PREDICTIVE MODEL OF THE
ORBIT DECAY OF THE
SOLAR MESOSPHERE EXPLORER

by

William Kent Tobiska

B.A., University of Colorado, 1972

A thesis submitted to the

Faculty of the Graduate School of the

University of Colorado in partial fulfillment

of the requirements for the degree of

Master of Science

Department of Aerospace Engineering

1985

This thesis for the Master of Science degree by

William Kent Tobiska

has been approved for the

Department of

Aerospace Engineering

by

Robert D. Culp

Robert D. Culp

Charles A. Barth

Charles A. Barth

Date May 9, 1985

Tobiska, William Kent (M.S., Aerospace Engineering)

Predictive Model of the Orbit Decay of the Solar Mesosphere Explorer

Thesis directed by Professor Robert Culp

The Solar Mesosphere Explorer (SME), a NASA science satellite operated by the University of Colorado, has been operational since launch in October 1981. It has a nearly circular, polar orbit which is gradually contracting due to atmospheric drag.

This study investigates the SME orbit decay. It aims to give an accurate short term prediction and a range of long term predictions for the satellite altitude. Starting with the theoretical basis in classical equations of motion and including the first order perturbing force of aerodynamic drag, this semi-analytic method achieves excellent results. After 37 months of prediction, the altitude is less than one percent off the actual value. The lifetime of SME extends over ten more years. The equations are based upon thirteen assumptions, including the shape of the planet, the characteristics of the atmosphere, the solar flux over the next solar cycle, and the geometry of the satellite.

There are extensive derivations of the computational equations, including the radius as a function of density, atmospheric density as a function of 10.7 cm solar flux, thermospheric temperature as a function of solar flux, satellite effective area as a function of roll angle, and the error analysis. In addition, the empirical data of the altitude change over the first three

years and the derived atmospheric density is discussed in detail. Predictions for the 10.7 cm solar flux over the next solar cycle, and the subsequent effects upon density and orbit altitude are explained.

The study concludes with an evaluation of this improved technique for determining orbit decay. It also makes recommendations for future areas of work. The validity of this semi-analytic method and the justification of the predictions is discussed.

To my wife, Susan, who has given me strength and boundless encouragement to aim for the highest goals, and to my two step-daughters, Elizabeth and Catherine, who have courageously sacrificed time and financial security to allow me the opportunity to complete this work. May their contributions continue to inspire myself and others to make human society productive, creative and peaceful.

ACKNOWLEDGEMENTS

It has been a privilege and honor for me to work with Dr. Robert D. Culp and Dr. Charles A. Barth in this study.

Dr. Culp, a Professor of Aerospace Engineering, encouraged me, from the beginnings of my graduate career, to pursue problems which are related to Astrodynamics. From him, I was able to gain a fundamental understanding of the field. For his efforts in assisting me, I am indebted.

Dr. Barth, the Director of the Laboratory for Atmospheric and Space Physics and a long-established scientist in the field of atmospheric physics, made my study possible. In my position as a graduate research assistant at LASP, he encouraged my studies of science and engineering problems related to SME by challenging me with new ideas. In my role as a teaching assistant to him, he pushed forward my conceptual understanding of this particular orbit decay problem as it is related to atmospheric physics. I thank him for this.

Many faculty members at the University of Colorado and professional staff members at LASP have given me tremendous assistance in this study. While it is not possible to single out every individual, the following people deserve special attention and thanks. Dr. N.X. Xinh and Dr. C.Y. Chow, both of Aerospace

Engineering, took time from their busy schedules, reviewed this material, and added useful comments. This was in addition to participating in my thesis defense. John Cowley of LASP made several good, timely comments in this work. He also put up with three years of numerous questions from me in a gracious manner, and for this he deserves special note. Dr. George Lawrence of LASP provided many useful suggestions and ideas in the formative stage of this study. Alan Stern of LASP played the role of my "sounding board" and his experience helped aim me in a good direction.

Two staff members worked above and beyond the call of duty in assisting my graduate work and this study. Ms. Joann Button of Aerospace Engineering truly eased my passage through the red tape of graduate school and has been enormously helpful through three years of big and small problems. Ms. Libby Peevy of LASP spent many, many long hours battling a word processor to produce this document. Under her labor, it finally reached an acceptable form. To these two people, I express my deepest thanks.

I could not write these acknowledgements without giving very special credit to my parents, Aron and Barbara Tobiska, who not only raised me with an inquisitive mind, the most precious gift of all, but also materially aided my family through very difficult early graduate years. This credit also goes to Ms. Sally Romayne, my mother-in-law, who has been tremendously supportive. Bob Hennig, a good personal friend, provided encouragement and hope during the difficult times of my transition to graduate school and Bob Anyon, also a friend of many years, aided me with one of the schematics in this study, helping provide a professional touch. To my many friends at LASP, Engineering school, and the CU GAS Project, thank you for three years of support and hundreds of useful discussions.

I could not have begun the long road leading to this point without the inspiration which I gained from over a decade of work with many people in the labor movement. They, and the people of China who hosted me on a visit there several years ago, showed me that human society can indeed advance. No effort in science and engineering has value unless it opens our eyes to a brighter path in the future and makes our life a little easier today. For this lesson, thank you.

CONTENTS

TABLES

Table

FIGURES

CHAPTER I

INTRODUCTION

1.1 History of orbit decay problem

For nearly twenty-three centuries, there is a written record of men and women attempting to explain the motions of celestial bodies. For a period of time much greater than that, human eyes have looked skyward, in awe of the motions of worlds and suns whose light they could see, but whose detail they could never imagine.

Over the last four centuries, humans have begun to understand better the mechanics and composition of the celestial bodies, both large and small. Copernicus accounted for the celestial motions with the Earth orbiting the Sun in his work De Revolutionibus (1543). Kepler (1571-1630) gave us a mathematical understanding of the laws of planetary motion. His contemporary, Galileo (1564-1642), developed a better fundamental understanding of the relationship between acceleration and force, as well as gave us the first real look at new worlds beyond our own with his telescope. Newton's (1643-1727) contributions firmly set the stage for human potential in space. His Law of Universal Gravitation, following on the heels of the three fundamental laws governing matter and motion in his work Principia (1687) and the mathematical methods of calculus to explain this motion, were outstanding contributions to our understanding of the universe around us. Einstein, with his breakthroughs in the concepts of Special and General Relativity, will allow us to expand our grasp of worlds around us, and possibly allow us to someday visit those worlds in person.

However, despite these monumental accomplishments of the past, it has not been until quite recently that many of these concepts have been put to practical use. Prior to October 1957, most of us had little concern for the solutions to problems in the specialized field of astrodynamics. This subset of celestial mechanics has been concerned with "the determination, integration, and improvement of specific 'real-world' orbits."[1] Much less were people concerned with the problem of orbit decay.

Sputnik opened an entire new era. Space travel and navigation had suddenly become a reality. The giant step of placing men on the Earth's moon, several times over only a decade later, forced upon us, in an electrifying and exhilarating way, the vast potential for human life off of this planet.

This study takes place in the context of our contemporary era. Trained people regularly travel into near Earth space several times a year. There exists a several years old space transportation system with the space shuttle as well as with numerous unmanned rockets of nearly a dozen nations being launched on a constant basis. Within the next decade or less, the first permanent space station will be in place, with a variety of scientific and research activities operating, under manned supervision, 24 hours a day. There will be low Earth orbiting unmanned satellites, platforms and transfer vehicles numbering in the hundreds or even thousands over the next decade. This is not to mention the crowded region of geosynchronous orbit, already now being populated regularly with communications satellites.

Particularly for low Earth orbiting satellites, there is a pressing need for accurate predictions of their orbital decay. This study analyzes the orbit decay over the past three years of one satellite in particular, the Solar Mesosphere Explorer (SME). It also makes a prediction for the orbit decay of this satellite during the next ten years. It is hoped that this small contribution will aid in our continuing efforts toward improving space navigation in particular and toward utilizing space for the benefit of all people in general.

There are two types of orbit decay predictions which are widely used today.

1.2 Types of predictions

Short term orbit predictions stem from the need to determine an accurate and narrow range of time and space for spacecraft reentry or location problems. The effort of solving this problem is driven by the need to know debris trajectories for particles after spacecraft breakup in the upper atmosphere, for rendezvous and docking maneuvers between spacecraft at the top of the atmosphere, and militarily, for potentially hostile missile tracking.

Long term orbit predictions, on the other hand, aim for a general determination of spacecraft lifetimes which are often measured in years. These predictions are useful for long term science and mission planning, studies of the density of space debris in regions of low Earth orbits, and in the coming years, assessing the scenarios for efforts of the space shuttle and space station to carry out spacecraft recapture and refurbishment tasks.

1.3 Description of the Solar Mesosphere Explorer (SME)

1.3.1 Scientific objectives

In the mid 1970's there was a general concern expressed among researchers and the public alike regarding the potential depletion of the ozone layer surrounding the Earth. Ozone is predominantly located in the sections of the middle atmosphere called the stratosphere and the mesosphere. Neither nature's nor humans' effects upon those layers were well known.

1.3.2 Construction and launch

During that period, the Laboratory for Atmospheric and Space Physics (LASP) at the University of Colorado in Boulder proposed to NASA the concept of a low budget satellite, designed exclusively to study the processes and elements creating and destroying ozone. In the late 1970's this proposal was accepted. NASA extended contracts for the scientific investigation of ozone depletion and formation, for the construction of a satellite bus system, for the building of several instruments to be used on the spacecraft and for the operations of the satellite from a Project Operations Control Center (POCC) in Boulder, Colorado.

SME has a mass of 415.5 kg and an effective area of 1.6 to 3.6 square meters. The actual effective area depends upon the satellite attitude. See Chapter 7 for a more detailed discussion. A look at Figures 1.1a and 1.1b shows the flat circular aluminum plate to which is attached the solar cells, the flattened cylindrical shape of the spacecraft bus and the generally rectangular module of the science instruments. The spacecraft also includes a long, parabolic cooling horn and an antenna stand. For reference, the spin axis of the satellite is through the horn and normal to the circular plate containing the solar cells. From the plane of the solar cells to the tip of the horn, SME measures 1.688 meters. The diameter of the circular plate is 2.235 meters.

SME was launched into a polar orbit, with an inclination near 97.5 degrees, on October 6, 1981 from the Western Test Range (WTR). The expected nominal altitude of 540 km was achieved in a near circular orbit, with eccentricity less than 0.0032. The orbit was sun synchronous, with an equator crossing of the ascending node at approximately 3 pm local time. This geometry, which still generally describes SME's orbit, allows an angle between the sun line and the orbit plane of the satellite of approximately 45 degrees and also allows the orbit plane to precess, or shift, eastward about 1 degree per day. This enables the orbit

SOLAR MESOSPHERE EXPLORER

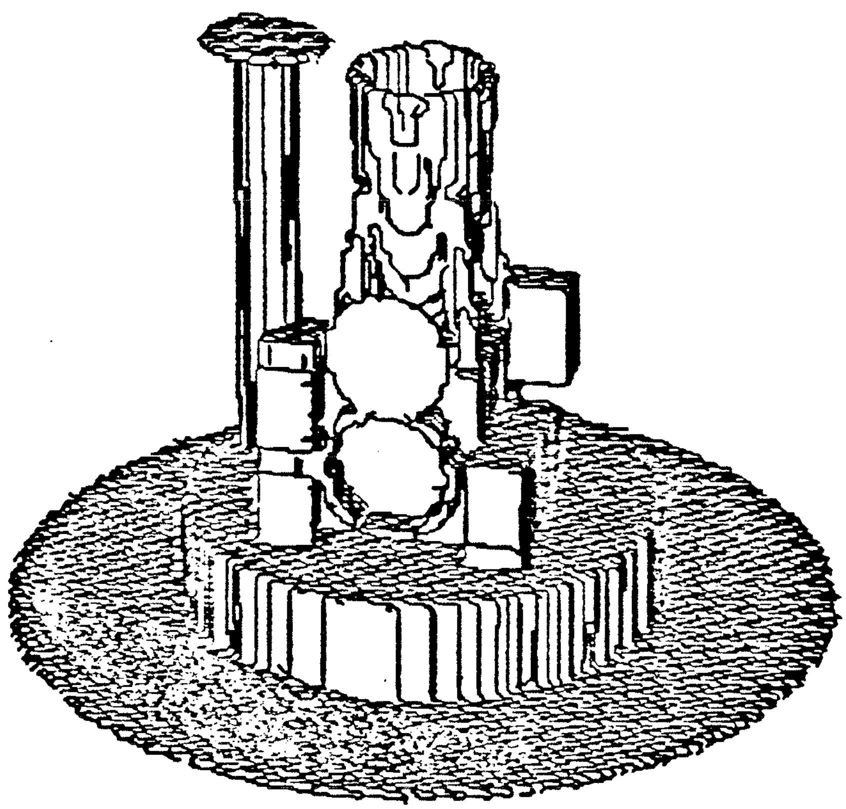

LABORATORY FOR ATMOSPHERIC AND SPACE PHYSICS
UNIVERSITY OF COLORADO

Figure 1.1a The Solar Mesosphere Explorer (SME), showing the solar array, the spacecraft bus, and the observatory module. (Courtesy of SME Mission Operations).

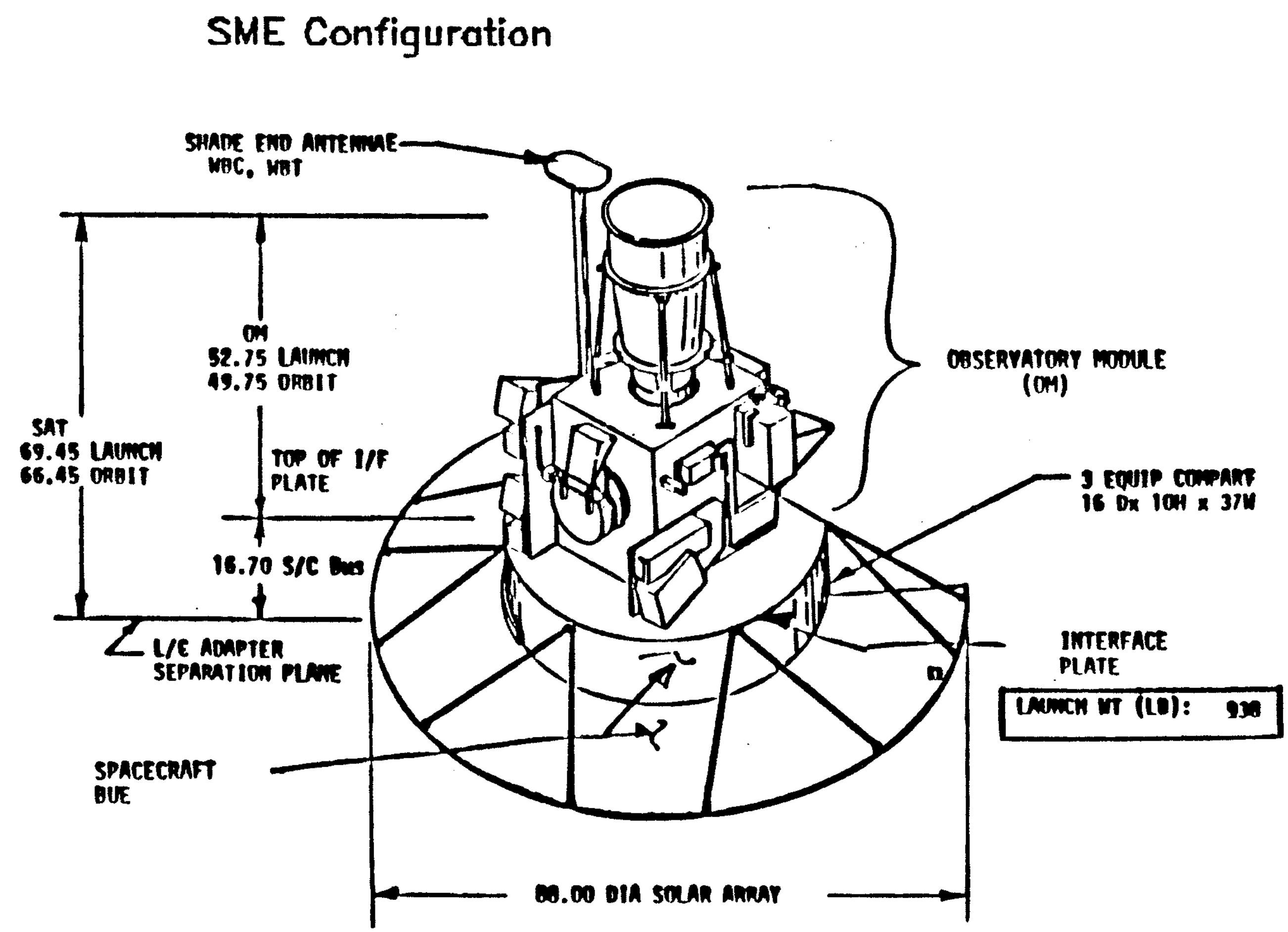

Figure 1.1b Schematic of the SME satellite with dimensions. (Courtesy of SME Mission Operations).

plane to keep up with the Earth's yearly rotation about the sun. Section 9.3 on the ascending node drift rate details this process. SME spins about an axis with a rotation rate of one revolution per 12 seconds, creating both stability, with a constant angular momentum vector, as well as a method for limb (horizon) scanning of the Earth by most of the major science instruments. See Figure 1.2.

1.3.3 Operations

Data is collected by the SME science instruments, stored on a tape recorder, and transmitted to Earth via a transponder. Engineering data is also collected in the same manner. Both the NASA Ground Station Tracking and Data Network (GSTDN) and the Tracking and Data Relay Satellite System (TSRSS) are used for the SME - Boulder POCC communication link. Commanding is done by the Boulder POCC. These are sent in a throughput mode from Boulder, to NASA's Goddard Network Control Center (NCC) and then on to the appropriate tracking and data relay station. The telemetry link from SME to Boulder follows the exact opposite path. The diagram of Figure 1.3 outlines this link.

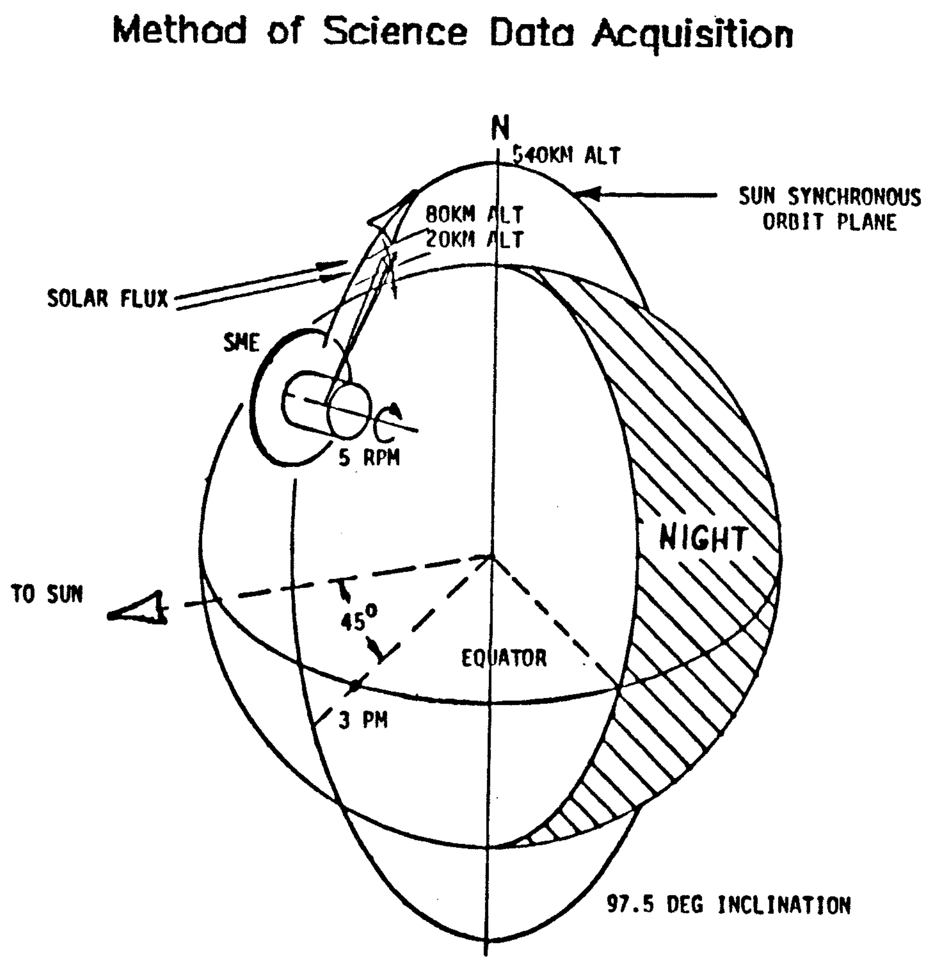

Figure 1.2 Orbit geometry of the SME satellite. (Courtesy of SME Mission Operations).

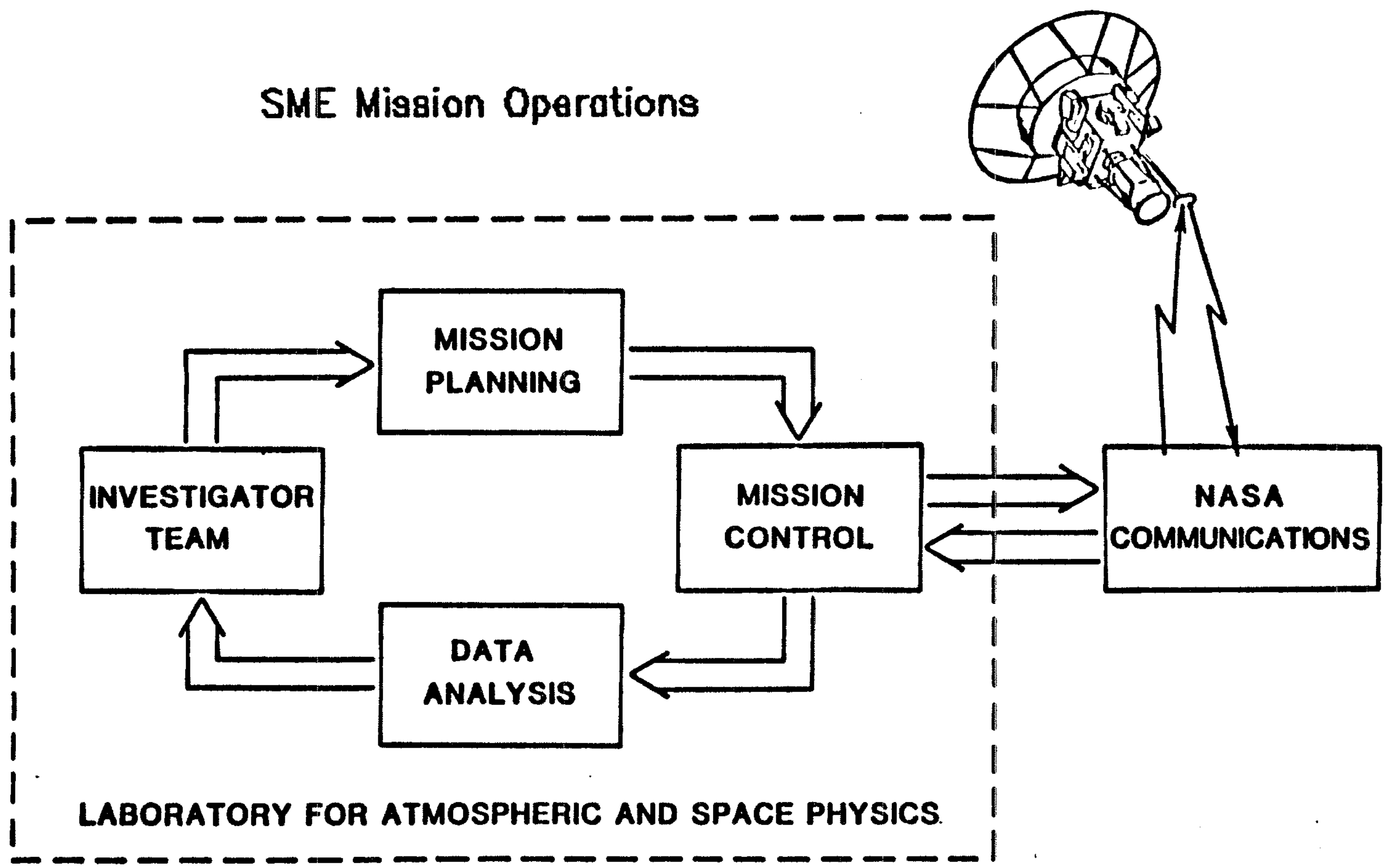

Figure 1.3 The Boulder Project Operations Control Center (POCC) at the Laboratory for Atmospheric and Space Physics (LASP) and the communication link with SME. (Courtesy of SME Mission Operations).

CHAPTER II

STATEMENT OF THE PROBLEM

2.1 Approaches to the orbit decay problem

There are three overall approaches to the problem of orbit decay. Each approach is useful under different conditions.

An analytical approach is most useful when one tackles a problem with little previous practical experience in orbit about a particular planet or with limited empirical data at hand. In this situation, the equations describing the physical behavior of a spacecraft must be derived from first principles, accounting for any of the reasonable perturbations which may exist.

An empirical approach to an orbit determination problem is applicable when a large quantity of data has been gathered. In addition, the general outline of the problem has been previously well-described and analyzed and there exists a good set of equations. In this case, one may be looking for the second, third or higher order effects in a problem such as orbit decay.

The semi-analytic approach may be used successfully when one has both a good data set and the opportunity to seek the best possible set of equations which may govern the behavior of a spacecraft.

2.2 Theoretical basis

In developing a set of equations which will adequately describe the motion and behavior of a spacecraft, there are several sources. Classical equations including equations of motion, Newton's and Kepler's laws, relations describing the gas in an atmosphere, and equations outlining the geometry of the spacecraft are all applicable, among others. This study uses a semi-analytic approach to the orbit decay problem. It also modifies the classical set of orbit determination equations, using a variety of assumptions which are outlined in Chapter 4.

2.3 Perturbations

In addition, the perturbations upon an Earth orbiting spacecraft from a variety of sources must be considered. Generally, in order of decreasing effect for a low Earth orbiting satellite in a nearly circular orbit, one may list perturbing forces due to thrust, aerodynamic drag, gravity gradient, oblate planet influences, solar radiation pressure, geomagnetic and electric field torques, sun and moon gravitational influences, and even the difference between relativistic mechanics and Newtonian mechanics. This study accounts for aerodynamic drag and the related spacecraft effective area as the major perturbing force. The others are taken to be of small magnitude and were neglected.

CHAPTER III

METHODOLOGY

3.1 Motivation for this study

The motivation for this work comes from two sources. First, from a survey of the literature, there is still room in the field for improvements in the techniques of spacecraft lifetime determination. From King-Hele, Cook and Jacchia in the late 1950's to the present (for example, the Workshop on Satellite Drag, Boulder, March 1982), many researchers have investigated the orbit decay and determination problem. An outstanding feature of the discussion continues to be the reliable prediction of solar activity as a dynamic driver of atmospheric density and thus orbit decay.[2] Second, the author has personal experience with the Solar Mesosphere Explorer satellite. There is extensive orbit data available and the opportunity exists to estimate the altitude during the 1987-89 time frame and beyond.

On this basis, the present study was undertaken.

3.2 Method of this study

The method of determining the altitude of SME as a function of time and solar flux is as follows: the density at a specified altitude is first determined by numerical integration. Density here is a function of the variable 10.7 cm solar flux

(F10.7). Next, the rate change of the orbit period is established. To conclude the iteration, the orbit radius on each day is calculated. The iteration proceeds through every day of the year, starting from a reference date and altitude, and terminates when the altitude reaches 120 km or lower.

The results of the iteration at the end of a month are stored in a table and printed both on the CRT display as well as inserted into a data file for later hardcopies. Examples of the program, it's subroutines and tabulated results are found in Appendix A and Appendix B.

CHAPTER IV

BASIC ASSUMPTIONS

There are a number of basic assumptions which lay the foundation for evaluating the orbit decay of SME. These assumptions help simplify the problem, even though they add a source of error in the results.

4.1 Circular orbit

The first assumption is that SME follows a circular orbit, with an eccentricity equal to 0.0. This is not the actual case, as the orbit eccentricity reaches 0.0032 at times. However, this small difference between the assumed and actual value of the eccentricity allows us to approximate a nearly circular orbit. By doing this, we can equate the semi-major axis of the orbit to the radius at all times, thus simplifying the equations of motion and the subsequent derivation of the radius as a function of atmospheric density. This is also in line with the general analytic result that atmospheric drag on a satellite is greatest at the periapsis and that the effect of this is to take energy out of the orbit, drop the apoapsis and circularize the orbit over a long period of time. Thus, we see that the general trend is to circularize the orbit.[3]

4.2 Spherical planet and atmosphere

Second, it is assumed that the Earth is perfectly spherical and that the atmosphere follows this contour above the planet. In reality, the Earth is oblate, bulging at the equator and flattened at the poles. The difference between the mean equatorial radius and the radius at the poles is not large (approximately 21.5 km), but it is certainly there.[4] The problems with this assumption, and the related effects on the Keplerian orbit elements of SME, are discussed in 4.5 below. However, here it should be mentioned that for long term orbit predictions, the use of a spherically distributed atmosphere greatly simplifies the calculations used in the prediction.

4.3 Concentric mass distribution of planet and atmosphere

In addition, the Earth has "lumps" in its mass distribution. One will find differences in the gravitational attraction around the planet which cause a satellite to momentarily speed up or slowdown in the course of one orbit. These effects have been neglected in this study. Their influence on long term orbit decay is negligible.

We may note that the above effects of planet asphericity and nonhomogenous planet mass distribution apply to the atmosphere above the planet surface. It is affected by the surface contour as well as the gravity differences since the atmosphere has mass. However, by assuming these effects to be small, especially at altitudes above 120 km, we greatly simplify the problem of modeling the distribution of gas molecules and ions in the atmosphere and hence the density.

4.4 Mean equatorial radius as Earth radius

For the purposes of numerical computation on the computer, we take the mean equatorial radius of the Earth as 6378.164 km.[5] This simplification introduces some error due to the planet asphericity mentioned above. However, computational speed is inversely proportional to the number of variables used in the programs, and this value was chosen as the best approximation constant to help decrease processing time.

4.5 Other orbit elements constant

4.5.1 Earth gravitational field, lunar and solar perturbations

The effect of the planet's asphericity on the orbit elements of an SME type satellite (i.e., very small area to mass ratio, circular low Earth orbit) can be summarized according to both secular (steady) and periodic perturbations. Table 4.1 from King-Hele[6] outlines these effects. Here, we have neglected all periodic lunar and solar perturbations on the orbit elements, and all secular and periodic Earth gravitational field effects. The neglect of the secular effects is not accurate, but over the time of a medium range orbit prediction for SME we can neglect this effect for simplification. The following arguments can be made.

The longitude of the ascending node Ω and the argument of periapsis ω do change for SME type satellites, and the SME orbit

Satellite Perturbations

	Secular		Periodic	
Perturbing source	large	small	moderate	small
Earth grav. field	Ω,ω	–	e	i,Ω,ω
Atmosphere	a,e	i	–	Ω,ω
Luni–solar	–	–	–	a,e,i,Ω,ω

Table 4.1 Secular and periodic perturbations on a satellite with perigee below 600 km.

plane precesses about one degree per day. This phenomenon, designed into the SME mission, keeps the orbit plane at approximately 45 degrees to the sun and an ascending node equator crossing of about 3 pm local time each day. Refer to Figure 1.2. Here, SME experiences about the same atmospheric density (slightly less than maximum) for each orbit.

However, small deviations in the above process have led to accumulated orbit plane deviation from this model. Presently, SME's orbit plane now has about a 4 pm local time ascending node each orbit. This is after three years of flight.

Over the second half of the 1980's, one might expect the precession rate, $\dot{\Omega}$, to continue increasing, although at a slower rate. This means that the longtitude of the ascending node will continue its (positive) eastward drift towards the dusk terminator, although at a slower rate of drift than we have seen over the past three years. We have two forces affecting the precession rate: one is the constant effect of the Earth's gravitational field variation due to the planet's oblateness (which is the major effect and constantly pushes the Ω eastward). The other is the variable effect of the atmospheric drag which is dependent upon solar flux (which affects the rate of ascending node drift). The equations describing these two effects are as follows[7]

$$\dot{\Omega} \approx -9.97\left(\frac{Re}{a}\right)^{3.5} (1-\varepsilon^2)^{-2} \cos i \tag{4.1}$$

$$\frac{di}{dt} = f_n r \cos u \, (\mu p)^{-1/2} \tag{4.2}$$

$$f_n = -\frac{\rho v \delta r \omega}{2\sqrt{F}} \sin i \cos u \tag{4.3}$$

where Re is the mean equatorial radius of the Earth, a is the semi-major axis of the satellite orbit, ε is the eccentricity and i is the orbit plane inclination. f_n is the aerodynamic force per unit mass and includes inclination as well as ω, which is the angular rotation of the atmosphere. We see that the rate change of ascending node $\dot{\Omega}$ changes secularly with the change in the semi-major axis. In other words, as the orbit contracts due to aerodynamic drag, a becomes smaller and $\dot{\Omega}$ (the ascending node drift rate) becomes larger. In addition, as i changes over time (slightly increases), the $\dot{\Omega}$ also increases. From equation 4.2, we notice that i changes over time proportional to aerodynamic force.

A discussion of the empirical results of the SME ascending node drift rate change is below in section 9.3. However, as far as assumptions are concerned, this is a small effect and this study neglects it, taking Ω, ω, and i to be essentially constant orbit elements. Eccentricity, ε, is considered to be 0.0 since we have a circular orbit approximation, as mentioned above in section 4.1.

4.5.2 Atmospheric drag perturbations

In referring again to Table 4.1, we find that by neglecting small periodic variations on Ω and ω from atmospheric drag, the remaining terms which we must account for are the large secular perturbations on the semi-major axis, a, and the period, P, due to atmospheric drag. For a circular, low Earth orbiter such as SME, we will discover later from the empirical data that these assumptions can certainly be made.

4.6 Non-rotating atmosphere

A common assumption is often made that the Earth has a non-rotating atmosphere, whereas in fact, it does have angular velocity. A non-rotating atmosphere contributes no tangential velocity components to the ions and molecules. The result is a distribution of random motion of the particles which cancel out any tangential components contributed to the drag on the satellite. By thinking of the atmosphere in this way, one can simplify the equations of motion and aerodynamic drag, allowing them to be written in non-vector form. Refer to Sections 4.5.1 above and 9.3 below for further discussion on this topic.

4.7 Three constituent atmosphere[8]

4.7.1 Troposphere

The atmosphere is normally broken into five layers, each having its own distinct characteristics. See Figure 4.1. Along the surface of the Earth, to an altitude of about 15 km at mid-latitudes is found the troposphere. Here the clouds form, there is turbulence and the temperature generally drops from an average of 288 K at the Earth's surface to 200 K at the tropopause. This is indicated in Figure 4.1.

4.7.2 Stratosphere

The next level of the atmosphere is the stratosphere where the temperature profile goes an opposite direction. A maximum temperature is achieved in the stratopause of approximately 270 K. This is due principally to the large amounts of ozone, O_3, located in this region. O_3 is a triatomic molecule and is a good radiator of infrared radiation. Solar flux penetrating into the O_3 layer is absorbed by that molecule and is reradiated as thermal energy.

4.7.3 Mesosphere

Above the stratopause at 50 km and extending to about 85 km is the mesosphere. Here the temperature profile again changes,

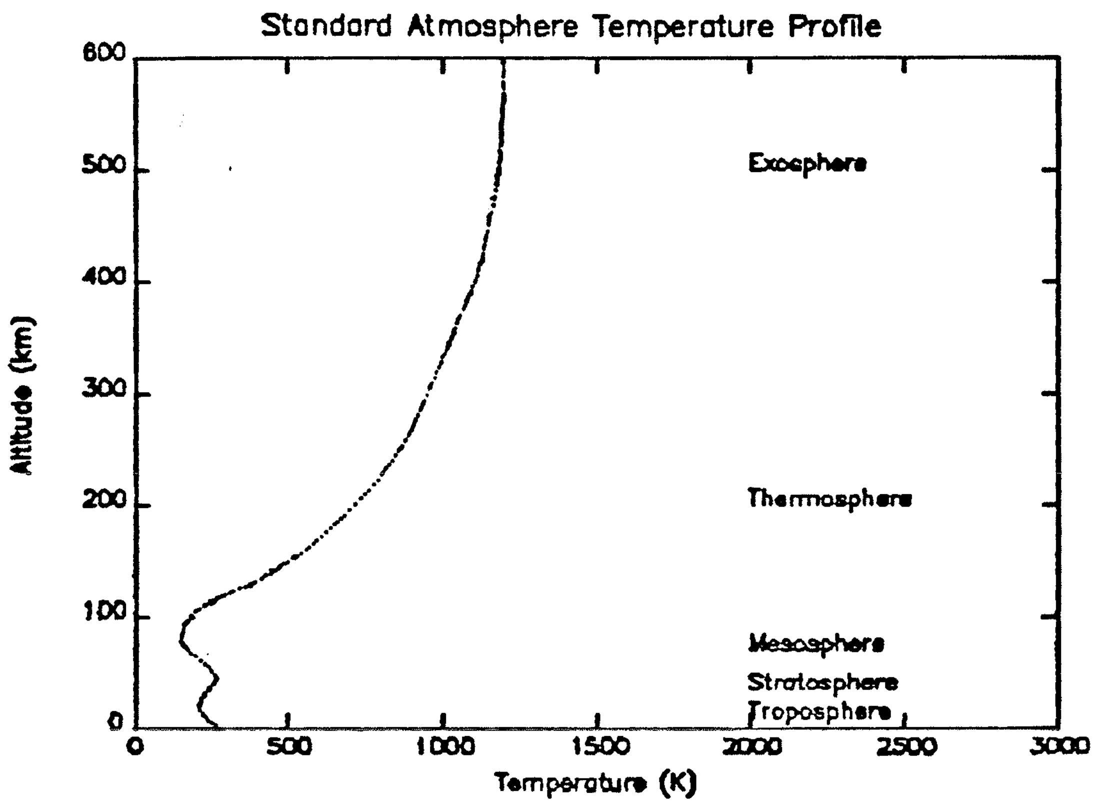

Figure 4.1 Kinetic temperature profile of the standard atmosphere. Adapted from the US Committee on Extension to the Standard Atmosphere (COESA, 1962).

with a temperature drop as the altitude increases. The main process identified as a heat exchanger here is convection and radiation from the O_3 layer below. At the mesopause near 85 km, the temperatures have dropped to about 180 K.

4.7.4 Thermosphere

In the thermosphere, extending from 85 km to approximately 500 km, the (kinetic) temperature again rises, approaching an asymptote or stable temperature known as the exospheric temperature or T_∞. As we will see later in section 6.2, this temperature varies considerably, depending upon day or night and solar activity.

The thermosphere above 120 km (that point chosen because it approximates the inflection point on the temperature curve) contains a number of constituents, including both neutral species as well as ions. Among these are O, N_2, O_2, Ar, He, H, NO^+, O^+, O_2^+ and N_2^+. However, only three constituents between 120 and 600 km constitute the bulk of the gas. Due to the processes of photoionization and dissociative recombination, neutral species and ions are transformed into a specific set of ions. Predominant among these are O^+, N_2^+, and O_2^+. The energy for these processes comes from solar ultra-violet radiation penetrating into the upper atmosphere. One finds that the total density of the atmosphere is just the sum of the individual species densities. See Figure 4.2. Helium, hydrogen and argon are also found in this region, as are other constituents, but they comprise only a small fraction of the total density.[9] Only above 600 km, as the other constituents drop off, do the lighter elements of hydrogen and helium play a more significant role in density calculations. This region has been neglected in this study since SME has never flown at those altitudes.

4.7.5 Exosphere

Above the thermosphere, beginning near 500 km, is the exosphere. Here the mean free paths of the ions and particles (the distance it must travel before it hits another particle) extend to infinity. Particle motion in this region is ballistic, as they follow trajectories which place them in near orbits.

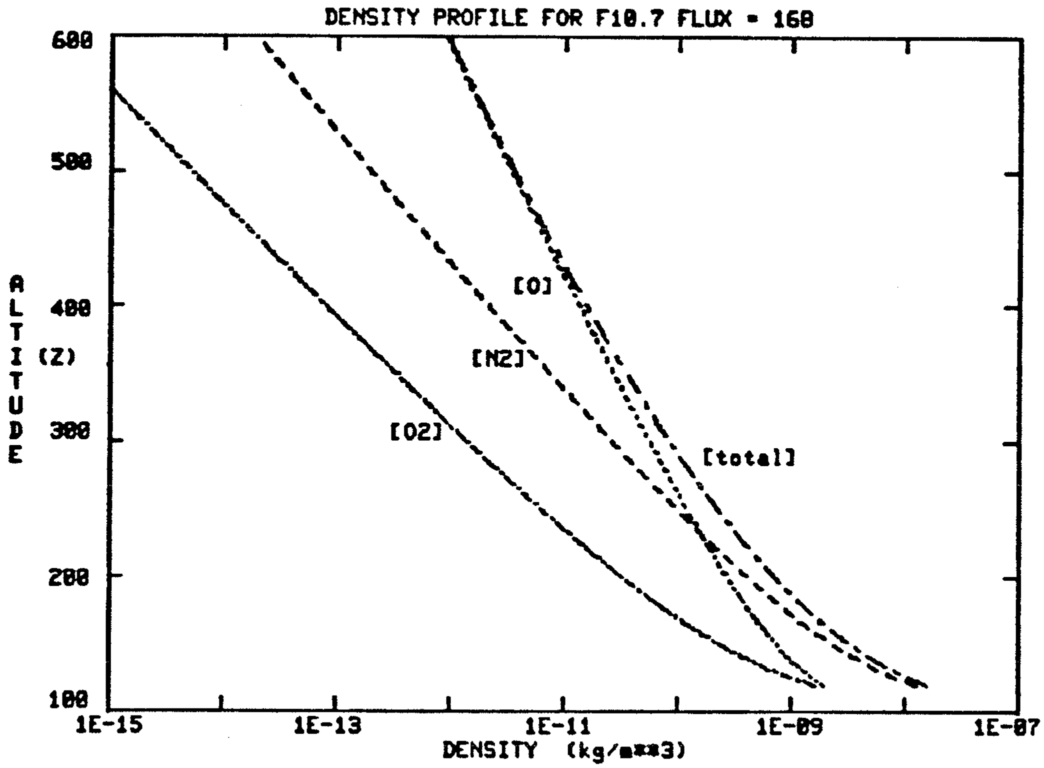

Figure 4.2 Model atmosphere with species densities and total density above 120 km. Plot based on a 10.7 cm solar flux of 168.

4.8 Non-mixing atmosphere

An eighth important feature of the atmosphere is the non-mixing of the elements above 120 km. The troposphere, stratosphere and mesosphere below this altitude sustain varying amounts of turbulence, convection and radiative heat transfer and, as such, the constituent gases are not found in stratified layers. On the other hand, the upper atmosphere feels little if any of these perturbations and the neutral species and ions tend to align themselves in strata. As a result of the greater gravitational attraction upon the heavier species, the process of diffusive separation tends to separate the constituents. Since there is little mixing, each constituent in the thermosphere has its own scale height H, and this must be accounted for in the calculations of total atmospheric density.

4.9 Exponential decay of density

In the thermosphere, an exponential curve best describes the temperature distribution. See Figure 4.3a and section 6.2. This is a result of the linear relation between pressure and temperature in the ideal gas law ($p = nkT$) and the subsequent derivation and substitution of variables into the barometric law ($p = p_0 \, e^{-h/[kT/mg]}$). Since ion density is derived from this relation, as we will see below, it follows that the total atmospheric density is described by an exponential decay curve above 120 km.

4.10 Average exospheric temperature

A tenth assumption simplifies the calculation of the exospheric temperature. We know that a general relationship (which can be described adequately with linear relations) exists between the day and night exospheric temperatures. The day temperature rises to a value about 1.3 times that of the night value. If one imagines a satellite in a circular polar orbit passing through both the nighttime and daylight sections of the atmosphere during one orbit, then one can suggest that there may exist some average temperature between the minimum night value and maximum day value. If this average value were to be substituted for the variety of temperature distributions experienced over one orbit, one might expect to see the same overall net effect in the derived atmospheric density as that actually felt by the satellite.

If we integrate the temperatures from the minimum to the maximum values as the satellite passes through one half of an orbit, we can arrive at an averaged, integrated exospheric temperature which can be treated as a constant at a given solar flux. See Figures 4.3a and 4.3b. This simplification is a modification of existing atmospheric models. Section 6.2 shows the derivation of this average exospheric temperature.

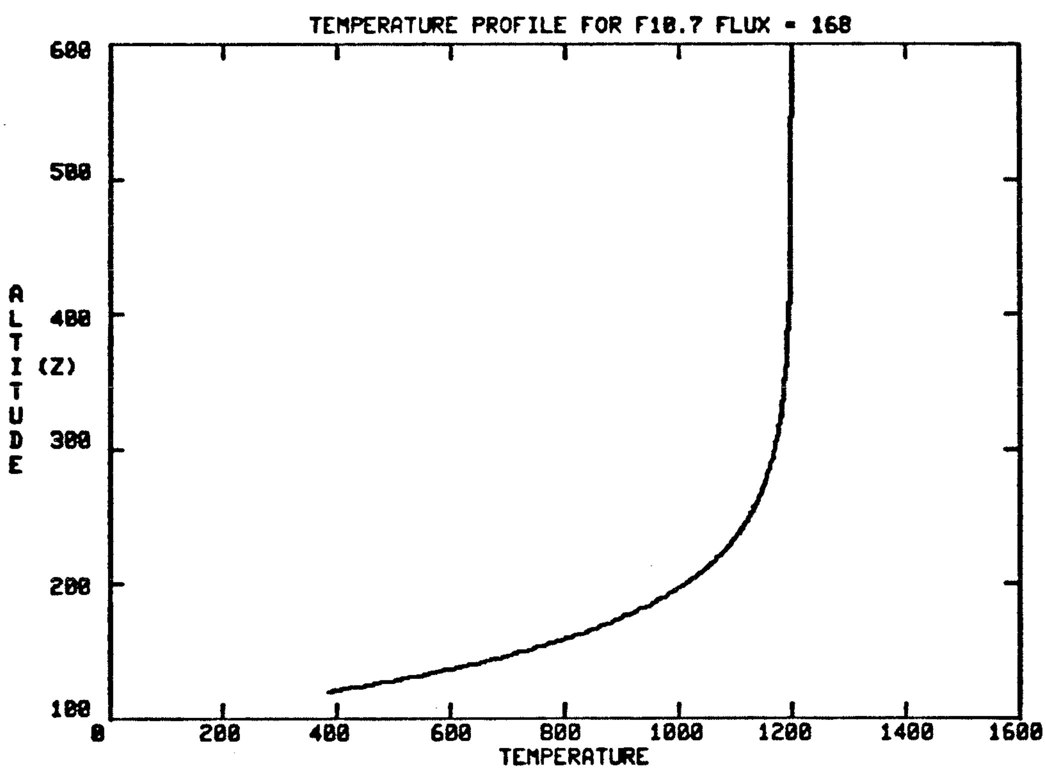

Figure 4.3a Model thermosphere kinetic temperature profile above 120 km at a 10.7 cm solar flux of 168.

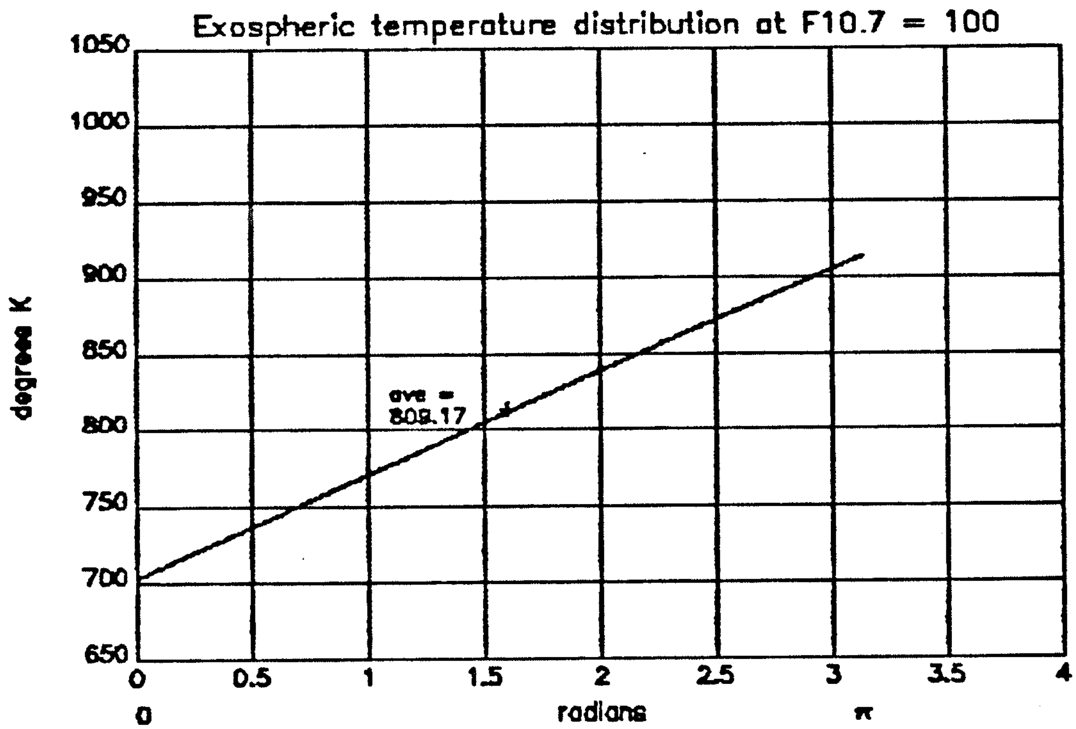

Figure 4.3b The distribution of exospheric temperatures between night minimum and day maximum for a 10.7 cm solar flux of 100. The average kinetic temperature is 809.17 degrees K in this example.

4.11 Solar flux correlates with atmospheric density

Experience among atmospheric, solar and planetary researchers has shown us that the changes in the 10.7 cm solar flux can be highly correlated with the changes in atmospheric density. One can use a fairly straightforward relationship to arrive at the total atmospheric density, based on work done by many researchers. This study uses the general method of Jacchia in correlating 10.7 cm solar flux with density. While Jacchia's models also include the geomagnetic index A_p in the calculations, the model in this thesis simplifies the calculations by using only the solar flux indicator. As an example of the correlation between variations in 10.7 cm flux and atmospheric density, see Figures 4.4, 4.5, 4.6, and 4.7.

4.12 Solar rotation effect negligible

The 27 day solar rotation cycle has a demonstrated effect upon satellite drag[10]. This phenomenon is especially noticeable as a second order effect during solar maximum periods. A possible (and very small) effect has been seen in the SME derived density data. This study assumes that there is a negligible effect from 27 day solar rotation on the long term orbit decay of a satellite. We can simplify the solar flux model by eliminating this term in the calculations.

4.13 Constant effective area of SME

A final assumption treats the effective area of the SME

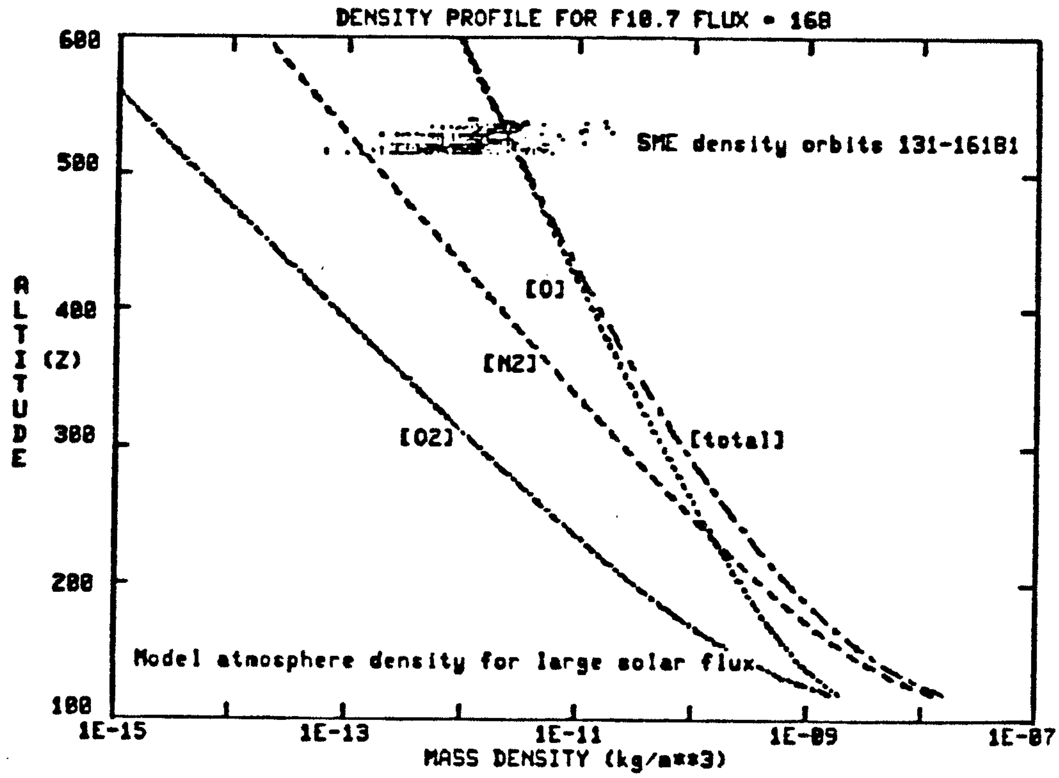

Figure 4.4 Model atmosphere with species densities and total density above 120 km at F10.7 = 168. Overplotted on the graph are the actual data points of SME derived density for orbits 131 - 16181 (33 months), representing the altitude range of 534 - 516 km.

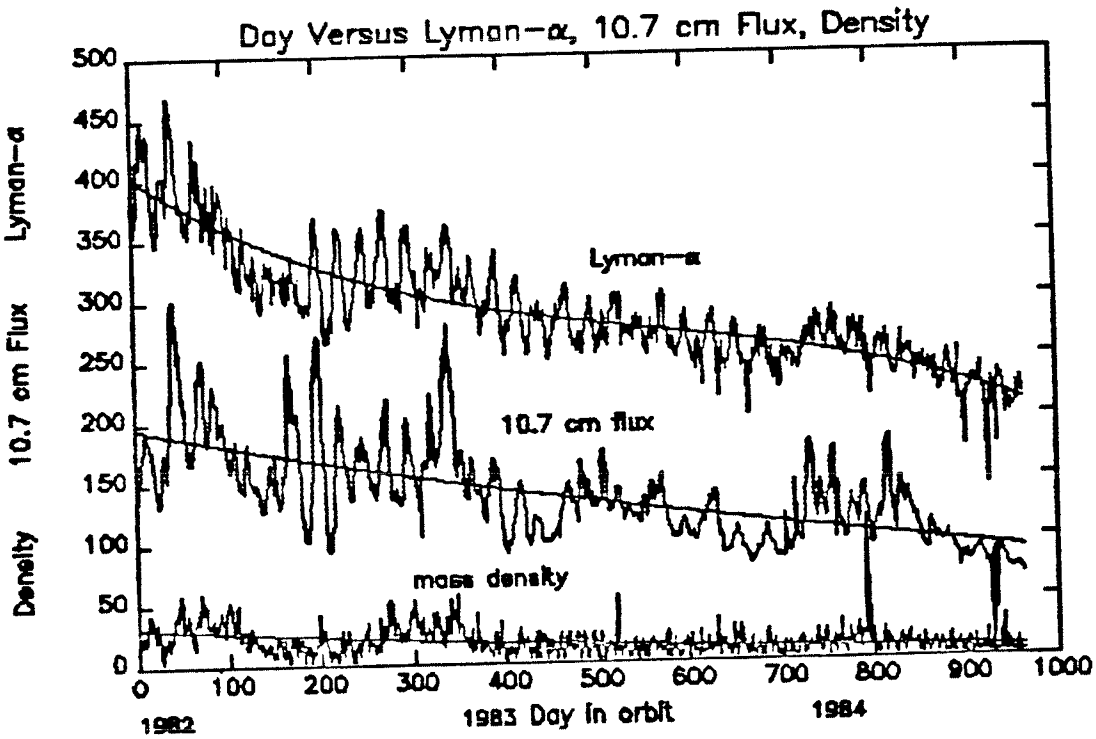

Figure 4.5 Thirty-three months of Lyman-α, F10.7 fluxes and the mass density of the atmosphere as observed by SME. The data has been offset from its actual values to fit a relative scale for illustration purposes.

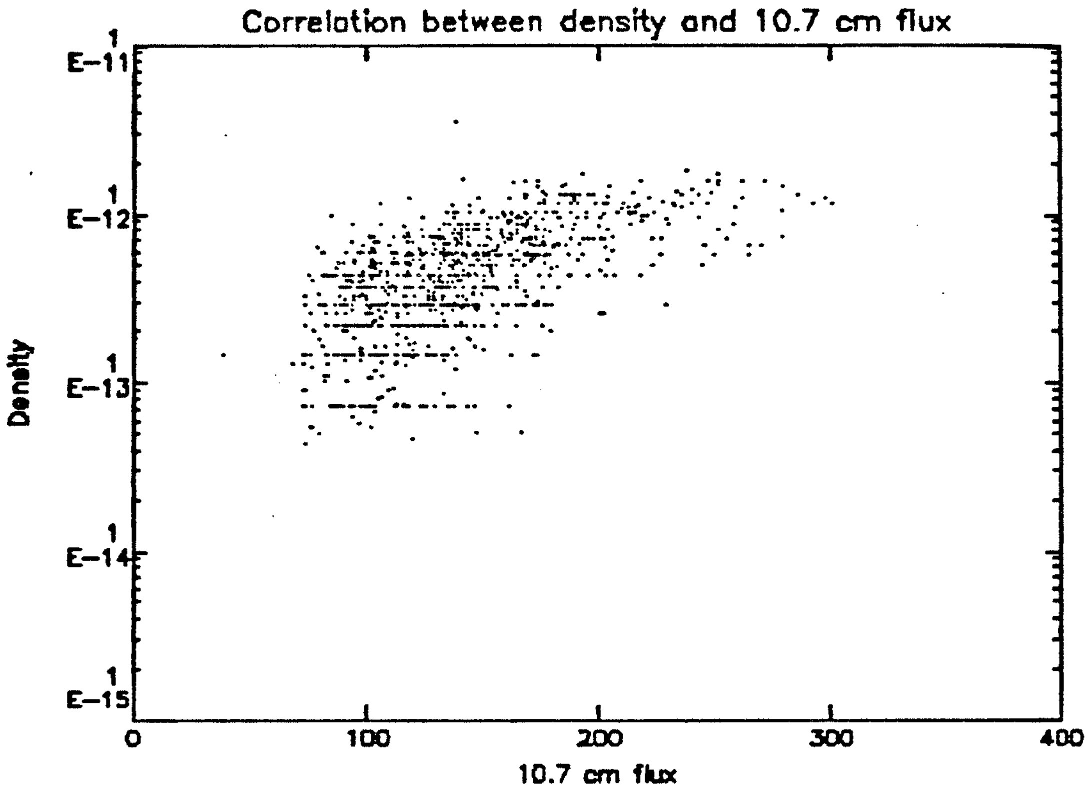

Figure 4.6 A correlation plot between the SME derived density and the 10.7 cm flux over thirty-three months between January 1982 and September 1984. There is one data point for each day. [Note: horizontal streaks in the data are artifacts of truncation error in the plotting routine.]

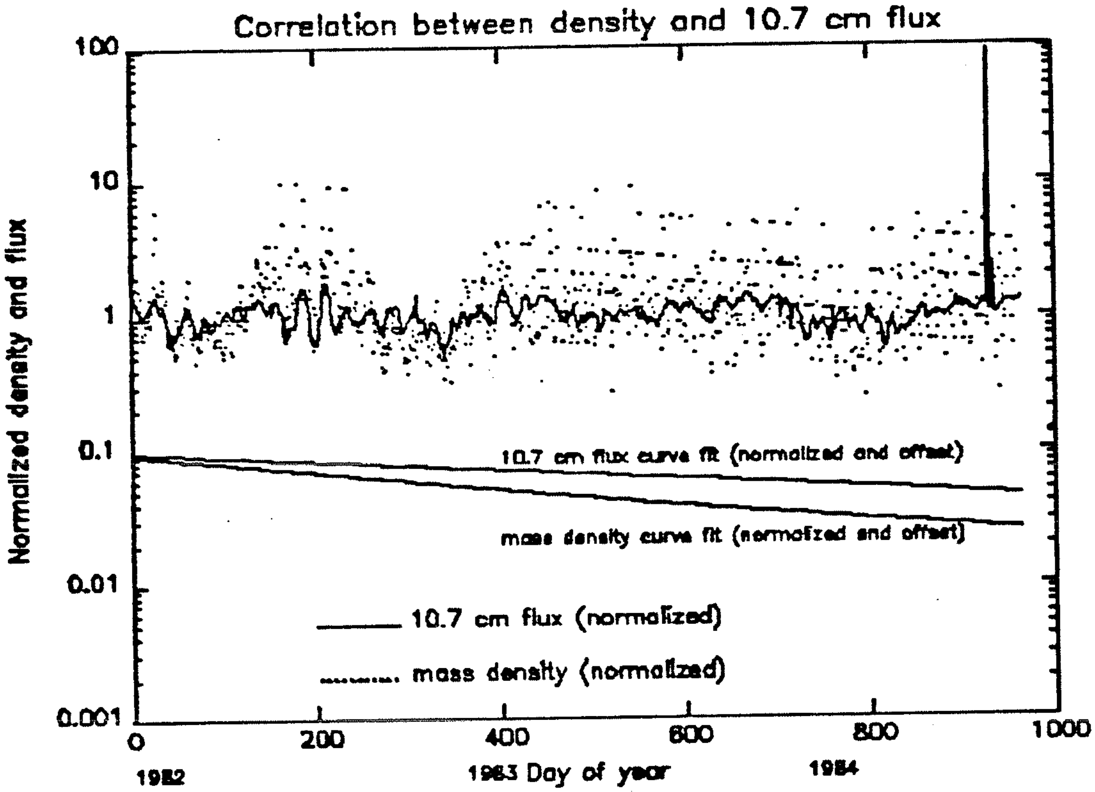

Figure 4.7 The normalized SME derived mass density variation versus day of year is overplotted with the normalized 10.7 cm flux variation versus day of year. The offset slopes of the lines fit to these two data sets are also plotted, showing the close correlation.

satellite as a constant. By letting the area = 2.0 m^2, another computational variable is reduced to a constant. When carrying out an analysis of the surface areas of the satellite, their relation to each other, to the velocity vector, and to the (coupled) roll/-yaw angles, one can arrive at a reasonable constant value. Confidence was gained with this value from three independent sources: knowing the exact dimensions of the satellite (see Figure 1.1b), knowing the observed radar cross-section of the satellite as seen by NORAD radar (2.59 m^2)[11] and by matching the predicted decay with the actual orbit decay over 33 months. The drag coefficient, which is near 1 for spherical satellites and near 2 for satellites having total particle adhesion or total reflection, should reasonably be somewhere between the two values and should be a constant in free molecular flow[12]. Empirical studies have shown this author that a value of 1.25 for Cd matches well the predicted versus actual decay rate.

CHAPTER V

DERIVATION OF THE ALTITUDE

The following derivation of the radius and altitude of the SME orbit follows from the classic equations of Newton's Second Law, Newton's Law of Gravitation, the equations for conservation of total energy and angular momentum, Kepler's equation, the equation describing aerodynamic drag, the equivalence of the rate changes of total energy and work, and finally the process of variable substitution. Numerical integration on the computer is used to step through the time period, achieving the best guess altitude on each particular date.

5.1 General relations

In order to derive the radius as a function of density, we establish the general relations for μ, the Earth gravitational constant

$$\mu = G(M + m) \text{ or } \mu \cong GM \tag{5.1}$$

where M is the mass of the Earth, G is the universal gravitational constant and m is the mass of the satellite. From Newton's Second Law

$$F_r = ma_r = m(\ddot{r} - r\dot{\theta}^2) \tag{5.2}$$

$$F_\theta = ma_\theta = m(r\ddot{\theta} + 2\dot{r}\dot{\theta}) \tag{5.3}$$

and the Law of Gravitation, where r is the distance from the center of the Earth

$$F_r = -\frac{GMm}{r^2} \tag{5.4}$$

By noting that under gravitational attraction there is no transverse force, we can show that angular momentum, h, per unit mass is conserved

$$r^2\dot{\theta} = h = \text{constant} \tag{5.5}$$

5.2 Radius as function of energy

We can solve for the radius, r, as a function of energy if we let

$$r = \frac{1}{u} \tag{5.6}$$

$$\dot{\theta} = hu^2 \tag{5.7}$$

The velocity in the radial direction is

$$\dot{r} = -\frac{1}{u^2}\frac{du}{dt} = -\frac{1}{u^2}\frac{du}{d\theta}\frac{d\theta}{dt} \tag{5.8}$$

$$= -r^2\dot{\theta}\frac{du}{d\theta}$$

$$= -h\frac{du}{d\theta}$$

and the acceleration in the radial direction is

$$\ddot{r} = -h \frac{d^2 u}{d\theta^2} \frac{d\theta}{dt} \tag{5.9}$$

$$= -h\dot{\theta}\frac{d^2 u}{d\theta^2}$$

$$= -h^2 u^2 \frac{d^2 u}{d\theta^2}$$

By substitution we arrive at the following

$$\frac{d^2 u}{d\theta^2} + u = \frac{\mu}{h^2} \tag{5.10}$$

This 2nd order differential equation is similar to the undamped mass-spring system with a constant forcing term. Its solution is well known and is given by

$$u = \frac{\mu}{h^2} + C \cos (\theta-\theta_o) \tag{5.11}$$

where C and θ_o are constants. We can evaluate $\theta = \theta_o$ when $r = 0$. Bearing this in mind, we will solve for the constant C and end up with the orbit equation in which the radius is written in terms of the energy of the system.

If we let the total energy per unit mass, e, equal the kinetic energy plus the potential energy of a system, then by substitution

$$e = \frac{1}{2} v^2 - \frac{\mu}{r}$$

$$= \frac{1}{2} h^2 u^2 - \mu u \tag{5.12}$$

where the velocity $v = r\,\dot{\theta}$ (5.13)

and by substitution, we can rewrite the energy per unit mass as

$$e = \frac{1}{2} h^2 \left(\frac{\mu}{h^2} + C\right)^2 - \mu\left(\frac{\mu}{h^2} + C\right)$$

$$\rightarrow e = \frac{1}{2} h^2 C^2 - \frac{1}{2} \frac{\mu^2}{h^2} \tag{5.14}$$

At this point, we solve for C in terms of energy

$$C = \sqrt{\frac{2}{h^2} \left(e + \frac{1}{2} \frac{\mu^2}{h^2}\right)} = \sqrt{\frac{2e}{h^2} + \frac{\mu^2}{h^4}} \tag{5.15}$$

and by allowing $\theta_o = 0$ then

$$u = \frac{\mu}{h^2} \left[1 + \sqrt{1 + \frac{2eh^2}{\mu^2}} \cos \theta\right] \tag{5.16}$$

or by rewriting u in terms of the radius, r, we arrive at the orbit equation where the radius is written in terms of energy per unit mass

$$r = \frac{h^2/\mu}{1 + \sqrt{1 + \frac{2eh^2}{\mu^2}} \cos \theta} \tag{5.17}$$

5.3 Conic section geometry

Shifting our focus momentarily, we set aside the orbit equation derived above and review some of the elements in the geometry of conic sections. See Figure 5.1. These are fundamental relations in orbit mechanics since they describe the mathematical properties of an ellipse, one of the 3 geometries of orbital motion. We remember that

$$r = \frac{\ell}{1 + \varepsilon \cos \theta} \tag{5.18}$$

where ℓ is the semilatus rectum and ε is the eccentricity. For the true anomoly, $\theta = 0$ and $\theta = \pi$, equation (5.18) reduces to

Ellipse Notation

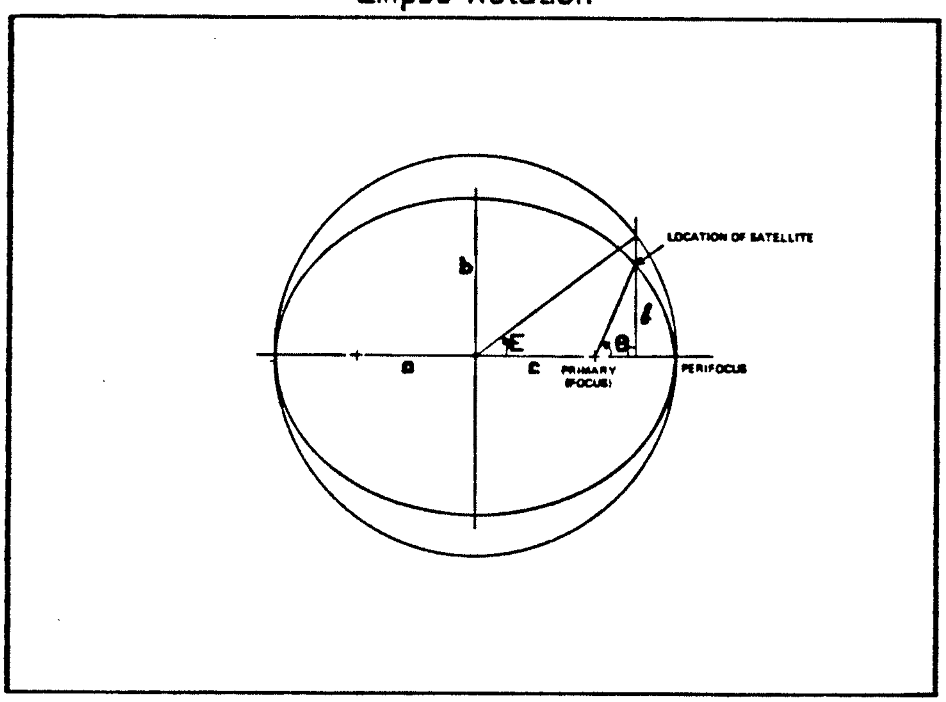

Figure 5.1 The geometry of an ellipse is shown, with the definition of the eccentric anomaly, E, and the true anomaly, θ.

$$r_p = \frac{\ell}{1 + \varepsilon} = a(1-\varepsilon)$$

$$r_a = \frac{\ell}{1 - \varepsilon} = a(1+\varepsilon) \qquad (5.19)$$

for the periapsis and the apoapsis, respectively. The semi-major axis, a, the eccentricity, ε, and the semilatus rectum, ℓ, may be written as

$$a = \frac{r_p + r_a}{2} \qquad (5.20)$$

$$\varepsilon = \frac{r_a - r_p}{r_a + r_p} = \frac{r_a - r_p}{2a} \qquad (5.21)$$

$$\ell = a(1-\varepsilon^2) \qquad (5.22)$$

where, by substitution into equation (5.18)

$$r = \frac{a(1-\varepsilon^2)}{1+\varepsilon\cos\theta} \qquad (5.23)$$

5.4 Vis-viva integral

By comparing the expression for the radius in the orbit equation (5.17) and in the conic section equation (5.23), we find a classic result. The eccentricity term can be written as a function of energy per unit mass, the semilatus rectum can be written as a function of angular momentum and the semi-major axis can be written as a function of both angular momentum and energy per unit mass

$$\varepsilon = \sqrt{1 + \frac{2eh^2}{\mu^2}} \tag{5.24}$$

$$\ell = \frac{h^2}{\mu} \tag{5.25}$$

$$a = \frac{\ell}{(1-\varepsilon^2)} = \pm \frac{h^2}{\mu(1-\varepsilon^2)}$$

$$\rightarrow a = \mp \frac{\mu}{2e} \tag{5.26}$$

We should note here that the (-) sign indicates an elliptic shape whereas the (+) sign indicates a hyperbolic shape of an orbit. An optional way to write equation (5.26) is

$$e = \mp \frac{\mu}{2a} \tag{5.27}$$

and $e = \frac{1}{2} v^2 - \frac{\mu}{r}$

(where e is also $e = \frac{1}{2} h^2u^2 - \mu u$ from equation (5.12))

By substitution, we then see that

$$\mp \frac{\mu}{2a} = \frac{1}{2} v^2 - \frac{\mu}{r} \tag{5.28}$$

or, rewriting this, we arrive at the vis-viva integral

$$v^2 = \mu\left[\frac{2}{r} \mp \frac{1}{a}\right] \tag{5.29}$$

5.5 Radius as a function of density

Up to this point, we have reviewed the classical equations relating to satellite orbits, both from the energy and the geometric standpoints. Below, we take these equations a step further. With simplifying assumptions, we arrive at an expression for the radius of an orbit as a function of both the atmospheric density and the rate change of the orbit period.

First let us define the aerodynamic drag force as

$$F_d = \frac{1}{2} C_d A\rho v^2 \tag{5.30}$$

where C_d is the drag coefficent, A is the effective area, ρ is the atmospheric density, and v is the velocity.

Recalling the expressions for work and rate change of work

$$W = \int_1^2 F ds \tag{5.31}$$

$$\dot{W} = F\dot{s} = Fv \tag{5.32}$$

we can then substitute equation (5.30) if we let the force in the rate change of work equation be the drag force by the atmosphere upon the satellite

$$\dot{W} = \frac{1}{2} C_d A\rho v^3 \tag{5.33}$$

Now, recalling that total energy in the system is

$$E = T + V \tag{5.34}$$

and that from equation (5.27) $e = \mp \frac{\mu}{2a}$, we can make an assumption for the case of SME that we have a satellite with a circular orbit where $a = r$ and

$$e = -\frac{\mu}{2a} = -\frac{\mu}{2r} \tag{5.35}$$

Taking the time derivative of this equation, we find the rate change of energy per unit mass can be written

$$\frac{de}{dt} = \dot{e} = \frac{\mu\dot{r}}{2r^2} \tag{5.36}$$

and likewise the rate change of total energy is

$$\text{and } \dot{E} = \frac{\mu m\dot{r}}{2r^2} \tag{5.37}$$

From Kepler's work, we know that the orbit period, P, is

$$P = \frac{2\pi r^{3/2}}{\mu^{1/2}} \tag{5.38}$$

and the rate change of the period is simply the first time derivative, or

$$\frac{dP}{dt} = \dot{P} = \frac{2\pi}{\mu^{1/2}} \frac{3}{2} r^{1/2} \dot{r} \tag{5.39}$$

or by simplifying the equation by resubstituting in the expression for P

$$\frac{\dot{p}}{p} = \frac{3}{2}\frac{\dot{r}}{r}$$

$$= \frac{3}{2} \frac{A}{m} C_d \rho v^3 \frac{r}{\mu} \qquad (5.40)$$

Here, for the right hand side of the equation (5.40), the reader should note that we can equate $\dot{W} = \dot{E}$ or

$$\dot{W} = \frac{1}{2} C_d A \rho v^3 \quad \left(\frac{kgm^2}{s^3}\right)$$

$$\dot{E} = \frac{\mu m \dot{r}}{2r^2} \quad \left(\frac{kgm^2}{s^3}\right)$$

$$\dot{W} = \dot{E}$$

$$\dot{r} = \frac{C_d A \rho v^3 \; 2r^2}{2\mu m} \qquad (5.41)$$

By rewriting equation (5.40), eliminating terms and remembering that we are assuming a circular orbit where $v_c = \sqrt{\frac{\mu}{r}}$

$$\frac{\dot{P}}{P} = \frac{3}{2} \frac{A}{m} C_d \rho v_c \qquad (5.42)$$

and therefore the rate change of the period can be written as

$$\dot{P} = 3\pi r \frac{A}{m} C_d \rho \qquad (5.43)$$

Finally, rewriting this equation to solve for density as a function of radius and rate change of period

$$\rho = \frac{1}{3\pi r \frac{A}{m} C_d} \dot{P} \tag{5.44}$$

or solving for the radius as a function of density and the rate change of period

$$r = \frac{1}{3\pi \rho \frac{A}{m} C_d} \dot{P} \tag{5.45}$$

which is the result we wanted to achieve. The nice thing about equations (5.44) and (5.45) is that they lend themselves to numerical integration on the computer quite readily. By taking a constant time interval, dt, we can step through the iteration and find the density or radius at each interval. Of course, the equations can be solved analytically, too, for any particular time interval.

A related derivation of density as a function of rate change of period can be found in King-Hele.[13]

CHAPTER VI

DERIVATION OF THE DENSITY

The density of the atmosphere can be described by the following set of equations. We build on the Ideal Gas Law, the Barometric Law, the known composition of the upper atmosphere and equations simplifying the exospheric temperature. Other useful items are the known number density of atmospheric ions and their sum, equations presenting a reasonable prediction of the 10.7 cm solar flux over the next solar cycle, and the techniques for numerical integration. The latter gives us the ability to achieve a density value of a species at a given altitude for a given solar flux.

6.1 General relations and classical equations

An important starting point in understanding the physics of the upper atmosphere is the Ideal Gas Law, where pressure, p, (force per unit area) is defined as a function of the density of a gas at a specific temperature

$$p = nkT \tag{6.1}$$

Here, n is the number of molecules per unit volume of a gas, k is Boltzmann's constant (k = 1.38062 E-23 Joules/degree Kelvin), and

T is the kinetic temperature of the gas in degrees Kelvin. We also note that mass density ρ is defined as

$$\rho = nm \tag{6.2}$$

where m is the mass of the gas molecule (or ion). We remember that the force on a gas particle in the atmosphere from gravitational attraction is just equation (5.4) where $F = -\frac{GMm}{r^2}$, or, if we let $r = Re + z$ where r is the radius from the center of the Earth, Re is the Earth radius and z is the height above the surface, then

$$g = g_o\left(\frac{Re}{Re+z}\right)^2 \tag{6.3}$$

where we can define g_o as

$$g_o = \frac{GM}{Re^2} \tag{6.4}$$

These relations lead to the hydrostatic equation where we write the change in pressure per unit area Δp as a function of two variables: gravitational force on the gas particle and the change in height above the surface Δz

$$\Delta p = -nmg\ \Delta z \tag{6.5}$$

Another way of looking at this equation is a balance between the pressure and the weight of the overlying section of air on top of that volume. Dividing both sides of equation (6.5) by the pressure terms and integrating both sides, we get

$$\frac{dp}{p} = \frac{-nmgdz}{nkT} \tag{6.6}$$

and

$$\int_{p_o}^{p} \frac{dp}{p} = - \int_{z_o}^{z} \frac{dz}{(kT/mg)} \tag{6.7}$$

which gives us the barometric law

$$p = p_o e^{-[(z-zo)/(kT/mg)]} \tag{6.8}$$

where pressure drops off exponentially with altitude. See Figure 6.1 for a plot of this function. We note that the quantity kT/mg has the units of length and is defined as a scale height H.

$$H = \frac{kT}{mg} \tag{6.9}$$

$H \sim kT \sim$ kinetic energy and is inversely proportional to force. If we let $kT = mgH$, then by substitution (and letting $dz = z - z_o$) we have the density equation

$$n = \frac{Po}{mg(z)} e^{-\frac{dz}{H}} \tag{6.10}$$

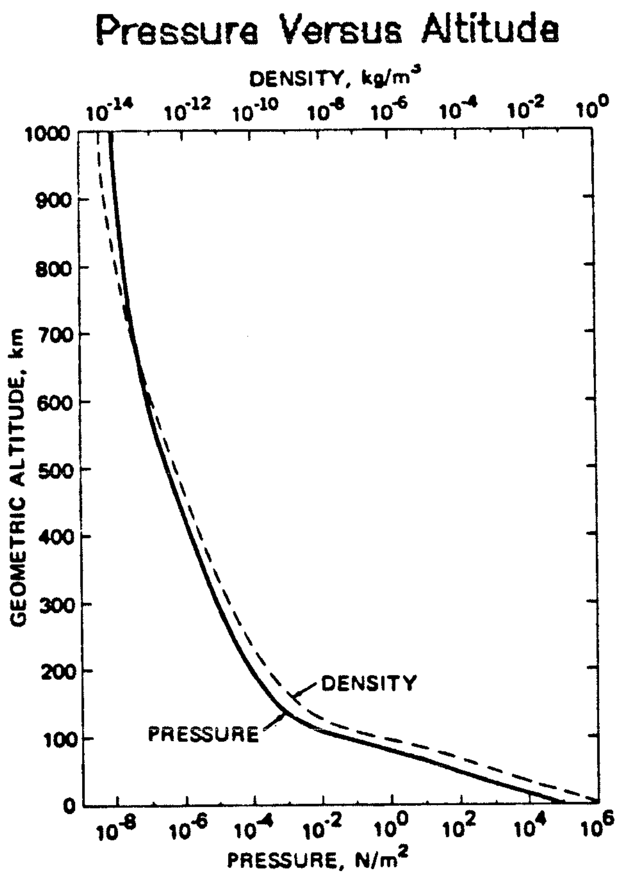

Figure 6.1 The total pressure and mass density are plotted against the geometric altitude. (Reproduced from the US Standard Atmosphere, 1976).

or

$$n = n_o e^{-\frac{dz}{H}} \tag{6.11}$$

It has generally been found[14] that up to about 90 km altitude, there is relatively good mixing of air in the atmosphere, as mentioned in the assumptions, section 4.8. This leads to a close estimate of average air mass = 29 mean molecular weight (see Table

6.1). Using the values of T = 288 degrees Kelvin, g = 9.8 m/s^2 and Avogadro's number of 6.022 E+23 molecules per mole, we find an average H to be approximately 8 km in the lower and middle atmosphere.

Lower Atmosphere Composition

Species	At Wgt	Percent	Contribution
O_2	32	21	6.72
N_2	28	78	21.84
Ar	40	1	0.40
			28.96

Table 6.1 Constituents contributing to the mass of the lower atmosphere.

As indicated earlier in this study, all our measurements are calculated for altitudes between 120 and 540 km for SME. Above 120 km, diffusive separation of the constituents and a non-mixing atmosphere cause us to consider each species separately. Therefore, while we can apply the same equations of ideal gas, hydrostatic balance and barometric law for each individual gas, we should also remember that higher temperatures in the thermosphere (see Figure 4.3a) will drive the scale height to larger values than those below 120 km. The reference altitude for the density equation (6.11) and the barometric law (6.8) we will use is z_o = 120 km. The reference pressure p_o and number density n_o are the pressure and density at 120 km for this study. If we consider the fact the Boltzmann's constant, k, and the atomic mass of a constituent, m, are fixed, then in equation (6.9) we note that only temperature, T, and gravity, g, are altitude dependent. Therefore, we write

$$H(z) = \frac{kT(z)}{\frac{m}{Av.} g(z)} \qquad (6.12)$$

where Av. is Avogadro's number.

If we also rewrite equations (6.3) and (6.11) as functions of altitude

$$g(z) = g_o \left(\frac{Re}{Re+z}\right)^2 \qquad (6.13)$$

$$n(z) = n(z_o)e^{-\frac{dz}{H(z)}} \qquad (6.14)$$

then the remaining term needing to be defined as a function of altitude is temperature. Completing this will give us a set of equations which will determine atmospheric density as a function of altitude for a given flux.

6.2 Averaged exospheric temperature

Jacchia has derived a general relationship between the 10.7 cm solar flux (F10.7) and the night time exospheric temperature.[15] This relation is

$$T_\infty = 379 + 3.24(\bar{F}10.7) \tag{6.18}$$

and does not include a term for the 27 day solar rotation effect. In addition, the day temperature is generally 1.3 times the night temperature, giving

$$T_{\infty d} = 1.3T_{\infty n} \tag{6.16}$$

Now, if we make the assumption that there exists an average exospheric temperature felt by a satellite over one orbit (as outlined in section 4.10), we can make the following derivation. Let us define an average exospheric temperature $\bar{T}_\infty$ where

$$\bar{T}_\infty = \lim_{m\to\infty} \sum_{n=1}^{m} f(\theta)\,\frac{1}{n} \tag{6.17}$$

where n is the number of temperature measurements we take and $f(\theta)$ is a function of the location around the orbit where we take the n_{th} measurement. Refer to Figure 6.2. If we now let each n_{th} increment be less than an integer value such that $\lim|n_{i+1} - n_i| \to 0$ and if we start at $n = 0$ and let $m = \pi$, then we can write

$$\overline{T_\infty} = \frac{1}{\pi} \int_0^\pi f(\theta)\, d\theta \qquad (6.18)$$

At this point we define $f(\theta) = A(\sin B\theta + 1)$ by the following reasoning: we can intuitively see that $f(\theta)$ will vary according to a sine function since T_∞ is at a minimum for $\theta = 0$ (the minimum temperature point in the night section of the orbit) and a maximum at $\theta = \pi$ (for the temperature maximum during the day portion of the orbit). But we also know that the temperature is not 0 at $\theta = 0$. Instead it is a definite value, which we call A here. This means that to the sine function we must add 1 such that when $\theta = 0$, the

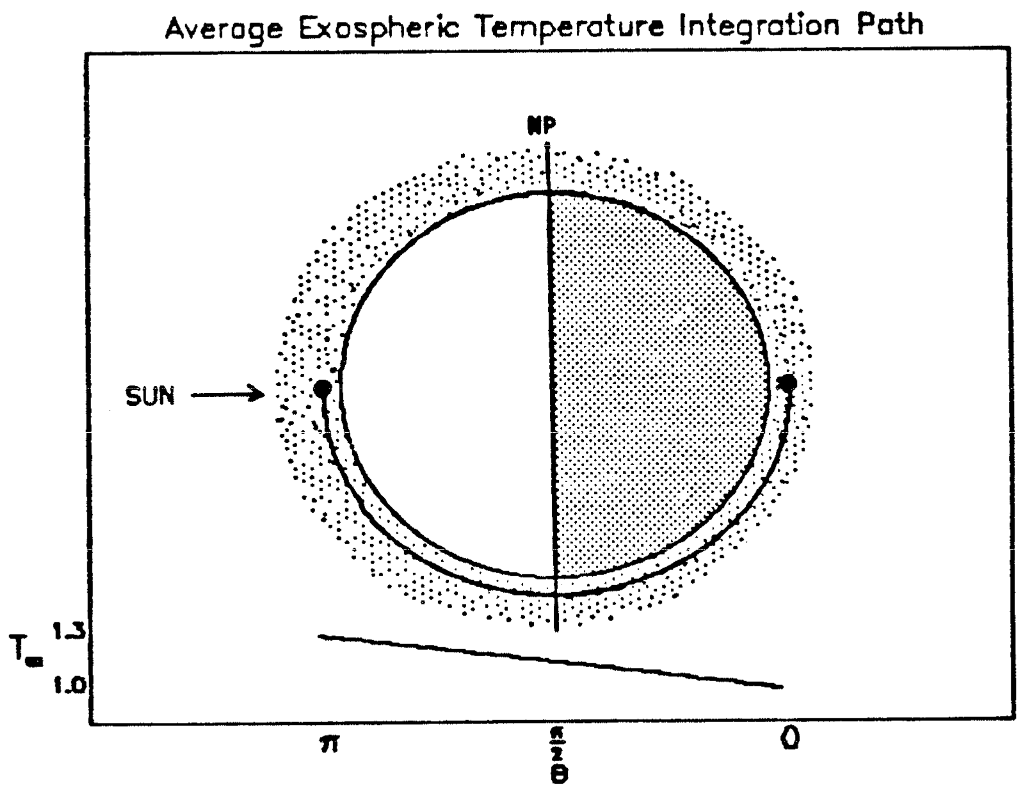

Figure 6.2 The schematic shows the Earth, the atmosphere in day and night, and one-half the SME orbit. The lower plot depicts the change in exospheric temperature as θ changes (the satellite position) from a value of 1.0 times the temperature (night) to 1.3 times the temperature (day). This schematic depicts the integration path for the average exospheric temperature calculation.

temperature equals the minimum constant value A. On closer inspection, A is simply Jacchia's formula for a specified F10.7 or A = 379 + 3.24($\bar{F}$10.7). Therefore, the initial offset and amplitude of the function are just A.

Now, we also know that the maximum temperature for the day part of the orbit is not twice the night temperature, but a value around 1.3 times the night value. Hence, we see that when $\theta = \pi$, the result in the sine function must equal 0.3 to be added to the 1 we have already included. By allowing the constant B to equal a shaping constant for the sine function, we solve the equation $\sin B\pi = 0.3$ and find that B = 0.09699. We now define the following relations

$$\bar{T}_\infty = \frac{1}{\pi} \int_0^\pi f(\theta)\, d\theta \tag{6.18}$$

$$f(\theta) = A(\sin B\theta + 1) \tag{6.19}$$

$$0 \leq \theta \leq \pi$$

$$A = 379 + 3.24(\bar{F}10.7) \tag{6.20}$$

$$B = 0.09699 \tag{6.21}$$

and therefore by substitution and integration

$$\overline{T_\infty} = \frac{1}{\pi} \int_0^\pi A(\sin B\theta + 1)\, d\theta \tag{6.22}$$

$$= \frac{A}{\pi}\{\int_0^\pi \sin B\theta \, d\theta + \int_0^\pi d\theta\}$$

$$= \frac{A}{\pi} \{- \frac{1}{B} \cos B\theta \Big|_0^\pi + \theta\Big|_0^\pi\}$$

$$= \frac{A}{\pi} \{ - \frac{1}{B} \cos B\pi + \frac{1}{B} + \pi\}$$

$$= \frac{A}{\pi} \{\frac{1-\cos B\pi + B\pi}{B}\} \tag{6.23}$$

or by substituting A and B, we find, where $f = \bar{F}10.7$

$$\bar{T}_\infty = \frac{(379 + 3.24f)\ (1 - \cos[0.09699\pi] + [0.09699\pi])}{0.09699\pi}$$

$$\overline{T_\infty} = (379 + 3.24f)\ (1.15) \tag{6.24}$$

This is our equation describing an average exospheric temperature between the lowest and highest temperatures in an orbit. It is not too hard to see that integrating from the maximum to the minimum, we will also get the same temperature.

This result is valid over a full orbit. However, our iteration step is a little bigger than this - actually one day. The F10.7 we use in the model is the flux over that day, and thus we are extending the assumption of an average exospheric temperature over one orbit to be generally the same temperature over one day. This assumption is valid if we assume that the solar flux will not jump drastically in one day. The monthly averages in the flux prediction and the interpolated values to the day of the month insure that assumption.

In completing our set of equations describing thermospheric temperature at a specific altitude, T(z), we remember from the substitutions leading to equation 6.14 that a similar result can be achieved for T(z).

$$p = nkT \tag{6.1}$$

$$T_o = \frac{p_o}{n(z)k} \tag{6.25}$$

$$p = p_o e^{-[(z-z_o)/(kT/mg)]} \tag{6.8}$$

$$n(z)\ kT(z) = p(z) \tag{6.26}$$

$$T(z) = \frac{p}{n(z)k}\ e^{-\frac{(z-zo)}{(kT/mg)}} \tag{6.27}$$

Setting this result aside for a moment, let us think of the temperature in the thermosphere in a little different way. Let us say that there is a relationship between the change in temperature with altitude and the actual temperature we measure. This, of course, is reasonable. Mathematically, we may write this as

$$\frac{dT}{dz} = \sigma T(z) + A \tag{6.28}$$

where σ is a shaping parameter and A is an arbitrary constant. The solution for this first order nonhomogenous differential equation is just

$$T(z) = -Ce^{-\sigma(z-zo)} + A \qquad (6.29)$$

where we have defined $z = z - z_0$. Evaluating this solution at the boundary conditions of $T = T_0$ at $z = z_0$ and $T = T_\infty$ at $z = \infty$, we arrive at the following solution

$$T(z) = T_\infty - (T_\infty - T_0)\ e^{-\sigma(z-zo)} \qquad (6.30)$$

where $A = T_\infty$ and $C = T_0 - T_\infty$. This equation we can use in our iteration to determine the mass density of a species.

σ is a shaping parameter for the above equation, and it is also simply a ratio of the change in temperature over the total temperature interval if we think about it physically. In other words, to make this a dimensionless term and to let the change in temperature over the change in altitude approach 0 as the altitude increases to infinity, we let[16]

$$\sigma = \frac{\frac{dT}{dz}}{T_\infty - T_0} \qquad (6.31)$$

We note that σ has the units of m^{-1} which is the same as H^{-1}.

6.3 Upper atmosphere composition and number density

In referencing standard sources[17], we find that the upper atmosphere (thermosphere) is composed of neutral and ion species.

Included in these are the consituents listed in section 4.7.4. There, we also made the assumption that the thermosphere, in the region relevant to SME, consists of only three constituents (O^+, N_2^+ and O_2^+). In Table 6.2, we can see the atomic mass and number density at 120 km for each of these.

Thermosphere Composition

Species	At/Mol Wgt	Number density (120 km)
O^+	16	7.69E+16
N_2^+	28	2.98E+17
O_2^+	32	3.38E+16

Table 6.2 Composition of the thermosphere.

6.4 10.7 cm solar flux - predicted

The computer algorithm used to generate the first 33 months of F10.7 values are based upon a curve fit to the data points discussed in section 10.1 below. A VAX 780 Interactive Data Language library routine POLY_FIT fits the actual monthly F10.7 averages to a least squares polynomial. In our case, a cubic curve fit was used. The output of this function provides a coefficient vector for the curve as well as a vector of calculated values.[18]

The algorithm used to compute the F10.7 predicted values is a series of cubic and quadratic curve sections. They are matched at the endpoints to produce a single curve for the best predicted value and for each of the one standard deviation lines in Figure 6.3. The general equation and coefficients for each section are reproduced in Table 6.3 below. Following the definition of each curve section, data points are generated for every month in the time period covered by that curve. Refer to section 8.2 for additional discussion on this topic.

Monthly values for both the actual and predicted F10.7 data are then stored in a common table for later access in the processing.

F10.7 Best Estimate Curves

Time frame	Months	Values of t	Equation f(t)
Jan 82 – Nov 86	59	1–59	$f = -3.33831E{-5}(t)^3 + 4.08119E{-2}(t)^2 - 4.4542(t) + 193.92$
Dec 86 – Dec 87	13	60–72	$f = f(59)$
Jan 88 – Apr 91	40	73–112	$f = -0.0023(t-72)^3 + 0.13812(t-72)^2 + 66.337$
May 91 – Dec 92	20	113–132	$f = f(112)$
Jan 93 – Apr 99	76	133–208	$f = 0.00034(t-132)^3 - 0.03895(t-132)^2 + 140.0$
May 99 – Aug 02	40	209–248	$f = -0.00338(t-208)^3 + 0.2025(t-208)^2 + 65.0$

Table 6.3 Curve fit equations to solar cycle 22 flux. Best estimate prediction curves.

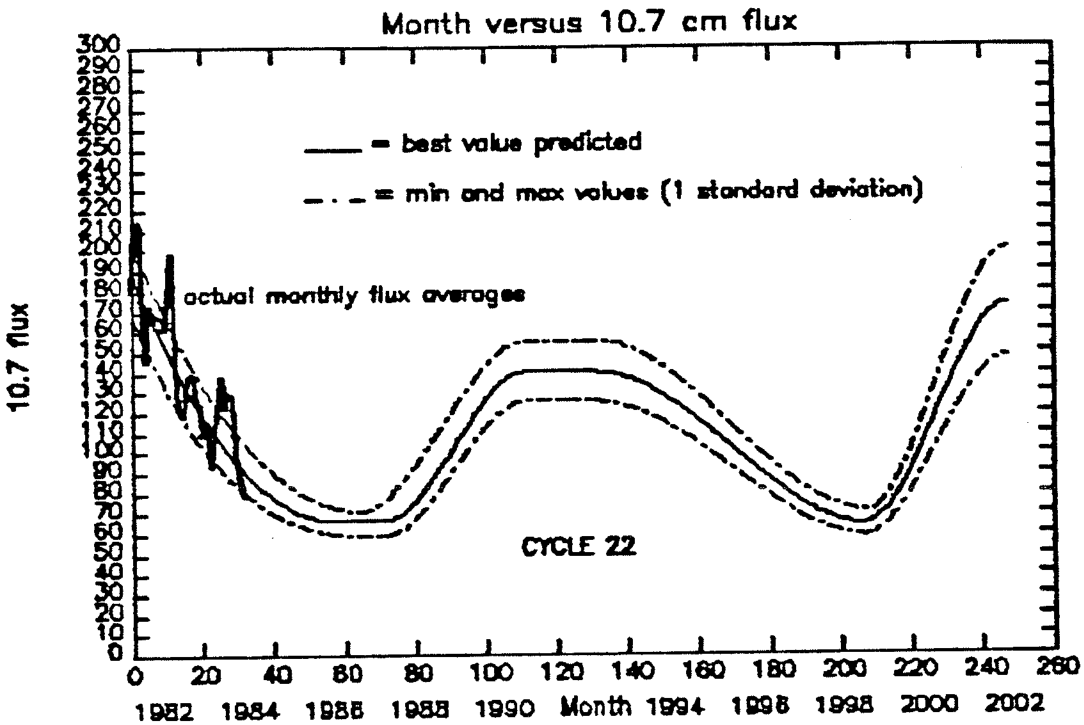

Figure 6.3 The best estimate and one standard deviation plot of the F10.7 versus month of year from January 1982. The actual monthly F10.7 averages are over-plotted for the first thirty-three months. The time span of the prediction covers solar cycle 22 and is based upon the predicted R_Z (sunspot) index by H.H. Sargent of NOAA.

CHAPTER VII

DERIVATION OF SATELLITE AREA AND C_d

7.1 SME effective area

7.1.1 Assumptions

A close approximation to the effective area of SME can be derived analytically. The effective area may be determined if we make the following assumptions.

First, we can imagine that there is a "shadow" created upon the bus of the spacecraft by the solar array preventing particles in the upper atmosphere from impacting upon SME. See Figure 7.1.

Next, we can assume that the particles in the upper atmosphere which impact upon SME have random motion. Therefore, the sum total of all their velocity vectors will cancel out in all directions, leaving only the single vector opposite to the direction of SME's velocity.

Third, we can develop a simplified model of SME. We will let the solar array be a circular flat plate with a slot cut out and the bus be a cylindrical unit with no supporting struts. The observatory module (OM) can be modeled as a cylindrical unit with a height to the tip of the radiative cooler and the diameter of the widest cross-section of the OM (i.e., the antenna stand is ne-

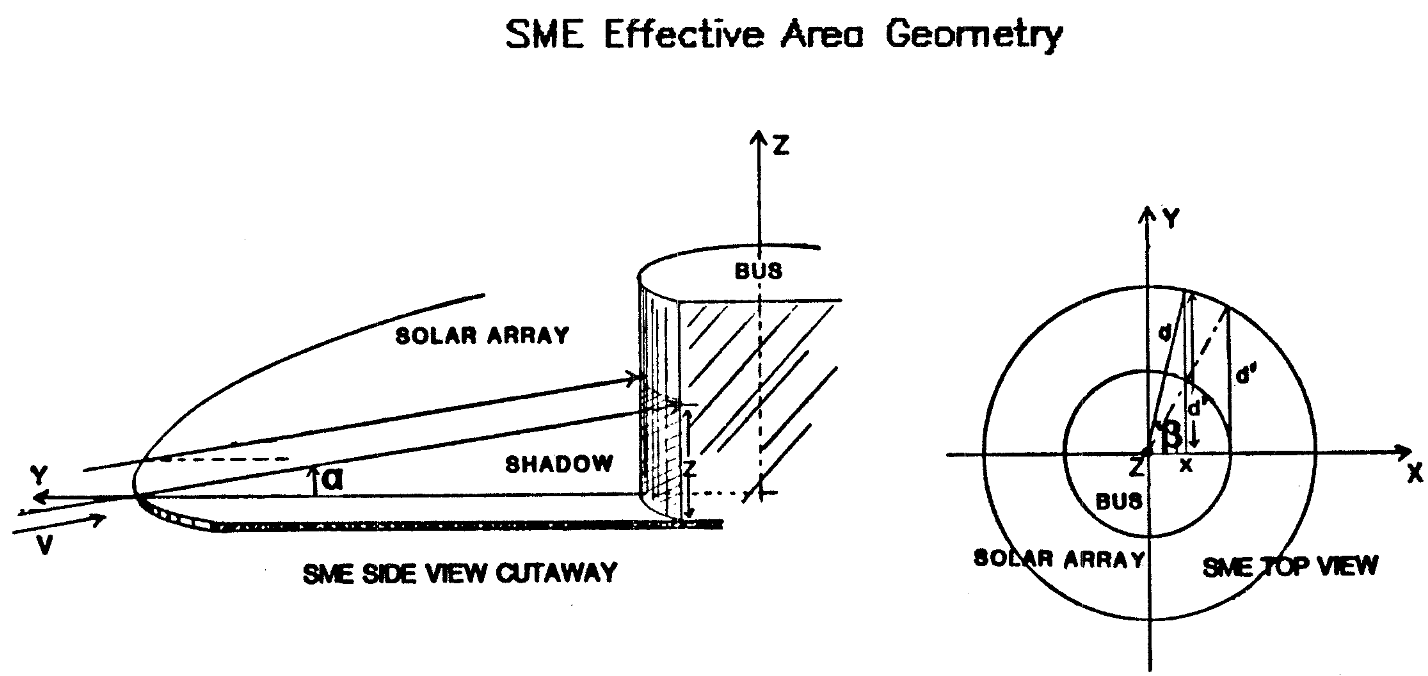

Figure 7.1 Geometry for the "shadow" area upon the SME bus created by the solar array blockage of upper atmosphere particles. Side view and top view.

glected). Finally, in this geometry, we will assume that particles passing through the slot in the solar array do not hit the bus or OM. Refer to Figure 1.1b.

7.1.2 Derivation of effective area

From Figure 7.1, we can see that the general relations are

$$r + d = R \tag{7.1}$$

$$R\cos\beta = x \tag{7.2}$$

$$R\sin\beta = y + d' \tag{7.3}$$

$$dx = -R\sin\beta \, d\beta \tag{7.4}$$

$$\beta = \cos^{-1}(x/R) \tag{7.5}$$

$$x^2 + y^2 = r^2 \tag{7.6}$$

$$y = \sqrt{r^2 - x^2} \qquad 7.7)$$

$$x^2 = R^2\cos^2\beta \tag{7.8}$$

$$d' = R\sin\beta - \sqrt{r^2 - x^2}$$

$$= R \sin(\cos^{-1} \frac{x}{r}) - \sqrt{r^2 - x^2} \qquad (7.9)$$

$$z = d' \tan\alpha$$

$$= [R \sin(\cos^{-1} \frac{x}{r}) - \sqrt{r^2 - x^2}] \tan\alpha \qquad (7.10)$$

Now, if we let $z = f(\alpha,x)$, we can define the shadow area of the solar array on the bus, the bus on the OM or the solar array on the OM as

$$A_s = \int_A f(\alpha,x)dA$$

$$= \int_\alpha \int_x f(\alpha,x)dxd\alpha \qquad (7.11)$$

or by substitution of equation (7.10)

$$A_s = \int_\alpha \int_x \tan\alpha \, [R \sin(\cos^{-1} \frac{x}{r}) - \sqrt{r^2 - x^2}] \, dxd\alpha \qquad (7.12)$$

If we allow α to vary from 0 to α and x to vary from -r to +r then

$$A_s = \int_0^\alpha \tan\alpha \int_{-r}^{+r} [R \sin(\cos^{-1} \frac{x}{r}) - \sqrt{r^2 - x^2}] \, dx \, d\alpha \qquad (7.13)$$

or

$$A_s = \int_0^\alpha \tan\alpha \, \{2\int_0^r [R \sin(\cos^{-1} \frac{x}{r}) - \sqrt{r^2 - x^2}] \, dx\} d\alpha \qquad (7.14)$$

This then gives us the effective area if we take the initial calculated area of the satellite A_i and subtract off the shadow area

$$A_{eff} = A_i - A_s \qquad (7.15)$$

For a given roll/yaw angle of SME, which gives us our α, we can then determine the satellite effective area by analytic evaluation of the integral or by numerical integration. See Figure 7.2, for the results of this work.

7.1.3 Determination of constant effective area

The above method would work great for determining the SME effective area if the coupled roll/yaw angle remained constant throughout the orbit. However, the complication here is that the SME roll/yaw angle varies from a maximum roll near the equator crossing to a maximum yaw at the pole each orbit. These maximum values themselves vary over time and are dependent on maintaining the SME sun angle (beta angle). See Figure 7.3. With some work, the relationship of the orbit position to effective area could be determined as well as a more specific average area which varied through a longer time period. This was not done here, however, due to the good results in the empirical data.

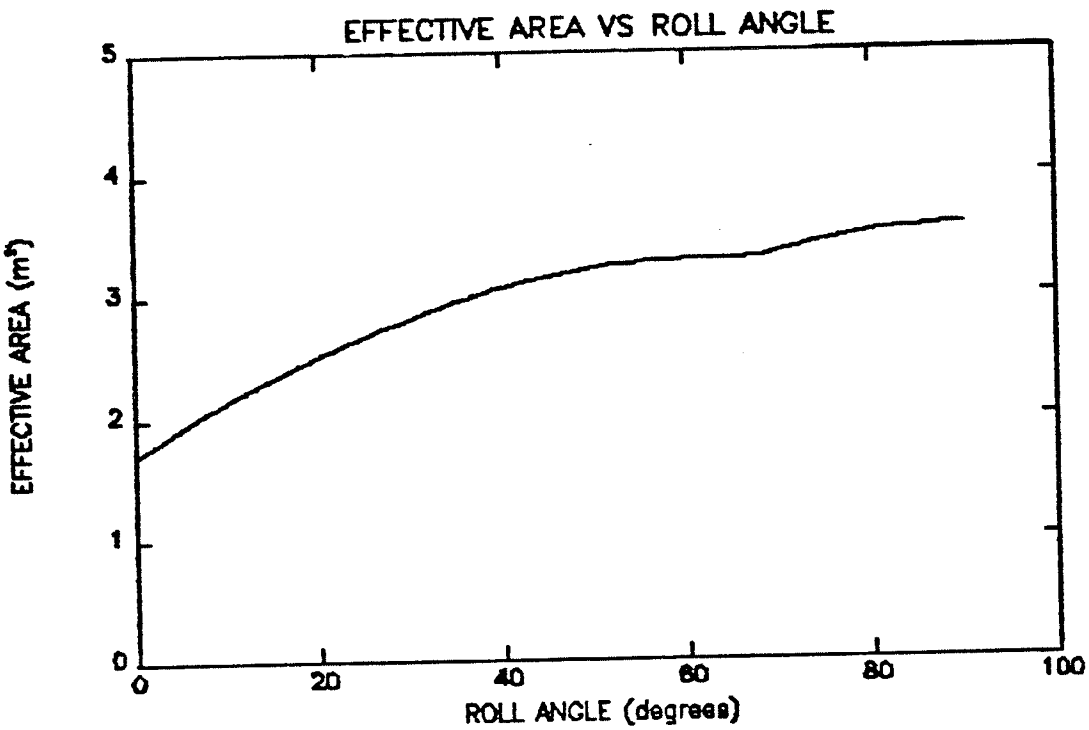

Figure 7.2 Effective SME area (analytic results) plotted as a function of roll angle (in degrees). The minimum and maximum points are approximately 1.6 m^2 and 3.6 m^2, respectively.

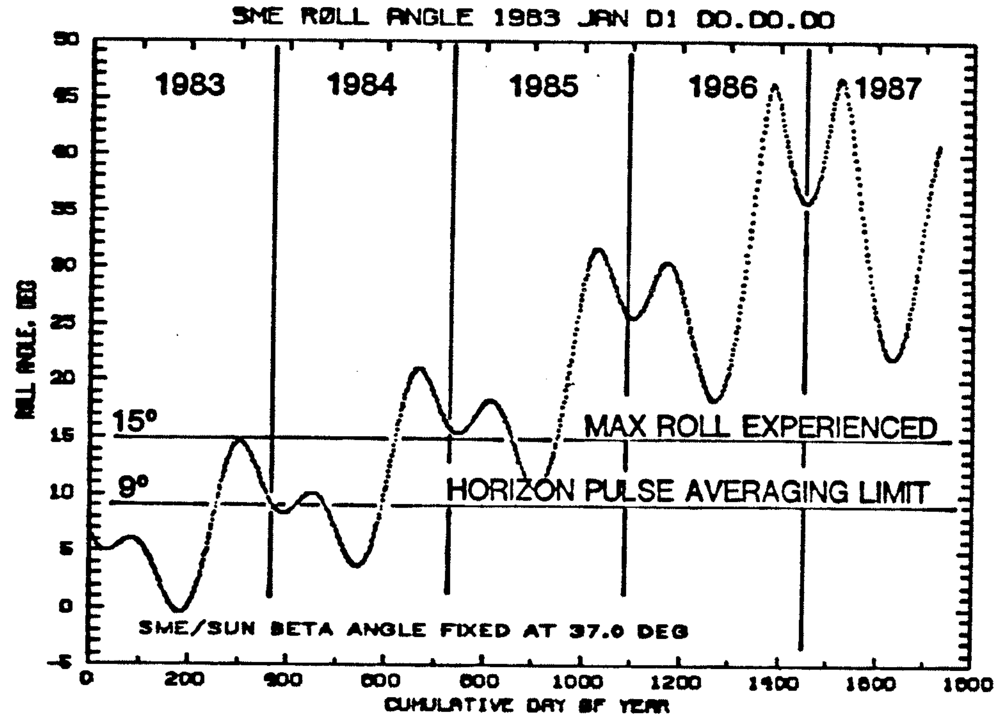

Figure 7.3 The predicted variation in the SME roll angle over the cumulative day of year, beginning January 1, 1983. The sun angle is fixed at 37.0 degrees. This plot represents the maximum roll angle experienced by SME over an orbit and the reader should remember that the same "minimum" angle will also be achieved each orbit. An example maximum roll experienced is indicated for the end of 1983. (Courtesy SME Flight Dynamics group).

Instead, the effective area of SME was assumed to be between the range of 1.6 and 3.6 m^2, as shown in Figure 7.2. The value of 2.0 m^2 was chosen because it is a reasonable, lower end estimate, given the smaller roll angle SME has experienced over the past three years and because that value fits empirically with the actual data.

7.2 Determination of the coefficient of drag C_d

It is reasonable to assume that the C_d is located at a value between 1 and 2, as mentioned above in section 4.13. By comparing various C_d's in the predicted data versus the ephemeris data, the best C_d was determined to be 1.25.

It should be noted that the value used by Goddard Space Flight Center (GSFC) for the effective area is 1.129 m^2. They also use a C_d of 2.3. Their value of $C_dA_{eff} = 2.5967 \approx 2.6$, whereas the numerical value of the same product used in this model is 2.5. In general then, the same constant is used, but with different terms.

CHAPTER VIII

ERROR ANALYSIS

8.1 Method

An error analysis of the prediction of SME altitude change over time is important to the overall understanding of the orbit decay problem. The method of first determining a best value and then determining the uncertainty is used. The Table 8.1 below gives the general equations which can be used for determining error propagation.

The best value of the orbit radius and thus the altitude is determined from the best values of two independent variables: the F10.7 over solar cycle 22 (which gives us mass density at a specified altitude) and the effective satellite area. The general equation describing the value of the radius r is

$$r = r_b \pm \delta r \tag{8.1}$$

where r_b is the best value of the radius and δr is the uncertainty in the radius. δr can be defined as

$$\delta r = \frac{\Delta r}{|r_b|} \tag{8.2}$$

Error Analysis

Uncertainty in products (8a & 8e)

$$q = x(\ldots)z \qquad\qquad q = Bx$$

$$\frac{\delta q}{q} = \sqrt{\left(\frac{\delta x}{x}\right)^2 + \ldots + \left(\frac{\delta z}{z}\right)^2} \qquad\qquad \delta q = |B|\,\delta x$$

Uncertainty in a function of one variable (8b)

$$q = f(x)$$

$$\frac{\delta q}{q} = \left|\frac{dq}{dx}\right| \delta x$$

Uncertainty in a power, n (8c)

$$q = x^n$$

$$\frac{\delta q}{|q|} = |n|\,\frac{\delta x}{|x|}$$

Uncertainty in a sum (8d)

$$q = x + \ldots + z$$

$$\delta q = \sqrt{\delta x^2 + \ldots + \delta z^2}$$

Table 8.1 General equations defining uncertainty.

The total uncertainty δr can be determined by summing in quadrature the individual uncertainties of the above factors. This technique can be used if one can reasonably show that the errors in the values are random and independent of one another.[19] First, the values of F10.7 (and subsequently density) and effective area come from independent and separate sources. Second, random error in area can be approximated by the sinusoidal variation of area during an orbit. Random error in F10.7 can be approximated by the undetermined oscillations of the daily flux about the monthly average. Therefore, we can safely use this method for determining the total uncertainty in the altitude. Double precision and REAL

16 computation is carried out to minimize machine bias. This is particularly true with the density uncertainty which has terms on the order of 1E-22. When we determine an uncertainty by summing in quadrature, we use

$$\delta q = \sqrt{\delta x^2 + \ldots + \delta z^2} \qquad (8.3)$$

where δx, ..., δz are the uncertainties of the individual quantities.

8.2 F10.7 best value and uncertainty

The best value of the F10.7 data comes from a set of predicted values defined by a series of minimum and maximum points matched in cubic equations. The first segment in the series making up the curve originally was a cubic fit to the monthly averaged flux over 36 months (January 1982 - December 1984). That curve was then extended for 23 more months to achieve a minimum point (November 1986) at the lowest expected values approaching solar minimum. For the following 5 segments the minimum/maximum points were chosen in time and amplitude to correspond with the general forecast by H.H. Sargent of NOAA, described in section 10.1 below. Referencing Table 8.2 reproduced here from section 6.4 above, we have the empirically determined equations describing the F10.7 best value curves.

For the error in the monthly averages of F10.7 during the

F10.7 Best Estimate Curves

Time frame	Months	Values of t	Equation f(t)
Jan 82 – Nov 86	59	1–59	$f = -3.33831E{-5}(t)^3 + 4.08119E{-2}(t)^2 - 4.4542(t) + 193.92$
Dec 86 – Dec 87	13	60–72	$f = f(59)$
Jan 88 – Apr 91	40	73–112	$f = -0.0023(t-72)^3 + 0.13812(t-72)^2 + 66.337$
May 91 – Dec 92	20	113–132	$f = f(112)$
Jan 93 – Apr 99	76	133–208	$f = 0.00034(t-132)^3 - 0.03895(t-132)^2 + 140.0$
May 99 – Aug 02	40	209–248	$f = -0.00338(t-208)^3 + 0.2025(t-208)^2 + 65.0$

Table 8.2 Curve fit equations to solar cycle 22 flux. Best estimate prediction curves (from Table 6.2).

initial 36 months of data, one standard deviation was used where

$$\sigma_f = \sqrt{\frac{1}{35} \Sigma(F_m - F_c)^2} \qquad (8.4)$$

where F_m is the monthly F10.7 value and F_c is the curve fit value. These uncertainty curves were extended another 29 months to a point near solar minimum for cycle 21 (May 1987). There, the minimum points for the upper and lower limits lines were established and new curves fit to those points. Table 8.3 gives the empirically determined equations describing both of the F10.7 one sigma curves. The minimum/maximum points in the uncertainty curves over cycle 22 were chosen to match an estimated one standard deviation error, based on the magnitude of the deviations from averages of

F10.7 One Sigma Curves

Time frame	Months	Values of t	Equation f(t)
Jan 82 – May 87	65	1–65	
			$f_{min} = -0.000204(t)^3 + 0.053302(t)^2 - 4.34(t) + 172.0$
			$f_{max} = -0.000029(t)^3 + 0.03626(t)^2 - 4.34(t) + 208.0$
Jun 87 – Apr 91	47	66–112	
			$f_{min} = -0.00206(t-65)^3 + 0.12375(t-65)^2 + 59.0$
			$f_{max} = -0.00162(t-65)^3 + 0.11408(t-65)^2 + 71.0$
May 91 – Dec 92	20	113–132	
			$f_{min} = f(112)_{min}$
			$f_{max} = f(112)_{max}$
Jan 93 – Apr 99	76	133–208	
			$f_{min} = 0.0003(t-132)^3 - 0.03428(t-132)^2 + 125.0$
			$f_{max} = 0.00039(t-132)^3 - 0.04415(t-132)^2 + 155.0$
May 99 – Aug 02	40	209–248	
			$f_{min} = -0.00275(t-208)^3 + 0.165(t-208)^2 + 59.0$
			$f_{max} = -0.00408(t-208)^3 + 0.24375(t-208)^2 + 70.0$

Table 8.3 Curve fit equations to solar cycle 22 flux. One sigma prediction curves.

previous even number cycles.

These two tables of equations provide the set of best data and uncertainty for the subsequent density calculations.

8.3 Density best value and uncertainty

We initially note that mass density is a function of the two independent variables altitude and solar flux. Other variables of temperature, gravity, scale height and number density are all dependent variables. Altitude is given in the iteration with no uncertainty and therefore can be treated as a constant for each step in the iterative process. This simplifies our problem of finding the uncertainty in the mass density of each species. Now we simply find the best value and the uncertainty based solely on the flux, f. The fractional uncertainty in a function of one variable $\rho(f)$ is

$$\frac{\delta\rho}{\rho} = \left|\frac{d\rho}{df}\right| \delta f \tag{8.5}$$

where ρ is density, $\delta\rho$ is the uncertainty in density and δf is the uncertainty in the flux. Knowing δf and being able to take the first derivative of ρ with respect to f, we can solve this equation analytically for a given flux and altitude.

$$\delta\rho = e^{(P+K)} \delta f \tag{8.6}$$

However, the equation is quite cumbersome since

$$A = 1.15(379 + 3.24f)$$

$$P = \frac{-m_i g(z)dz}{1000\ k} \left\{\frac{1}{A-[A-To]e^{\left(-\frac{dT}{dz}(z-zo)/(A-To)\right)}}\right\} \tag{8.7}$$

$$K = \ln(n_z m) \tag{8.8}$$

and as such, it is more convenient in an iterative process to find the uncertainty in each individual term step by step. This method of error propagation term by term may lead to slightly greater uncertainty in the final result but is adequate for this analysis.[20] Here, we achieve generally the same results. The computational algorithm uses the following equations to propagate the flux error and arrive at uncertainty in the mass density. See Subroutine error2 in Appendix A for the listing of these equations.

We now proceed to analyze the uncertainty in the thermospheric temperature T(z). Reproducing equation 6.30 here

$$T(z) = T_\infty - (T_\infty - T_0)e^{-\sigma(z-z_0)}$$

we can see that the uncertainty in T(z) is the sum of the uncertainty in the two quantities on the right hand side. The uncertainty in T_∞ is clear and can be written as

$$\delta T_\infty = (3.24)\ (1.15)\delta f = 3.73\delta f \tag{8.9}$$

The second term on the right hand side can be described as follows

$$x = (T_\infty - T_0)e^{-\sigma(z-z_0)} \tag{8.10}$$

where we let

$$y = T_\infty e^{-\sigma(z-z_0)} \tag{8.11}$$

$$z = T_0 e^{-\sigma(z-z_0)} \tag{8.12}$$

The fractional uncertainty in y is the quadratic sum of the fractional uncertainty in the two terms forming the product. Hence, if we let

$$p = e^{-\sigma(z-z_0)} \tag{8.13}$$

and the derivative of p with respect to σ is

$$p' = (z_0-z)e^{-\sigma(z-z_0)} \tag{8.14}$$

giving the uncertainty in p as

$$\delta p = \left|(zo-z)e^{-\sigma(z-zo)}\right| \delta\sigma \tag{8.15}$$

then by 8(a) above, the fractional uncertainty in term y can be given as

$$\frac{\delta y}{y} = \sqrt{\left(\frac{\delta T_\infty}{T_\infty}\right)^2 + \left(\frac{\delta p}{p}\right)^2} \tag{8.16}$$

or

$$\delta y = y\sqrt{\left(\frac{\delta T_\infty}{T_\infty}\right)^2 + \left(\frac{\delta p}{p}\right)^2} \tag{8.17}$$

and by a similar analysis, the uncertainty in z can by given by

$$\delta z = \left|-To(zo-z)e^{-\sigma(z-zo)}\right| \delta\sigma \tag{8.18}$$

which leads to the uncertainty in x as the quadratic sum

$$\delta x = \sqrt{\delta y^2 + \delta z^2} \tag{8.19}$$

and hence the uncertainty in exospheric temperature T_∞ is

$$\delta T_\infty = \sqrt{\delta T_\infty^2 + \delta x^2} \tag{8.20}$$

We assume there is no uncertainty in gravity, $g(z)$, as a function of altitude, the Boltzmann constant, k, or the mass, m, of the species. We continue then to find the uncertainty in the scale height propagated by the temperature uncertainty. If we let B be a constant defined as

$$|B| = \left| \frac{1000\ k}{m_i\ g(z)} \right| \tag{8.21}$$

then we note from equation 6.12 that the uncertainty in the scale height is just B times the temperature uncertainty, and from 8(e) above

$$H(z) = \frac{kT(z)}{m_i\ g(z)} \tag{6.12}$$

$$\delta H = |B|\, \delta T_\infty \tag{8.22}$$

The conversion factor of 1000 changes the B units from meters to kilometers. By 8(b), we find the number density, starting with equation 6.14 and ending with the uncertainty in the number density. We use the same method as above finding p to determine the density uncertainty

$$n(z) = n(z_o)\ e^{-\frac{dz}{H}} \tag{6.14}$$

$$\delta n = \left| n(z_o)\ \left(\frac{dz}{H^2}\right) e^{-\frac{dz}{H}} \right| \delta H \tag{8.23}$$

Mass density uncertainty is just the constant, m_i, mass of the species times the number density uncertainty, or by 8(e) above

$$\delta\rho = |m_i| \delta n \tag{8.24}$$

and this is the result we wanted to achieve.

8.4 Radius or altitude best value and uncertainty

The uncertainty in the radius and thus the altitude simply follows that same analytic method as in section 8.3. Bearing in mind the general relations 8(a) - 8(e), we will simply write the results which may also be seen in algorithmic form in Appendix A, Subroutine errorl. These equations find the error in the effective area of the satellite and combine that error with the flux initiated error in the density to find the altitude uncertainty.

C_2 is a constant used in the iteration which actually includes error from the area uncertainty. Therefore, the uncertainty in C_2 is just a constant K_2 times the area uncertainty which is analytically known from section 7.1.3 above. K_2 includes π, C_d and satellite mass - see Appendix A, Program Orbit_ decay. Since the area ranges from 1.6 to 3.6 m^2 and the constant area was set at 2.0 m^2, the maximum difference of 1.6 m^2 is a large percent if translated into fractional uncertainty. We probably do not want to do this. It is reasonable to expect the real uncertainty to be much less for two reasons: the roll angle deviation has never gone to its maximum of 90 degrees (which gives us 3.6 m^2) and SME never flies at a constant roll angle deviation relative to the velocity vector. In addition, empirical results over the last 3 years show us the real value of effective area can be 2.0 ±0.1 m^2, given a drag coefficient, C_d, of 1.25. The values compare favorably to the GSFC constants' product of (C_d) (area) = 2.5967 (compared to this study's value of 2.5). In summary, a constant uncertainty in area was set at 0.5 m^2 for this problem. This conservative approach allows us to account for the ±0.1 m^2 uncertainty in the empirical value as well as any greater uncertainty which may arise as the roll angle deviation increases with time. See Chapter 7 for a more detailed discussion on this. Here, we have the relation for the uncertainty in the area term

$$C_2 = K_2 \text{ (area)} \tag{8.25}$$

$$\delta C_2 = |K_2| \ \delta\text{area} \tag{8.26}$$

where $K_2 = 3000\pi C_d/\text{mass}$.

The uncertainty in the radius, needed during the calculation of the orbit period uncertainty during the iteration, is simply the uncertainty from the previous iteration propagated one more step. The initial uncertainty in the radius is from equation 8(c). This uses the initial uncertainty in the orbit period from the GSFC definitive ephemeris of 0.001 minutes (1E-5 fractional uncertainty). Thus, the following equation

$$\delta r = \left(\frac{2}{3}\right) \left(\frac{\delta P}{P}\right) r \tag{8.27}$$

starts our iteration, and δr is slightly modified each step. If we remember that the uncertainty in the mass density can be found by the process in section 8.3 above, we can subsequently find the total uncertainty in the radius each iteration (or over one day). First, we define our terms by letting

$$r = C_3 P_i^{2/3} \tag{8.28}$$

where P_i is the orbit period in the i_{th} iteration. But the period each iteration is defined as the previous period less the absolute value of the change in period, or

$$P_i = P_{i-1} - |dP| \tag{8.29}$$

$$dP = \dot{P} dt \tag{8.30}$$

$$\dot{P} = C_2 r \rho \tag{8.31}$$

$$P = C_1 \sqrt{r^3} \tag{8.32}$$

By substitution into equation 8.28, the radius can be rewritten as

$$r = C_3 (C_1 \sqrt{r^3} - C_2 r \rho dt)^{2/3} \tag{8.33}$$

By renaming some of these terms to conduct the error analysis, we let

$$x = C_1\sqrt{r^3} - C_2 r\rho dt \qquad (8.34)$$

$$y = C_2 r\rho dt \qquad (8.35)$$

and by 8(a) for the uncertainty in products, the fractional uncertainty in y is

$$\frac{\delta y}{y} = \sqrt{\left(\frac{\delta C_2}{C_2}\right)^2 + \left(\frac{\delta r}{r}\right)^2 + \left(\frac{\delta \rho}{\rho}\right)^2} \qquad (8.36)$$

which then leads us to the uncertainty in x (remembering that δr is the radius uncertainty from the previous iteration)

$$\delta x = \sqrt{\delta r^2 + \delta y^2} \qquad (8.37)$$

and the fractional uncertainty in r

$$\frac{\delta r}{r} = \left|\frac{2}{3}\right| \frac{\delta x}{|x|} \qquad (8.38)$$

Thus, by solving δr which has units of km, it is straightforward to add and subtract this uncertainty to the altitude each iteration to achieve the total altitude uncertainty for each day in orbit. This is the final result we seek. The minimum, best, and maximum values of the altitude are stored in a table for later plotting. The numerical results can be seen in Appendix B, where the program results are tabulated for the entire prediction.

This concludes our error analysis of the SME orbit decay problem.

CHAPTER IX

SME ORBIT DECAY EMPIRICAL DATA

9.1 Justification of the data

In justifying the assumption made above that the variation in F10.7 can be highly correlated with the change in the atmospheric density, we can look at the following results. In Figure 4.7 we note the plot of the 10.7 cm flux versus the total mass density of the atmosphere. The latter is derived from the SME orbit ephemeris data and equation 5.44 which is independent of the 10.7 cm flux. The normalized curves through the data points indicate the positive correlation. When one calculates a correlation coefficient, the value is .9, a value close to the independently derived value of .88 of Lawrence (see Section 11.3).

One should note that the F10.7 values are actual daily values recorded by the National Oceanic and Atmospheric Administration's Space Environment Services Center (NOAA SESC).

A second justification of the data is the correlation between the monthly averaged density using Jacchia's model and the SME derived density for 33 months of operation. See Figure 9.1.

9.2 Empirical results

A result from studying the SME data is the plot of the altitude change over the first thirty-three months. See Figure 9.2.

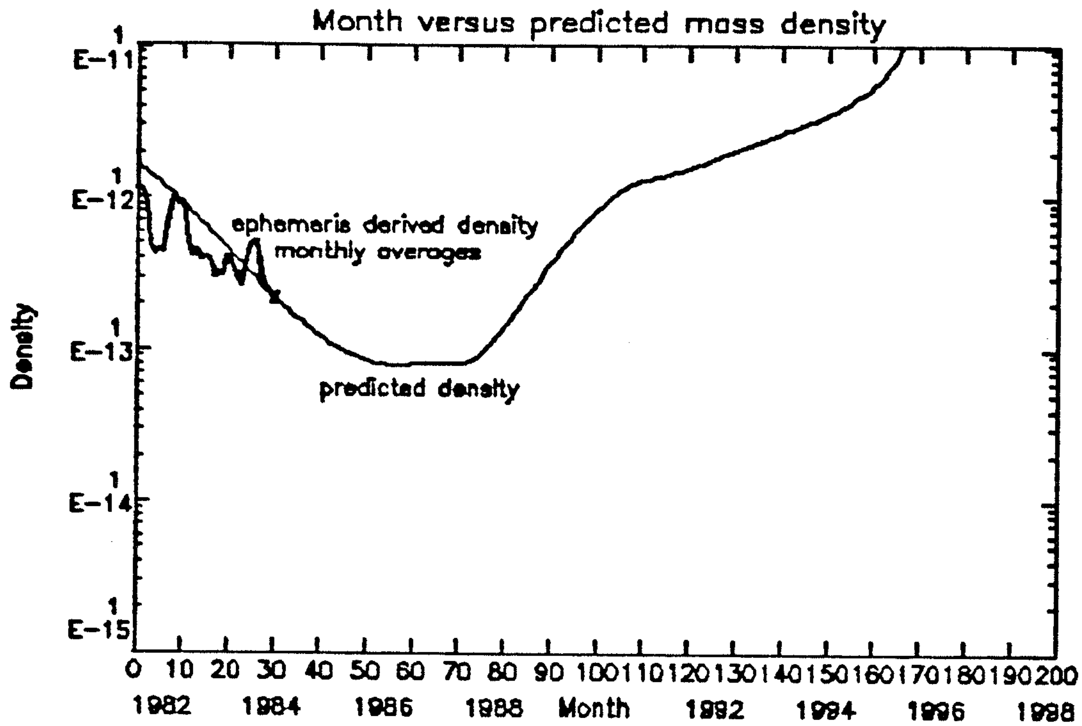

Figure 9.1 Predicted SME observed mass density based upon the predicted F10.7 over solar cycle 22. Overplotted are the SME derived monthly averaged density, based on equation (5.44).

This data was obtained by taking the definitive ephemeris orbit start times, determining the orbit period from this data, and thus deriving the orbit semi-major axis and altitude, assuming a circular orbit. An interesting note on Figures 9.3a and 9.3b is that SME experienced a greater density in the atmosphere at 534 km in early 1982 than at 516 km in late 1984. This seemingly contradictory data can be explained once one realizes the solar activity was at a much higher level in early 1982. The maximum for solar cycle 21 occurred in December 1979, and its effects were still being felt by SME into 1982. Because of this phenomenon, the orbit

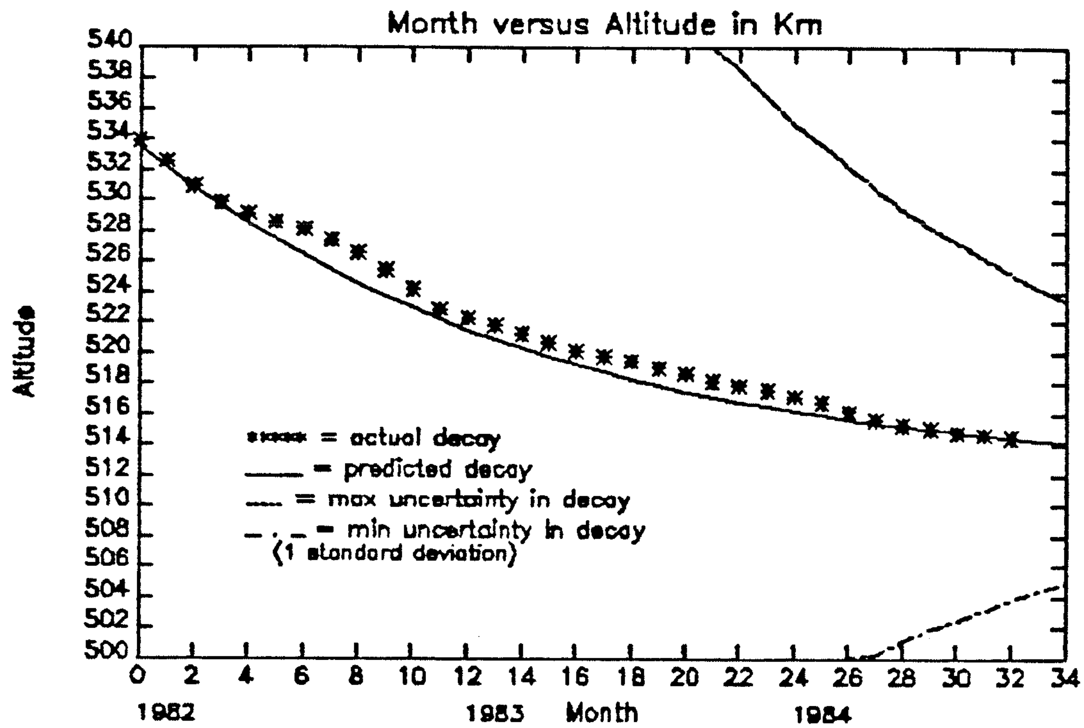

Figure 9.2 Altitude decay of SME over thirty-three months plotted against the predicted altitude decay. [Note: predicted decay does not represent a curve fit to the actual altitude data, but is a result of the derived altitude, starting from the monthly averaged F10.7.]

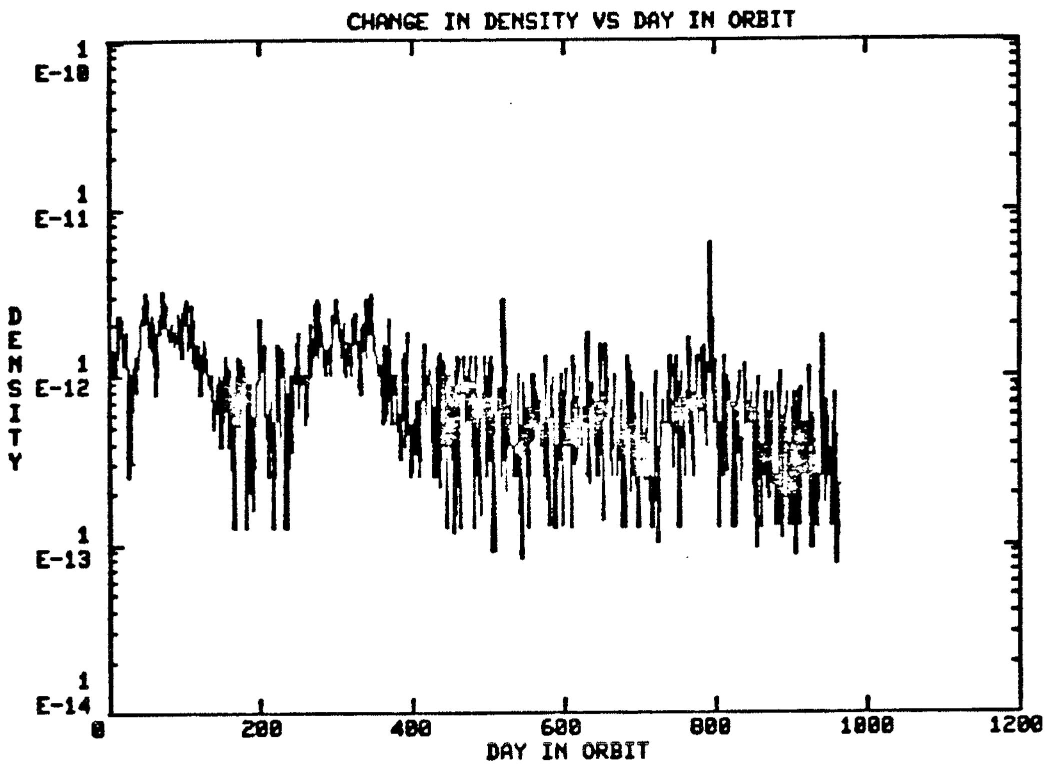

Figure 9.3a Smoothed SME derived mass density from equation (5.44) over thirty-three months between January 1982 and September 1984. Wild points as a result of no ephemeris data for that day were removed, with the previous day's point substituted instead (~ 1% of the data points). Plotted in histogram mode.

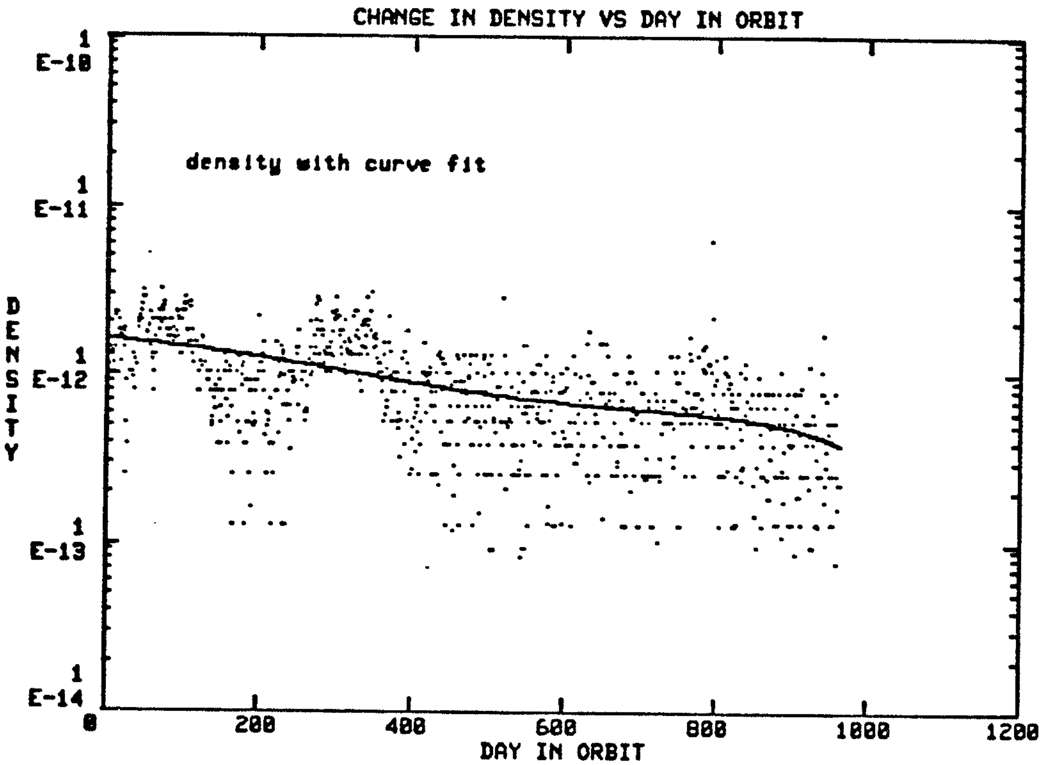

Figure 9.3b Same data as Figure 9.3a, plotted in data point mode with cubic curve fit through the data.

decay rate had a much steeper slope soon after launch, and it has since tended to level off as we approach the minimum of cycle 21.

A second result is the orbit period change and the rate of change over the first thirty-three months of operation. This plot in Figures 9.4a and 9.4b follows a path very similar to that of the altitude change. The slopes are much the same, again due to the solar activity.

Several interesting features appear in the SME data of period versus orbit number. When we improve the resolution of the plot, one notices that the curve defining the period change over

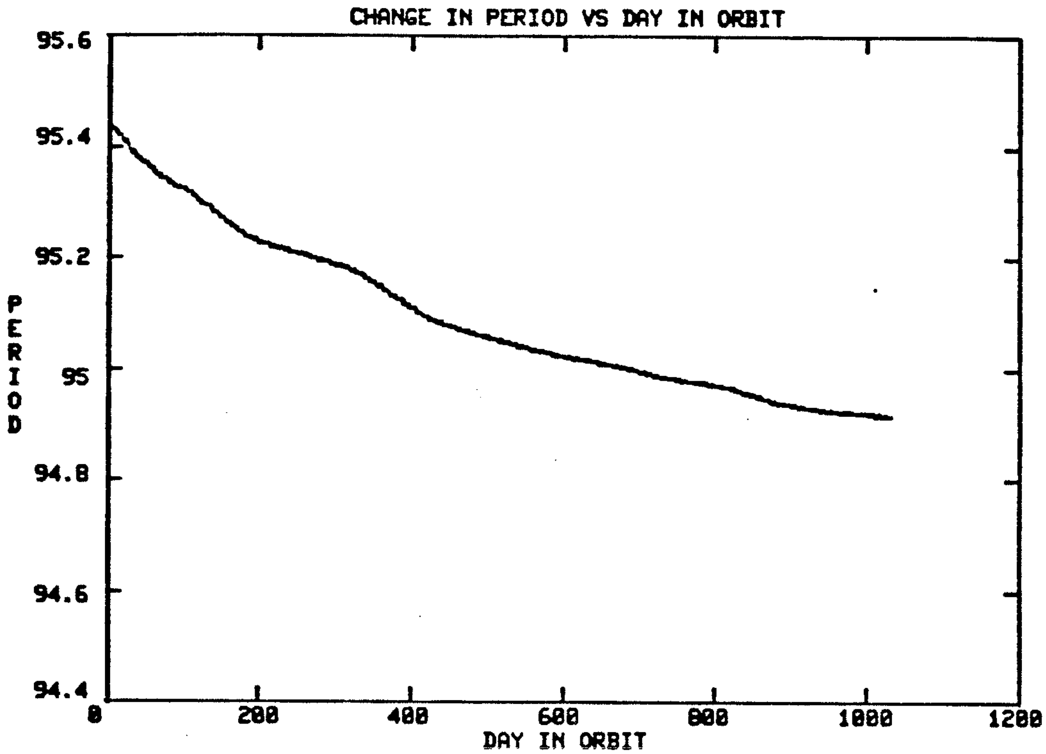

Figure 9.4a Change in period versus day in orbit between January 1982 and September 1984. One point plotted for each day. Period is in minutes.

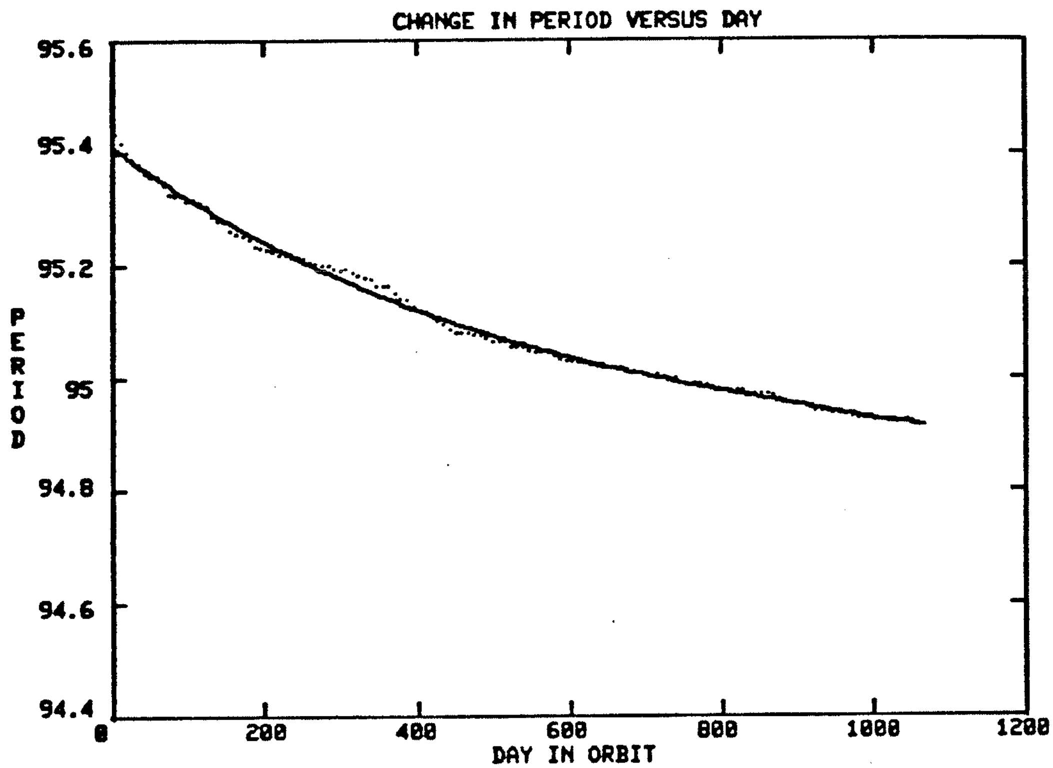

Figure 9.4b Same data plotted as in Figure 9.4a (dotted line) with the curve fit to the data points. Period is in minutes.

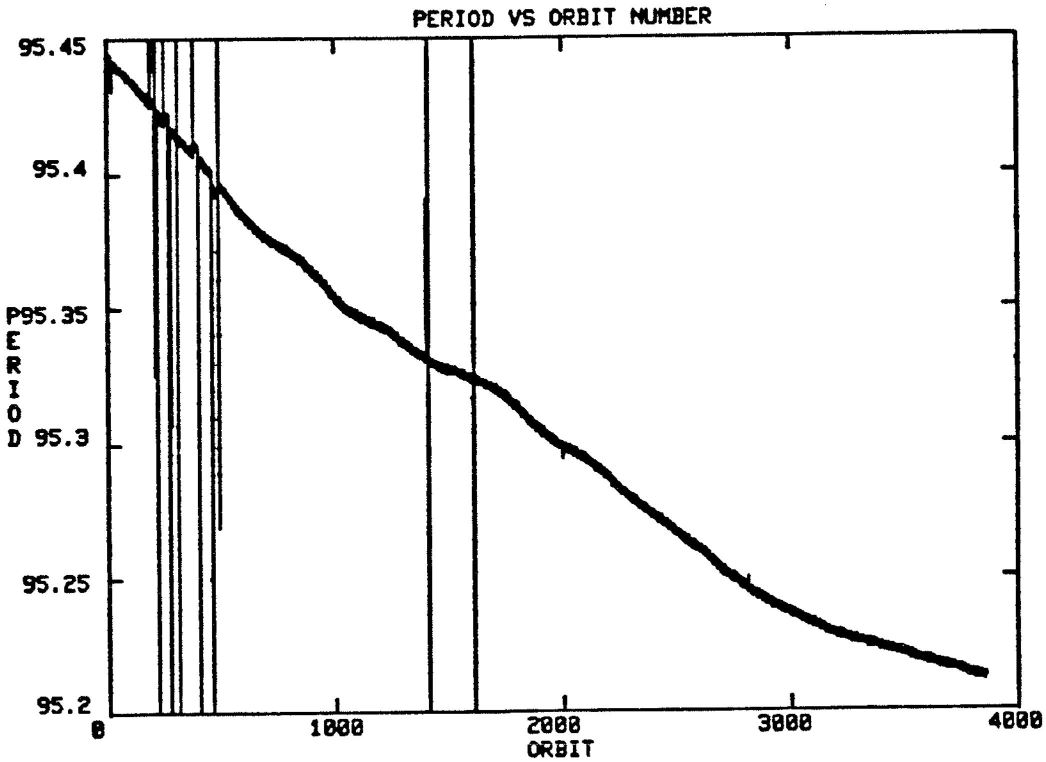

Figure 9.5 Raw data points of period (in minutes) versus orbit number (same time span as Figure 9.4a). Wild points left in. Unsmoothed data shows width to the curve.

time has width to it and is not simply one data point wide. See Figure 9.5. When the plot is expanded to look at the orbit period over fifty orbits, we find that indeed there is a definite perturbation pattern in the SME data. In Figure 9.6, we note that the period of the perturbation is on the order of a half day. There is roughly 150 milliseconds between the maximum and minimum values of the period twice a day (or fifteen data points). This translates to about 0.5 km deviation from the mean radius. It is reasonable to assume that we are looking at the effects of an oblate planet upon SME, and the lumpiness in the gravitational field. This perturbation is on the order of 1E-3, which corresponds to the J_2 term in the harmonic series. Figure 9.7 shows the reference geoid which these terms model.

9.3 Ascending node drift rate

An interesting feature which can be determined from the SME emphemeris data was mentioned earlier in section 4.5.1. From the work of Lawrence, Cowley and Figure 9.8, we can see the general drift of the longitude of the ascending node. This has some relevance to us since the location of the ascending node reflects which section of the atmosphere SME flies through and hence the density profile of the atmosphere.

It was noted earlier that the ascending node Ω was now located near 4 pm local time, having shifted from approximately 3 pm local time at launch. Using equation 4.1 which is reproduced here

$$\dot{\Omega} \approx -9.97\left(\frac{Re}{a}\right)^{3.5}(1-\varepsilon^{2})^{-2}\cos i \qquad (4.1)$$

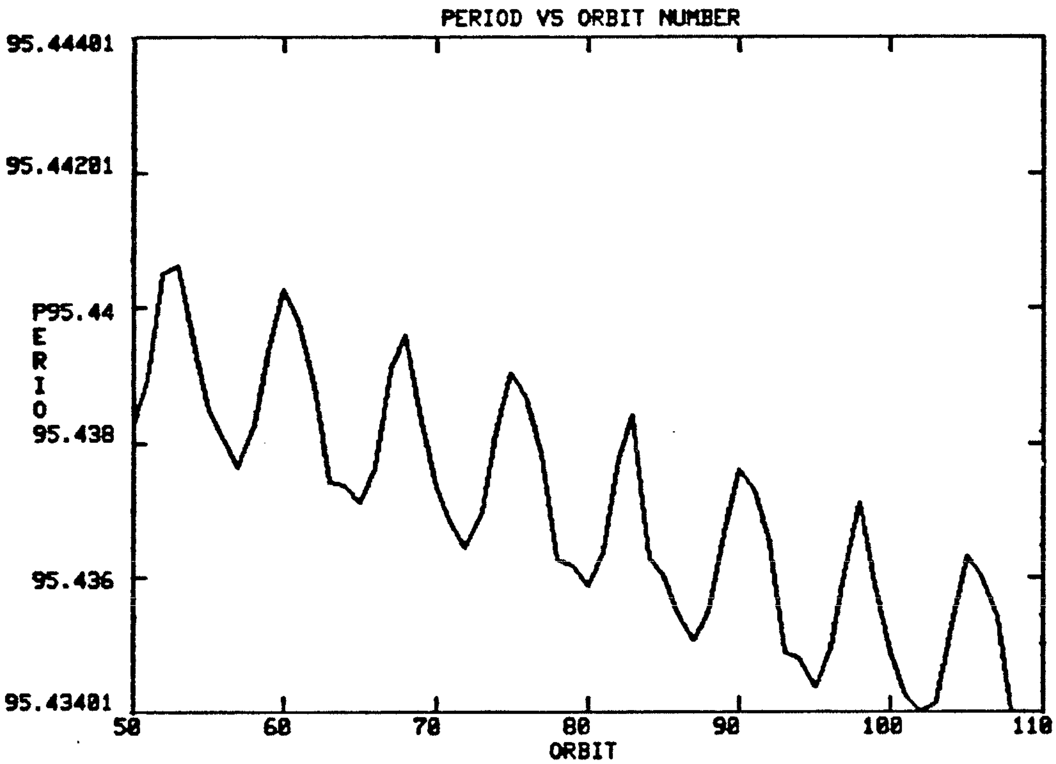

Figure 9.6 High resolution plot of period (in minutes) versus orbit number (50 - 109). There is a periodic variation in the data of approximately one-half day (7^{+} orbits), corresponding to a distance between maximum and minimum of about 150 msecs. This is in the range of one-half km variation in altitude and corresponds to the J_2 term in the harmonic series expansion. Physically, it is the effect of the "lumpy" gravitational field upon SME.

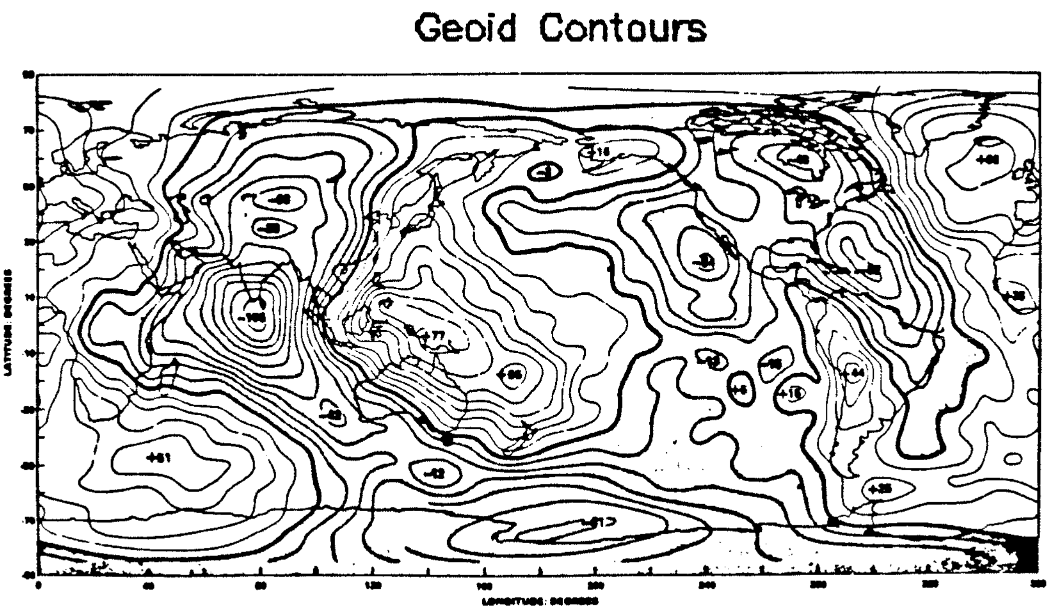

Figure 9.7 Geoid heights form Goddard Earth Model-8 (GEM-8). Contours are at 10 m intervals. The effects of gravitational field represented by this plot can be seen in Figure 9.6. (Reproduced from J. Wertz, "Spacecraft Attitude Determination and Control".)

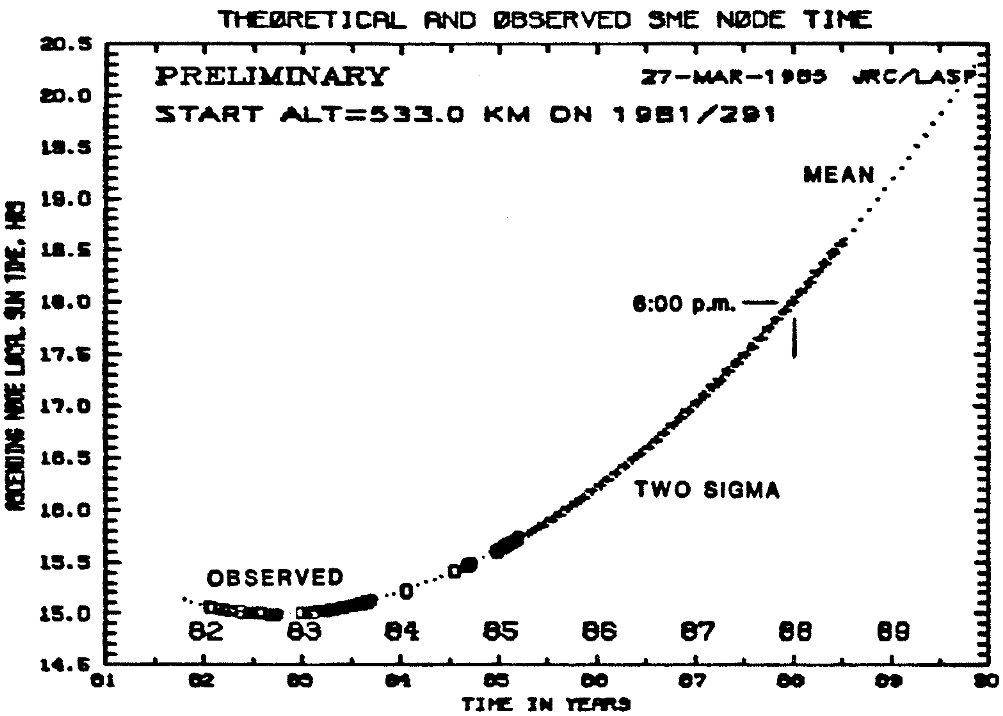

Figure 9.8 The longitude of the ascending node, Ω, both observed and theoretical, plotted as a function of time for SME. (Courtesy of SME Flight Dynamics group).

and using the values listed in Table 9.1 below, we find that the drift rate of Ω in November 1983 was 0.996 degrees per day and in January 1985 was 1.0065 degrees per day. This increase in the drift rate is due primary to the change in the semi-major axis, which is directly related to orbit decay from aerodynamic drag. However, upon further examination, we notice that the second time derivative (acceleration rate) of the ascending node has changed by 2.5E-5 degrees per day per day as a mean value. This term called $\ddot{\Omega}$ includes the time derivative of inclination i (equation 4.2). We remember that this latter equation was an expression of the effect of atmospheric rotation and atmospheric drag upon a satellite. $\ddot{\Omega}$ can be used to determine the contribution of the combined atmosphere rotation and atmospheric drag upon the ascending node precession. Specifically, we have

$$\dot{\Omega} \simeq -9.97\left(\frac{Re}{a}\right)^{3.5}(1-\varepsilon^2)^{-2} \cos i \qquad (4.1)$$

$$\ddot{\Omega} \simeq +9.97 \left(\frac{Re}{a}\right)^{3.5} (1-\varepsilon^2)^{-2} \sin i \frac{di}{dt} \qquad (9.1)$$

from equation 4.1 where the first time derivative of i (equations 4.2 and 4.3) are reproduced here[21]

$$\frac{di}{dt} = f_n \, r \cos u \quad (\mu p)^{-1/2} \qquad (4.2)$$

$$f_n = -\frac{\rho v \delta r \omega}{2F} \sin i \cos u \qquad (4.3)$$

where μ is the Earth gravitational constant, p is the semi-latus rectum of the orbit, $\delta = FSC_d/m$, v is the velocity of the satellite relative to the center of the Earth and ω is the angular velocity of the atmosphere. u is the arc from the ascending node to the satellite nadir position projected on the planet surface. ρ is the density of the atmosphere. We note that $\ddot{\Omega}$ may be a negative, or deceleration term, due to the negative sign from the aerodynamic drag term.

We can rewrite Ω as

$$\Omega = \Omega_0 + \dot{\Omega}_0 t + \frac{1}{2} \ddot{\Omega} t^2 \tag{9.2}$$

In the left hand side equation, we substitute the values from Table 9.1 below. When t = 1205 days (from October 6, 1981 launch to January 23, 1985), the acceleration term contributes about 18 degrees in longitude of ascending node drift eastward (positive direction) from launch to present. If we remember that $360^0/24$ hours = 15^0 for every hour on the equator, we have pretty much demonstrated, to a rough approximation, the main source of drift from SME's initial ascending node crossing time of 3 pm to the present ascending node crossing time of around 4 pm. In other words, aerodynamic drag coupled with the angular velocity of the atmosphere has effected this change. Since atmospheric angular velocity can be assumed constant, any noticeable rate change of this drift in the ascending node is due to change in density as a result of change in solar flux.

This topic can use more study.

Ascending node drift

28 Nov 83		23 Jan 85
a = 6899.610 (km)		a = 6893.848 (km)
ϵ = 0.001		ϵ = 0.001
i = 97.558 °		i = 97.616 °
	R_e = 6378.164 (km)	
	t = 1205 days	

$$\dot{\Omega} \sim -9.97 \left(\frac{Re}{a}\right)^{3.5}(1-\epsilon^2)^{-2} \cos i$$

$$\ddot{\Omega} \sim +9.97 \left(\frac{Re}{a}\right)^{3.5}(1-\epsilon^2)^{-2} \sin i \frac{di}{dt}$$

$$\Omega = \Omega_0 + \dot{\Omega}_0 t + \frac{1}{2} \ddot{\Omega} t^2$$

$\dot{\Omega}$ = 0.996 °/day		$\dot{\Omega}$ = 1.0065 °/day
	$\ddot{\Omega}$ = 2.497E−5 °/day/day	

acceleration term contribution ~ 18 °

Table 9.1 Calculation of the ascending node drift rate.

CHAPTER X

PREDICTIONS FOR ORBIT DECAY

10.1 Predicted solar flux

The driving force in predicting satellite orbit decay is a good model of solar activity. In our case, good estimates of the amplitudes and the time frames for the minimum of cycle 21 and maximum and minimum of cycle 22 are necessary. This study uses the 10.7 cm solar flux as a good indicator of solar activity relative to the Earth's atmosphere. This was outlined in the discussion above relating to basic assumptions (section 4.11). To date, the most satisfactory prediction for solar activity found by this author is the forecast developed by H.H. Sargent of the Space Environment Laboratory at NOAA.[22] He gives a general estimate of sunspot numbers (R_Z) for cycle 22. Some of the discussion below outlines the main points in that forecast.

10.1.1 Solar cycle description

Solar cycles can be numbered in even-odd pairs, with the characteristic that the preceeding even cycle generally predicts the maximum of the odd cycle. By observing the last six even-odd pairs, one can make a general comment that the slopes before and after maximum solar activity of the even cycle also tend to predict the slopes of the odd cycle. See Figure 10.1.

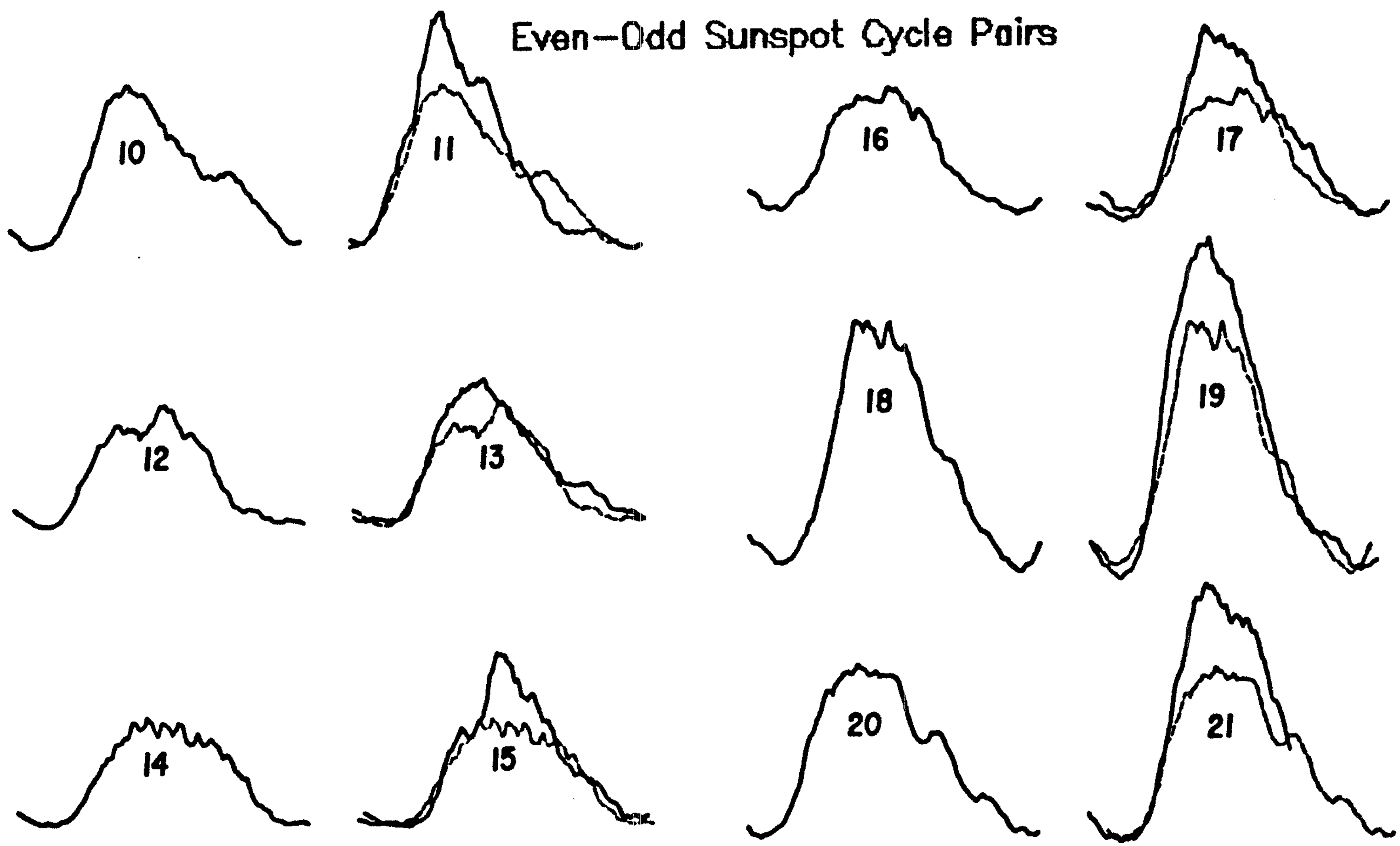

Figure 10.1 Even-odd solar sunspot cycle pairs for cycles 10-21. The preceeding even cycle is matched with each odd cycle. (Reproduced from H. Sargent, "An Early Forecast for Sunspot Cycle 22").

Sunspot Cycle Ratios

Even — odd cycle ratios

Cycle	Maximum	Ratio
10	97.9	1.44
11	140.5	
12	74.6	1.18
13	87.9	
14	64.2	1.64
15	105.4	
16	78.1	1.53
17	119.2	
18	151.8	1.33
19	201.3	
20	110.6	1.49
21	164.5	

$\bar{X} = 1.44$

Table 10.1 Even-odd sunspot cycle maximums and the ratio of each pair. Adapted from H. Sargent, "An Early Forecast for Sunspot Cycle 22."

10.1.2 Solar cycle amplitude

An important difference between the even and odd cycles in a pair is that the even cycle has its top "chopped off." See Figure 10.1. The sets of even-odd cycles (from 10 to 21) average approximately 10.1 years between minimums, with a total of about 22 years for a pair. See Figures 10.2 and 10.4. This even-odd cycle amplitude relation has been uniformly true for the past six pairs of solar cycles, or about 130 years. The average ratio of the odd cycle to the even cycle in the data is 1.44 (see Table 10.1) and this would be a good estimate for predicting the maximum of cycle 23 from cycle 22. Unfortunately, there is not a good relation like this for predicting the amplitude of an even

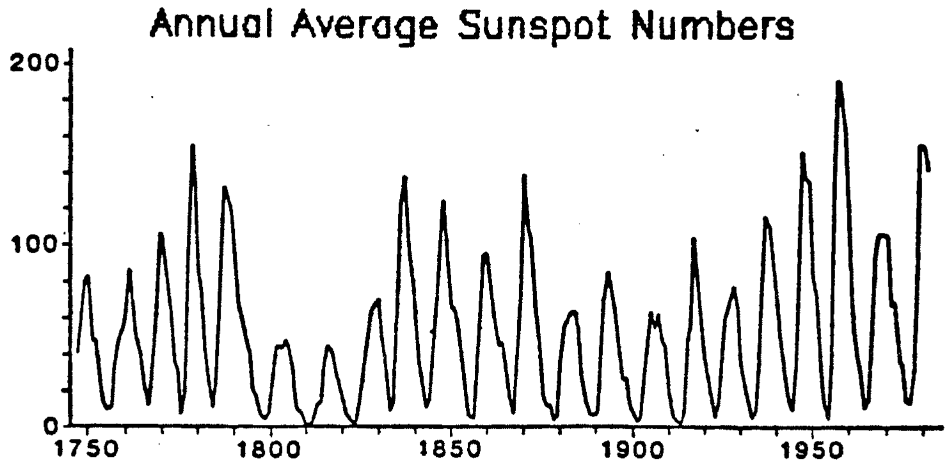

Figure 10.2 Annual average sunspot numbers from 1750 to 1980. Data prior to 1848 may not be entirely reliable. (Reproduced from H. Sargent, "An Early Forecast for Sunspot Cycle 22").

cycle following an odd cycle, as is our present case. As a result, we must look to other means to get a good estimate of the amplitude of the cycle 22 maximum.

In observing the amplitudes of solar cycles since 1848, the phenomenon of the Gleissburg cycle has been suggested. What appears in the data over the last 140 years is a general indication of an 80 to 90 year cycle. See Figure 10.2. With the beginnings of the present cycle, around the turn of the century, we see an increase in the solar maximums to a peak level in midcentury. It would seem that we should now be nearing the end of that cycle, if it exists.

For this reason, we could expect the maximum of cycle 22 (an even, low amplitude solar cycle) to be lower than the peak of cycle 20, the last low amplitude cycle. We note that the average of the sunspot cycles since 1848 is 117.5 (R_z). This translates to approximately 158 in F10.7.[23] We can use this as a likely value for the maximum of cycle 22. However, in doing so, we notice that cycle 20 had a maximum of 110.6 R_z or 152 F10.7. Refer to Figure 10.3. If we accept this, it means our prediction is going the wrong way if we still agree on the validity of the Gleissburg cycle. In rethinking the data, Sargent suggests a better value for the maximum R_z of cycle 22 might be between 90 and 100, which translates to F10.7 of 135 to 143. This would allow for a decrease in the solar maximum according to the Gleissburg cycle pattern, and would still be well within range of the average R_z values over modern times. This author believes this to be a reasonable assumption and has chosen a best estimate maximum value of 140 for the F10.7. Sargent also points out that in the modern era, R_z of 96.2 or F10.7 of 140 is the average for the even cycle maximum amplitudes, which gives us a little more confidence in selecting that value.

Sargent does not make a forecast for the minimum of cycle 21, which we are now approaching. In arriving at a F10.7 best guess value of 66, I took the average value of the minimums for the last five cycles, estimating that the minimum for cycle 21 would be similar to those.

10.1.3 Solar cycle length

The predicted time frame of the minimum of cycle 21, still

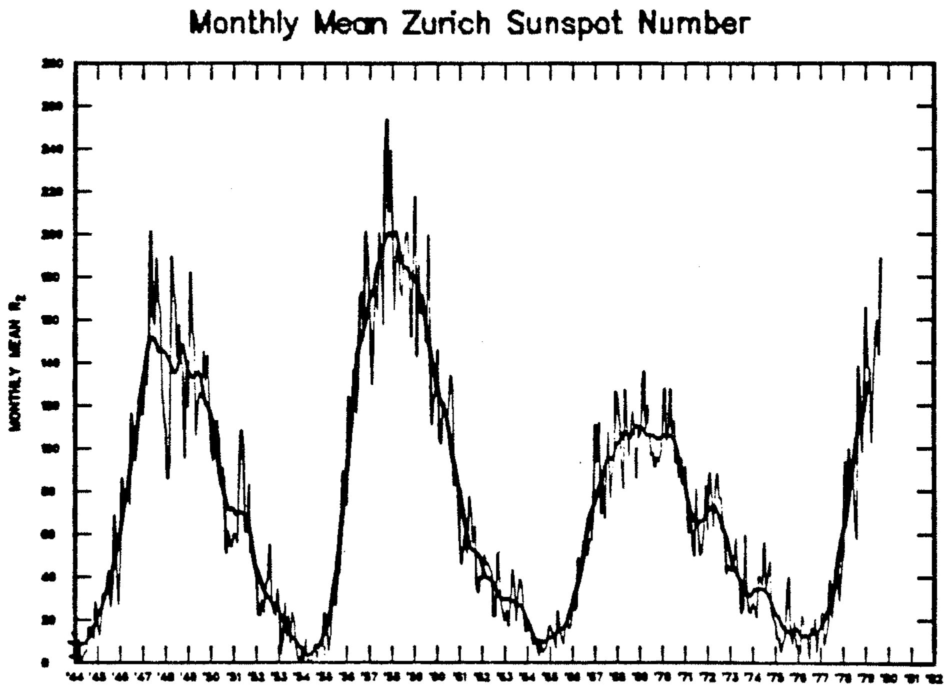

Figure 10.3 Monthly mean Zurich sunspot numbers (R_z) from 1944 to 1979. The heavy line indicates smoothed R_z. (Reproduced from "Solar Geophysical Data").

to come, ranges from June 1986 to November 1988, with a best predicted date in February 1988. This point in the cycle would reflect the general trend over the past 140 years where one average time between minimums is 140 months. I say one average time because Sargent points out that there are really two sets of data for sunspot cycle lengths. One set has lengths of 140 or 150 months while the other set has lengths in the range of 120 or 130 months. These sets seem to be organized in a series. See Figures 10.4 and 10.5. Sargent notes that the last series was of short length, with cycle 20 having just jumped into the long length range. Since there is no indication in the data that the cycles successively jump from long to short lengths in alternating cycles, we might reasonably accept a cycle 21 length somewhere near that of cycle 20. The average length for the longer series of cycles is around 140 months, which is the same range for the cycle 20 length. In fact, this is not much higher than the overall cycle length average of 133 months. For this study, the author will be conservative and use a happy medium between Sargent's value and the overall average, selecting a cycle 21 length of 138 months. This places the solar minimum in December 1987 and conveniently allows the computational model in this study to change its minimum point on the F10.7 curve at a natural break in an iterative cycle. See the predicted F10.7 data set in Appendix B.

For a final, graphic depiction of the above discussion, Figure 10.6, shown earlier, as Figure 6.3, is a plot of the predicted solar activity of cycle 22, based on the Sargent data. One notes that the maximum of cycle 22 occurs over a relatively large period of time, approximately 21 months. This plateau of average monthly F10.7 values follows the trend over the last four even solar cycles.

It should be noted that the curve section which approximates the predicted flux during the first 33 months of actual monthly F10.7 averages is simply a cubic fit to the real data. Hence, we cannot compare a predicted curve to the real data for

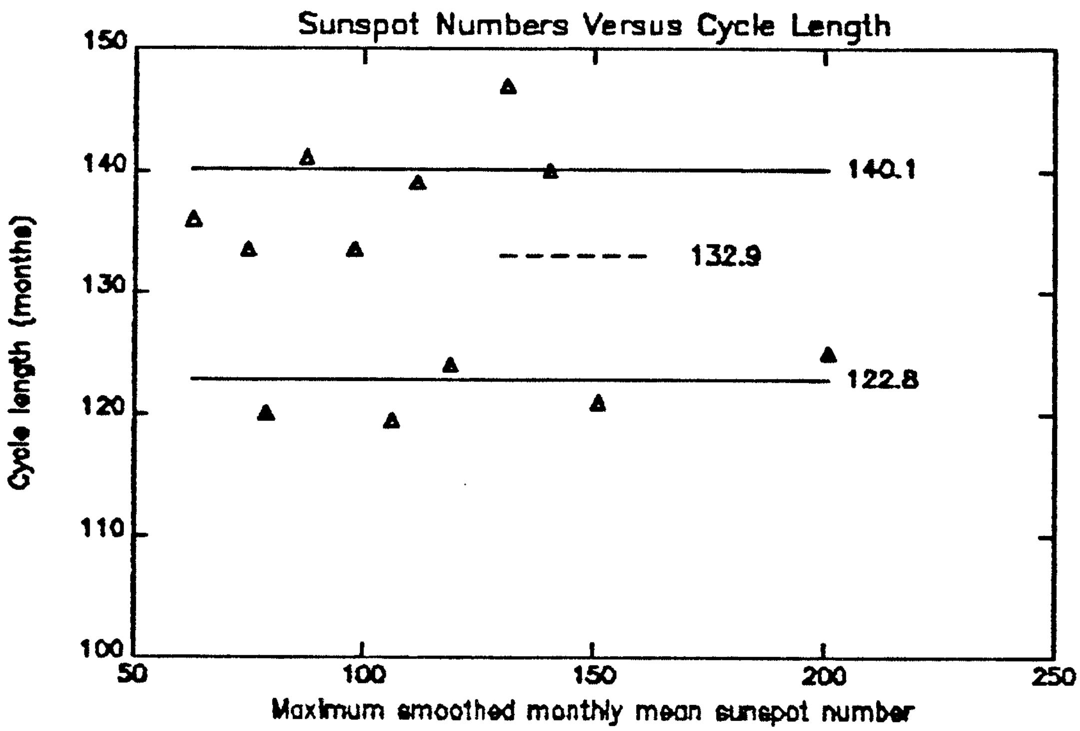

Figure 10.4 Maximum smoothed monthly mean sunspot number plotted with cycle length in months. (Adapted from H. Sargent, "An Early Forecast for Sunspot Cycle 22").

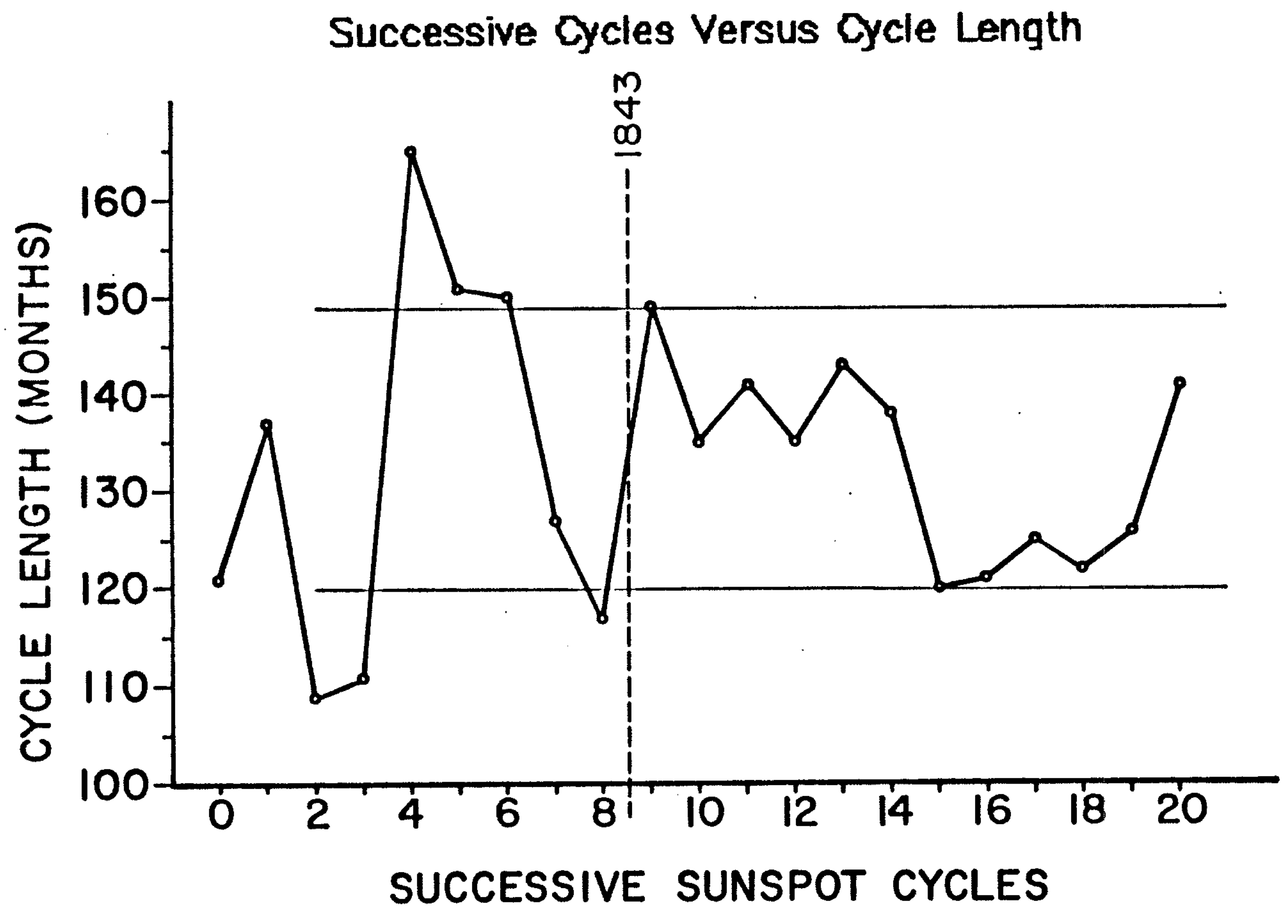

Figure 10.5 Successive sunspot cycles plotted with cycle length in months. (Reproduced from H. Sargent, "An Early Forecast for Sunspot Cycle 22").

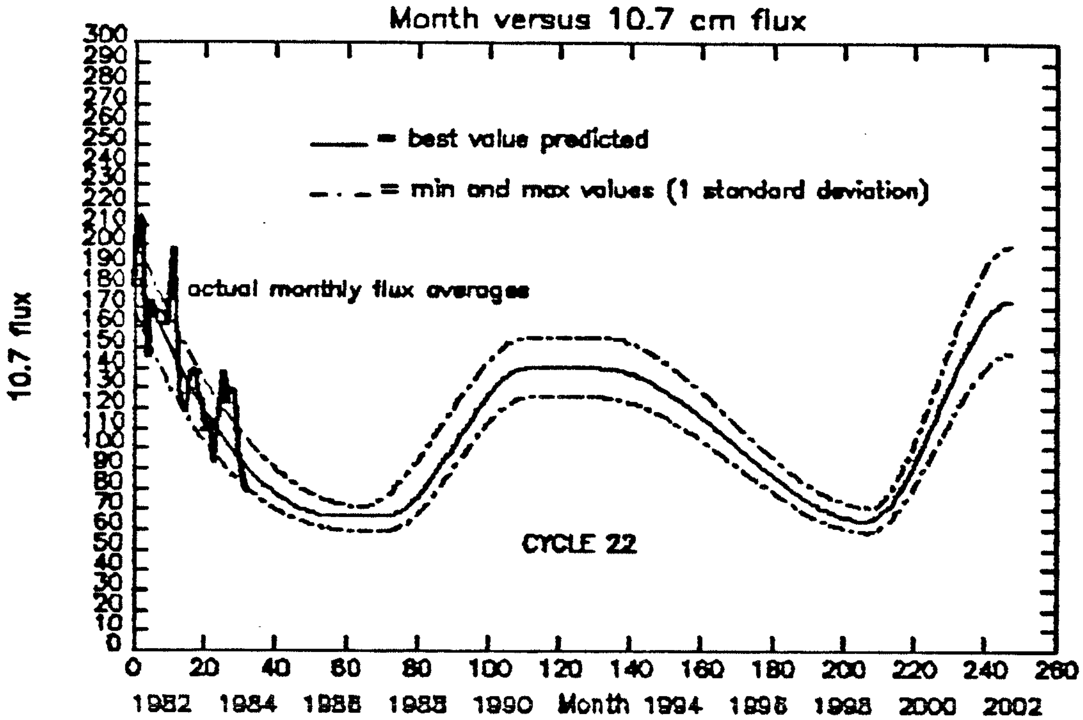

Figure 10.6 Figure 6.3 reproduced. 10.7 cm flux prediction over solar cycle 22, based upon H. Sargent sunspot predictions and conversion to F10.7.

that time period, nor do we need to.

10.1.4. Another F10.7 model

A second model which exists for F10.7 activity over the next solar cycle is one developed at Goddard Space Flight Center (GSFC). The general profile of the data from that forecast approximates the Sargent forecast in its general shape. Refer to Figure 10.7. Three important differences occur, however. First, the GSFC prediction indicates the minimum of cycle 21 will most likely oc-

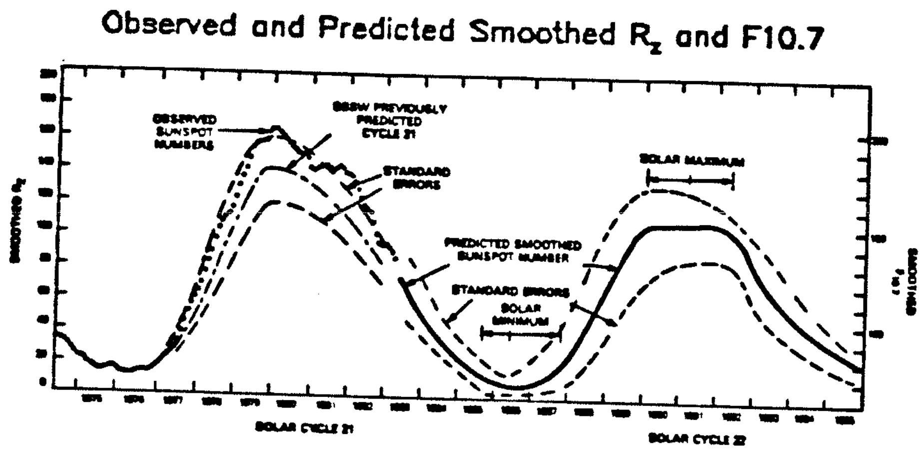

Figure 10.7 Predicted smoothed sunspot number and 10.7 cm flux over solar cycle 22 from another model. (Reproduced from K. Schatten, A. Hedin, "A Dynamo Theory Prediction for Solar Cycle 22: Sunspot Number, Radio Flux, Exospheric Temperature, and Total Density at 400 km").

cur in the early fall of 1986, which falls near the very earliest possible time in the Sargent model. Second, and as a result, the maximum of cycle 22 occurs over a year earlier in the GSFC forecast (early 1990) than in the forecast based on Sargent's predictions (April 1991). This difference in solar activity affects the orbit decay calculations. It causes the altitude in the 1987 - 1988 time frame to be lower than the altitude achieved in this study. The actual predicted altitude differences are discussed below in section 10.2.3.

10.2 Predicted altitude decay

10.2.1 General results

Probably the most exciting result of this work is the predicted altitude decay of SME. When studying the results, plotted in Figures 10.8a and 10.8b, we note immediately that the satellite reenters the lower atmosphere during the second half of the 1990's. In addition, the altitude remains quite stable in the period from the early 1985 until late 1988. The actual decay matches the predicted decay over the first 33 months of flight, remembering that the F10.7 values in the first part of the mission are the cubic curve fit to the actual data. By matching the predicted curve to the real curve of altitude decay, we gain confidence that other variables in the equations are relatively accurate. This is particularly relevant to the area/mass ratio and the drag coefficient C_d.

A comparison between the best predicted value for January 23, 1985 and the altitude given by the GSFC definitive ephemeris data for that date indicates a 1.7 km difference in altitudes. The study had the lower altitude (513.90 km) and was arrived at in the 37th month of prediction. The GSFC altitude was based on the semimajor axis value (515.65 km). For the same date, GSFC gave a periapsis altitude of 507.79 km and an apoapsis of 523.64 km. This result and range also give us high confidence in our short term predictive model, even though the GSFC values probably reflect osculating elements.

In Figure 10.8a, we notice that the one standard deviation confidence level for the maximum altitude will never go beyond a certain altitude, reflecting the fact the SME will not gain in altitude in later years. This is despite the plot of the orbit un-

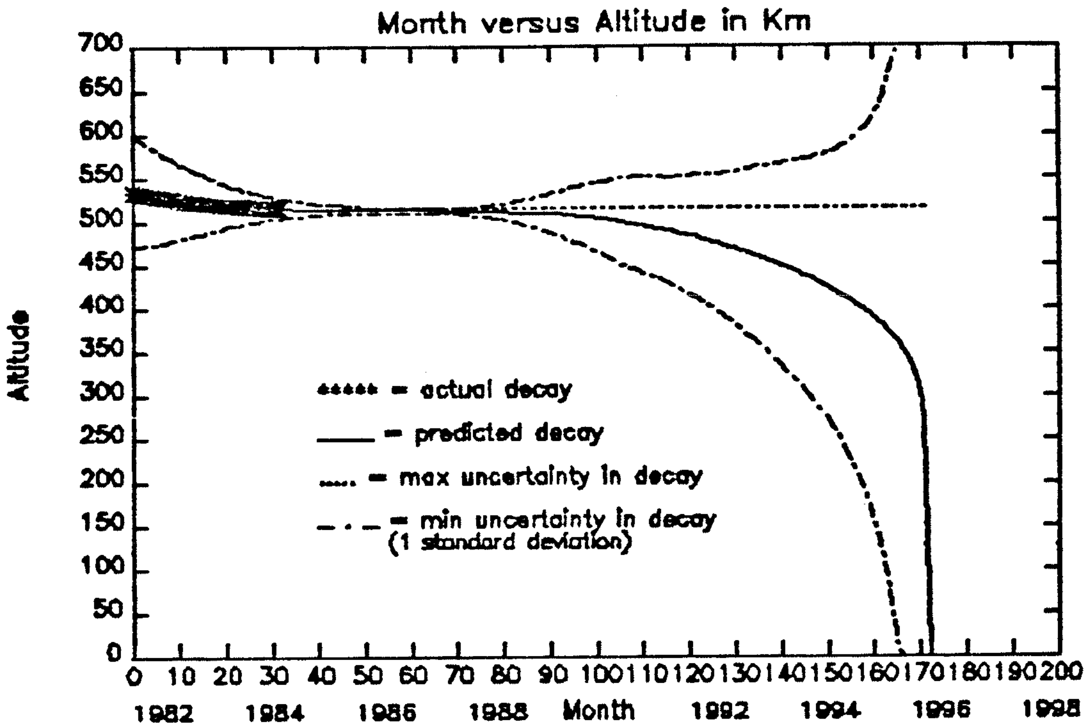

Figure 10.8a Predicted altitude decay versus month, beginning January 1982. Best estimate is solid line and one standard deviation is given by dashed line. Overplotted in asterisks are the actual altitude points for the first thirty-three months. The dotted line represents the maximum altitude for the upper uncertainty line, given that SME will not gain altitude after the minimum is reached during solar cycle 21 minimum. April 1996 is the predicted reentry date.

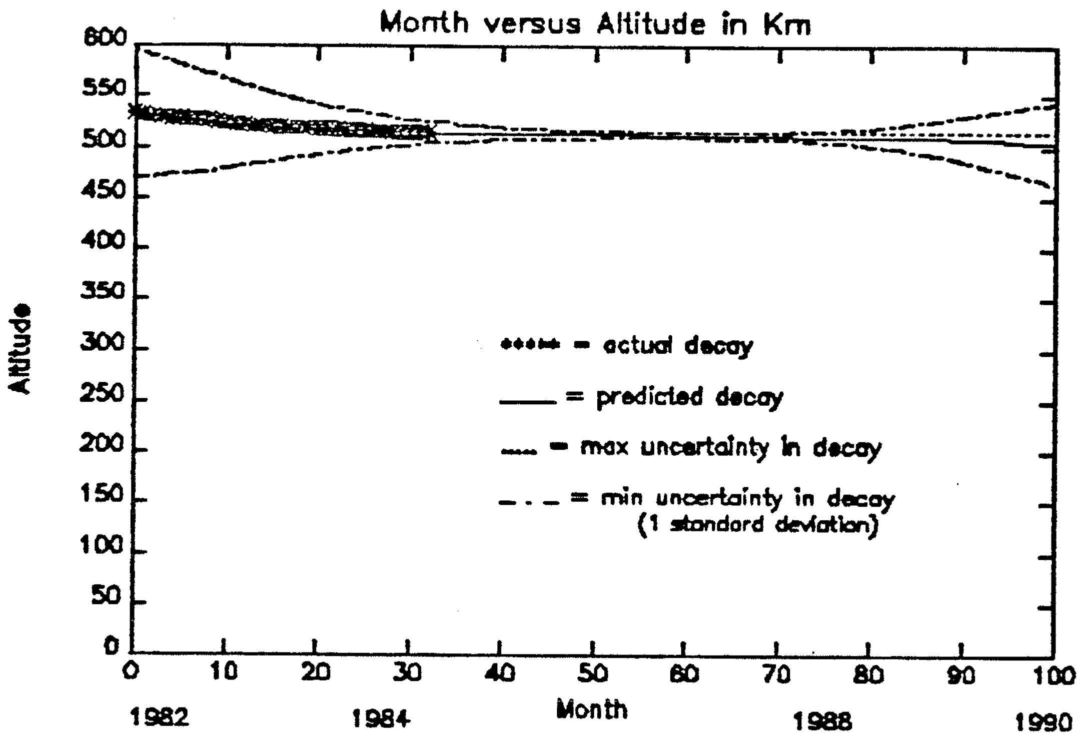

Figure 10.8b High resolution plot of Figure 10.8a. The time frame includes the actual altitude data plus the period of solar cycle 21 minimum.

certainty extending into that region. The upper uncertainty line was retained so that other features could be discussed below.

10.2.2 Other features

Some of these features, for example, include the uncertainty curve during the first forty months or so. The uncertainty in the data is quite high, even though our altitude is known accurately during that time period. The reason for this uncertainty is the wide monthly variations in the solar flux shortly after solar maximum. Cycle 21 maximum was in December 1979. In

1982 - 1983, we still saw fairly wide variations in the F10.7. When we observe monthly F10.7 averages over several solar cycles, we see that the maximums in solar activity have widely varying monthly averages over a period of one to four years, depending on the even or odd cycle characteristics. See Figure 10.3. Such a wide fluctuation spreads our uncertainty. On the other hand, solar minimums and the slopes from minimum to maximum generally contain moderate or small fluctuations. Hence, the period from 1985 through 1988 has low uncertainty due to the small F10.7 predicted variations. The period from 1989 through 1995 has quite a large uncertainty, since it covers the time of the next solar maximum. Finally, the uncertainty tends to diminish just about the time the satellite reenters the lower atmosphere due to the minimum of cycle 22 occurring during that time frame.

Other features include the solar maximum in cycle 22 which is quite visible around month 112 (1991). It shows up in the uncertainty lines as a bulge. The slope of the altitude decay curve takes a definite turn downward at that point in time, reflecting the increased solar activity and thus the increased atmospheric density.

10.2.3 Comparison to other studies

A final note comparing the predictions in this study and studies using MSFC data is that the altitude difference around 1987 or 1988 is about 10 km. A prediction of SME decay using the MSFC model was recently done by J. Cowley of LASP. His results, which also use a somewhat different computational algorithm, are generally similar to the results of this study. They are included in Figure 10.9 for the reader's comparison.

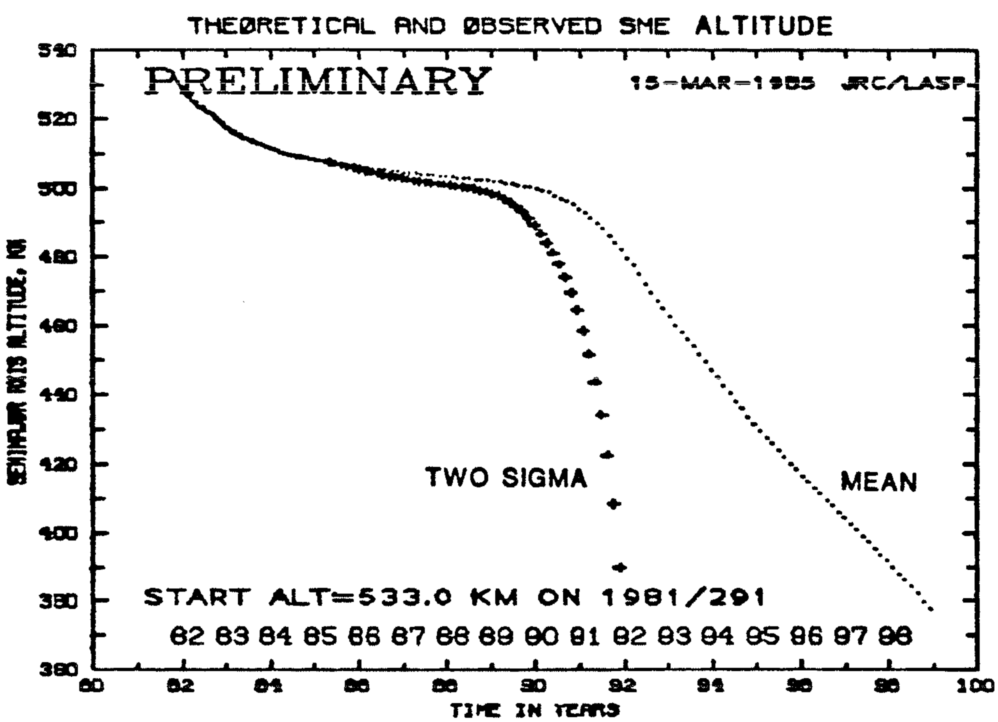

Figure 10.9 Another model's prediction of SME altitude decay, based on the F10.7 in Figure 10.7. (Courtesy of SME Flight Dynamics group and J. Cowley).

10.3 Other predicted variables

Additional confidence level indicators in the predicted versus the actual data may be studied.

First is the predicted orbit period change. By observing Figure 10.10, one sees little variation from the altitude plots reviewed above. This is not suprising, given the same equations of derivation and the linear relation between altitude and period.

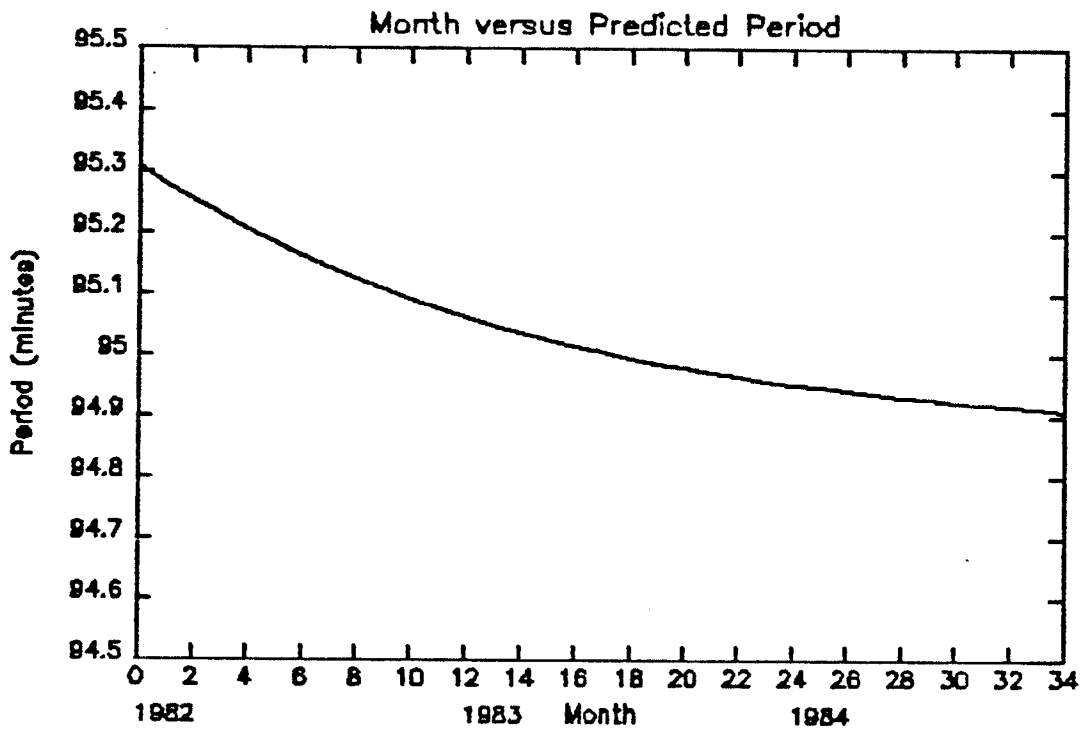

Figure 10.10 Predicted period change for the first thirty-three months. Based on the monthly averages of F10.7 data.

Secondly, a comparison of SME definitive ephemeris derived monthly averaged density and predicted density relative to SME can be seen in Figure 9.1. Here there is some difference which is noticeable. This discrepancy, while not ideal, can be accounted for by the fact that the actual density is smoothed data of monthly averages and the predicted density is the data derived from a curve fit to the F10.7 data and then calculated through several steps to arrive at density. Fortunately, and as an indication of the generally correct method of the work, the two lines tend to converge as we approach a solar minimum in cycle 21. The uncertainty also declines there. The largest difference could be expected near the maximum of the solar cycle due to large F10.7 fluctuations and nonlinearities in the calculation of density from that flux. That is precisely where we observe it.

CHAPTER XI

EVALUATION

11.1 Strengths of this method

Among the major positive results of this work include the good agreement with actual data compared to short term predictions. As noted above, the January 23, 1985 GSFC Ground Tracking and Data System Ephemeris Program determined the orbit semi-major axis at 515.65 km, with the SME perigee at 507.788 km and the apogee at 523.635 km (osculating). The same date in the orbit decay prediction program gave an altitude of 513.90 km. This difference of 1.7 km, or 0.33%, after 37 months of prediction is well within tolerable limits. It also shows that by making several assumptions to simplify the problem, our results for short range predictions are well within the uncertainty limits and provide usable data.

The overall method is straightforward, using valid assumptions, and is based on accepted theory. This gives a good analytic foundation upon which to base the predictions of orbit decay. The first 33 months of SME ephemeris data verify the overall method and approach.

Another feature in this work which stands out is the remarkable detail afforded to the observer in the SME ephemeris data. Resolution down to the level of one day is easily achievable, with second order perturbations being recognizable. While more study needs to be done in this area, there is much information to be gleaned from that detail.

Two final features which should be commented upon here are variations upon previous orbit decay models. In particular, the derivation of the average exospheric temperature and the codification of the Sargent sunspot number prediction for cycle 22, which is then translated into a predicted F10.7 curve with a one standard deviation uncertainty is noteworthy. In addition, the overall method of density and radius determination from the change in period over time is a straightforward approach to orbit decay problems of satellites of the SME type.

11.2 Weaknesses of this method

There are also features in this method which can contribute to error and uncertainty, and these must be mentioned. The assumption of a circular orbit initially will necessarily lead to some uncertainty about the actual altitude of a spacecraft at any given time. In addition, the neglect of planet oblateness, its effect on the gravitational field and its effect on the atmosphere will cause periodic variations in a single orbit as well as a long term secular effect in the Ω and ω terms. Also, the fact that SME has a variable effective area which is dependent upon a coupled roll/yaw angle, and that it varies with a period equivalent to one orbit, adds an additional source of error. This could change the overall effective area by a factor of two. It must also be noted that the maximum roll/yaw angle deviation (roll angle over the equator, yaw angle over the poles, and a coupling of the two everywhere else) itself varies sinusoidally over the year, with the amplitude gradually increasing over the duration of the mission. Finally, the processes between the generation of the 10.7 cm flux, its relation to overall cyclic solar activity and the subsequent relation to the Earth's atmosphere and its density variation are still only generally understood. While there is a good correlation between 10.7 cm flux variation and thermospheric density variation, there is also much room for improvement in this model.

11.3 Comparison with other methods

A comment on the comparison between the altitude decay predictions in this study and those of other studies should be made. The prediction by J. Cowley with a separate solar flux model shows remarkable general agreement with the present study. This was noted earlier in our discussion.

References to atmospheric density relative to the SME project have appeared in other, separate publications. Of particular note is the report entitled "Studies of the attitude of the Solar Mesosphere Explorer: Dynamics and horizon sensor performance" by G.M. Lawrence, et al.[24] mentioned earlier. Here, four different methods were used to compare atmospheric density related to the SME orbit. General agreement was found, with some methods yielding higher correlations than others to SME decay rate data. It is instructive to note that the J66 model used in that paper was similar to the method used in this study, and found comparable results in atmospheric density for the first 33 months of the SME mission.

CHAPTER XII

RECOMMENDATIONS

12.1 Future work on this problem

In three specific areas, this author has initiated work which relates to the problem of SME orbit decay. This work was originally intended for inclusion in the present study. However, after rethinking the basic assumptions of the problem, it became clear that the following areas describe second order effects or areas where more background needs to be gained. Therefore, these areas were left out of the present study, to be taken up at a later time.

12.1.1 SME effective area

One particular problem which stands out is the determination of the satellite effective area. Here, given the control over attitude of the satellite which we have through magnetic torquing, and the regular attitude control exercised by the flight dynamics group, it should be possible to work out an effective area which varies both with latitude in orbit and with increasing mission flight time as the yaw angle between the velocity vector and the spin axis changes. We are aware that the roll/yaw angle increases and decreases to maximum and minimum values during the course of an orbit. We also have derived analytic equations which describe the change in effective area as a result of roll angle instantaneously. See Chapter 7. With more work, it should be possible to analytically solve this problem and compare these variations to ephemeris derived data.

12.1.2 Oblate planet modeling

A second problem which may be tackled is to introduce the equations of zonal and tesseral harmonics into the analytic equations in order to describe oblate planet and geoid effects in orbit decay. While these effects will not play the major role in long term orbit determination, since atmospheric drag contributes most to the loss of altitude, there is a benefit to short term orbit decay prediction by including these terms.

12.1.3 Model comparison

A particularly useful problem related to SME orbit decay would be a comparison of the results of this semi-analytic model to a purely analytic model, such as that developed by Vinh, Busemann and Culp in their book Hypersonic and Planetary Entry.[25] This effort would serve to solidify the bridge between empirical results and analytic solutions, thus strengthening both.

12.1.4 Derivation of exospheric temperature

A further check on the average value of the exospheric temperature could and should be made by rederiving that temperature based on SME ephemeris derived data. This would give a good comparison between the theoretically predicted value based on a certain F10.7 values and its subsequent use in determining atmospheric density. This check is generally straightforward, but was eliminated from this study due to the late recognition of this need and related time considerations.

12.2 Future work on related problems

12.2.1 Questions from empirical data

As any good study should do, the solution of some problems opens up new, unanswered questions. While arriving at the results outlined in the empirical data above, several new questions arose which are still left unexplained. In particular, the variety of orbit perturbations, which emerged from the altitude and orbit period plots, deserve more study. Examples of this are the 150 millisecond twice daily variation in orbit period, numerous frequency spikes which were revealed in a power spectrum analysis of the orbit period, and sinusoidal variations in the orbit period rate change residue from a curve fit to that data for the first 4000 orbits.

12.2.2 Atmosphere rotation effects

A second problem which deserves to be studied in more detail is the small perturbation on satellite orbits caused by the rotation of the Earth's atmosphere. From the quick glance done here with the SME emphemeris data, it may be possible to derive an angular velocity ω of the atmosphere at the altitude of SME. The effects of the change in the semi-major axis in equations 4.1, 4.2, 4.3 and 9.1 must be uncoupled from the ω term, but this work could prove informative.

12.2.3 Upper atmosphere constituents

A separate area which has potential for more investigation is the determination of upper atmosphere constituents, their percentages and densities from other techniques and other spacecraft, whose data can be related to that of SME over the same time period. An example of a new approach to studying atmospheric composition is the investigation of vehicle glow on the space shuttle as well as other spacecraft. Ions in the upper atmosphere, which have velocities relative to a vehicle of seven or eight km per sec, absorb energy from impact with the vehicle surface in the four to eight electron volt range. The transitions from this excited state back down to the ground or lower energy state results in emissions of photons at wavelengths specific to each species. This process most likely occurs along with other reactions. Through spectrography, we can measure the intensity and wavelength of these emissions and theoretically determine the species creating them. Their relative number density may be determined from an intensity plot. This independent method of determining atmospheric composition and density at low Earth orbit altitudes could give us another basis by which to correlate our present data from satellite orbit decay studies. The importance of these studies holds no small place in the next decades as the space shuttles, the space station and a variety of low Earth orbit activities blossom.

CHAPTER XIII

CONCLUSION

The following conclusions can be made from this study.

13.1 Validity of semi-analytic method

First, by using simplifying assumptions, the problem of orbit decay prediction can be narrowed to a set of analytic equations and the results verified by comparison to empirical data. In this case, the classic equations of motion, of energy and momentum conservation, and of relations describing the Earth's atmosphere can be combined to produce valid orbit decay solutions. Within these calculations, it is possible to modify previous dynamic atmosphere models, improving the prediction accuracy.

13.2 Validity of predictions

Second, the actual predictions for SME orbit decay can be broken up into short, medium and long range estimations.

13.2.1 Short term prediction

The decay predictions for the short range (on the order of months to a year) are very accurate, being less than one percent off the actual orbit semi-major axis value.

13.2.2 Medium term prediction

For the medium range altitude estimations, we can determine the orbit altitude with considerable certainty. This is quite fortuitous, given that over the next two or three years we are experiencing the minimum of solar cycle 21. This allows us to fairly accurately predict the F10.7 values, the atmospheric density and the associated orbit decay. One can expect the actual orbit altitude to be within one or two percent of the best predicted value in early 1988.

13.2.3 Long term prediction

The long range orbit prediction for SME has quite a large uncertainty associated with it, due to the time period which extends nearly a decade into the future and due to the uncertainty associated with solar cycle 22 which has not yet begun. Given our best efforts, we may say that a reasonable guess of the expected lifetime of the SME satellite, in it present configuration, will be another ten years, more or less. Both this study and the Cowley study predict reentry in the second half of the 1990's.

Any studies which consider the capture and refurbishment of SME, whether from the space shuttle or the space station, should note that SME will be at accessible altitudes until reentry. However, given the energy needed to reach different orbits, weighed against the useful satellite lifetime and predictable rates of descent, the ideal time for such a capture would likely bridge the late 1980's and early 1990's.

REFERENCES

1. Herrick, S., Astrodynamics - Orbit Determination, Space Navigation, Celestial Mechanics, Volume I, Van Nostrand Reinhold Company, London, 1971, pp. 1-2.

2. Springer, B.D., "Session I Summary - Operational Problems of Satellite Drag", published Proceedings of a Workshop on Satellite Drag, March 18-19, 1982, Boulder, Colorado.

3. King-Hele, D., Theory of Satellite Orbits in an Atmosphere, Butterworths, London, 1964, p. 6.

4. Wertz, J.R., Spacecraft Attitude Determination and Control, D. Reidel Publishing Co., Dordrecht, The Netherlands, 1984, p. 98.

5. Allen, C.W., Astrophysical Quantities, 3rd Edition, The Athlone Press, William Clowes and Sons, Ltd., London, 1981, p.16.

6. King-Hele, p. 8.

7. Ibid., pp. 4,127.

8. United States Committee on Extension to the Standard Atmosphere, U.S. Standard Atmosphere, Washington, U.S.G.P.O., 1976, p. 13.

9. Ibid.

10. Altrock, R.C., "An Anomalous Twenty-seven Day Periodic Variation in Satellite Drag and Possible Solar-Induced Causes", published Proceedings of a Workshop on Satellite Drag, March 18-19, 1982, Boulder, Colorado.

11. McKnight, D., private communication.

12. King-Hele, p. 14.

13. King-Hele, p. 118.

14. Chamberlain, J.W., Theory of Planetary Atmospheres, Academic Press, New York, 1978, p. 63.

15. Jacchia, L.G., "Static Diffusion Models of the Upper Atmosphere With Empirical Temperature Profiles", SAO Special Report 170, 1964.

16. Bates, D.R., "Some problems concerning the terrestrial atmosphere above about the 100 km level", Proceedings of the Royal Society, A 253, 1959, pp. 451-462.

17. United States Committee on Extension to the Standard Atmosphere, p. 13.

18. Laboratory for Atmospheric and Space Physics, VAX780 Interactive Data Language system library, "POLY_FIT".

19. Taylor, J.R., An Introduction to Error Analysis, University Science Books, Mill Valley, California, 1982, p. 121.

20. Ibid., pp. 70-74.

21. King-Hele, p. 127.

22. Sargent, H.H., "An Early Forecast for Sunspot Cycle 22", Seminar Notes, HAO Colloquium Series, 1984.

23. Euler, H. and Holland, R., "Solar Activity Statistical Estimation Technique", published Proceedings of a Workshop on Satellite Drag, March 18-19, 1982, Boulder, Colorado.

24. Lawrence, G.M., Cowley Jr., J.R., Sparn, T.P., Arlton, P.E., Tobiska, W.K., "Studies of the Attitude of the Solar Mesosphere Explorer: Dynamics and Horizon Sensor Performance", prepared report for Goddard Space Flight Center, 1985.

25. Vinh, N.X., Busemann, A., Culp, R.D., Hypersonic and Planetary Entry Flight Mechanics, The University of Michigan Press, Ann Arbor, 1980.

APPENDIX A

Program Orbit_Decay and Subroutines

```
      Program Orbit_decay

C*************************************************************************
C       This program solves for the change in the orbit radius over time
C            of the Solar Mesosphere Explorer satellite (SME).
C
C       Assumptions:
C               1) Circular orbit (in reality the eccentricity = 0.001)
C               2) Spherical earth (actually oblate)
C               3) There exists a means equatorial radius for the Earth
C               4) Negligible long term effect on semi-major axis from
C                  oblate planet
C               5) Non-rotating atmosphere (does have angular velocity)
C               6) 3 constituent atmosphere above 120 km, non-mixing
C               7) Density of atmosphere an exponential curve above 120 km
C               8) Day/night temperatures of the atmosphere can be integrated
C                  into an average thermospheric temperature for all orbits
C               9) Solar flux variations at 10.7 cm is highly correlated to
C                  atmospheric density variations (Jacchia model)
C               10) 27-day (solar rotation) has negligible effect on the
C                  atmosphere
C               11) SME has a constant effective area
C
C       Author: Kent Tobiska, LASP
C*************************************************************************
```

```
Implicit        none
Parameter       months = 248      ! number of months for iteration
Parameter       mass = 415.5      ! mass of SME (kg)
Parameter       area = 2.0        ! area (sq meters) of SME
Parameter       Cd = 1.25         ! aerodynamic drag coefficient
Parameter       mu = 398600.64    ! Earth gravitational constant
Parameter       Re = 6378.164     ! Earth radius (equat. mean in km)
Parameter       dperiod = 0.001   ! uncertainty in period (min)

Integer*2       i,j,k             ! Loop control
Integer*2       year              ! Year of referencing orbit
Integer*2       lastyr            ! Previous year of referencing orbit
Integer*2       doy               ! Day of year
Integer*2       mo(12)            ! array of number of days per month
Integer*4       dt                ! time change (1 day in minutes)

Real*8          perdot            ! dP/dt (change in period over time)
Real*8          dP                ! change in period
Real*8          rho               ! density variable (min,best,max)
Real*8          pi                ! pi
Real*8          alt(3)            ! altitude of SME above the earth
Real*8          period            ! Final orbital period
Real*8          r(3)              ! Mean radius of SME at given period
Real*8          f107(3,6,248)     ! flux array
Real*8          den               ! averaged actual value of density
Real*8          c1                ! constant for period
Real*8          c2                ! constant for perdot
Real*8          c3                ! constant for r
Real*8          dr                ! uncertainty in the radius
Real*8          dalt              ! uncertainty in the altitude
Real*8          darea             ! uncertainty in area of SME (m**2)
Real*8          drho              ! uncertainty in the density
Real*8          K2                ! constant

External        den               ! input year, day,; get ave. density
Common  / solflx / f107
Common  /err1/  darea,K2,c1,c2,c3,dt,drho

Data mo / 31,28,31,30,31,30,31,31,30,31,30,31 /
Data dt / 86400 /
pi = 4.0*atan(1.0)
darea = 0.5                       ! uncertainty in area of SME (m**2)
period = 95.336                   ! initial period on Jan 1 1982
doy = 0                           ! initial day of year
c1 = 2.0*pi/sqrt(mu)              ! constant for period
K2 = 3000.0*pi*Cd/mass            ! constant
c2 = K2 * area                    ! constant for period-dot
c3 = (sqrt(mu)/(2.0*pi))**(0.6666666666667)

Open (unit=2,file='Orbit_decay.DAT',status='old')
Write (2,101) 'Year','DOY','Prd Per','Prd Dens','Act Dens',
2       '10.7','Min Alt','Bst Alt','Max Alt','Act Alt'
Write (6,101) 'Year','DOY','Prd Per','Prd Dens','Act Dens',
2       '10.7','Min Alt','Bst Alt','Max Alt','Act Alt'
Write (2,102) ' '
Write (6,102) ' '
```

```
        Call solarf                           ! initialise solar flux

        r(2) = ((period*60.0*sqrt(mu))/(2*pi))**(0.6666666666667)
        dr = (0.6666666666667) * (dperiod/period) * r(2)
        r(1) = r(2) - dr
        r(3) = r(2) + dr

        Do 10, i = 1,months
          year = 1982 + int((i-1.0)/12.0)
          If (year .gt. lastyr) doy = 0
          mo(2) = 28
        If (((((year .eq. 1984) .or.
     2          (year .eq. 1988)) .or.
     3          (year .eq. 1992)) .or.
     4          (year .eq. 1996)) .or.
     5          (year .eq. 2000)) mo(2) = 29    ! leap years

          Do 15, j = 1,mo(i-12*int((i-1.0)/12.0))! 1 day iteration step
            doy = doy + 1                        ! day of month
            alt(1) = r(2) - Re - dr              ! altitude (km) (min)
            alt(2) = r(2) - Re                   ! altitude (km) (best)
            alt(3) = r(2) - Re + dr              ! altitude (km) (max)
            If (alt(2) .le. 120.0) goto 11       ! satellite crashes
            period = c1*sqrt(r(2)**3)            ! period (sec)
            Call dens (year,doy,alt(2),rho,drho)! density (kg/m**3)
            perdot = c2*r(2)*rho                 ! change in period over time
            dP = perdot * dt                     ! change in period (sec)
            period = period - dP                 ! period (sec)
            r(2) = c3*period**(0.6666666666667) ! radius (km)
            Call error1 (r(2),dr,rho)            ! uncertainty in radius
15        continue

          Write (2,105)
     2      year,doy,period/60.0,rho,den(year,doy),
     3      int(f107(2,3,i)),alt(1),alt(2),alt(3),f107(2,6,i)
          Write (6,105)
     2      year,doy,period/60.0,rho,den(year,doy),
     3      int(f107(2,3,i)),alt(1),alt(2),alt(3),f107(2,6,i)

          lastyr = year
10      continue

11      continue                               ! SME crashes
        Write (2,105)
     2          year,doy,period/60.0,rho,den(year,doy),
     3          int(f107(2,3,i)),0.0,0.0,0.0,f107(2,6,i)
        Write (6,105)
     2          year,doy,period/60.0,rho,den(year,doy),
     3          int(f107(2,3,i)),0.0,0.0,0.0,f107(2,6,i)

        Close (2)

101     Format (X,A4,X,A3,X,A7,2(2X,A8),X,A4,4(X,A7))
102     Format (A1)
103     Format (A42)
104     Format (F7.4)
105     Format (x,I4,x,I3,x,F7.4,x,E9.3,x,E9.3,x,I3,x,4(x,F7.3))

        END
```

```
      Subroutine Dens (year, doy, z, densty, result)

C*****************************************************************************
C     This program determines both actual and predicted temperature and
C     density of the atmosphere at any altitude above 120 km up to 550 km,
C     given a reference date and a specific altitude.
C
C     Assumptions:
C             1) Non-mixing atmosphere above 120 km.
C             2) Exponential atmosphere above 120 km.
C             3) T (temperature), g (gravity) and H (scaleheight) are all
C                functions of altitude.
C             4) There are 3 primary ionic constituents of the atmosphere
C                above 120 km: O+, N2+, O2+ and the total density consists
C                of the sum of these individually.
C
C     Author:          Kent Tobiska    LASP
C*****************************************************************************

      Implicit        none
      PARAMETER       start = 120.0          ! 120 km reference altitude
      PARAMETER       go = 9.80665           ! m/s**2
      PARAMETER       Re = 6378.164          ! km
      PARAMETER       Avogad = 6.02217E23    ! molecules/mole
      PARAMETER       temp = 1.15            ! thermosphere temp constant

      REAL*8          densty                 ! total density
      REAL*8          pdens(3,120:550)       ! density each constituent
      REAL*8          m(3)                   ! element masses
      REAL*8          n(3,120:550)           ! number density
      REAL*8          nz                     ! temporary variable
      Real*8          T(120:550)             ! temp at altitude
      Real*8          g(120:550)             ! gravity at altitude
      Real*8          H(120:550)             ! Scale height
      Real*8          To                     ! Kelvin at 120 km
      Real*8          Tinf                   ! Temperature at infinity
      Real*8          sigma                  ! dimensionless factor
      Real*8          z                      ! altitude input
      Real*8          k                      ! Joules/K
      Real*8          zo                     ! reference altitude
      Real*8          sflux                  ! returned F10.7
      Real*8          f107(3,6,248)          ! 10.7 cm solar flux array
      Real*8          dh                     ! fractional uncertainty in alt
      Real*8          df                     ! fractional uncertainty in flu
      Real*8          dq(3)                  ! fractional uncertainty in den
      Real*8          result                 ! uncertainty in the density
      Real*16         ddq(3)                 ! fractional uncertainty in den
      Real*16         dden                   ! uncertainty in the density

      INTEGER*2       alt                    ! iteration control
      INTEGER*2       i,j                    !  "     "     "  elements
      INTEGER*2       year                   ! input year
      INTEGER*2       doy                    ! input day of year
      INTEGER*2       dT                     ! Kelvin
      INTEGER*2       dz                     ! km

      Common          /solflx/        f107
      Common          /err2/          Tinf,To,sigma,j,zo,k,dz
```

```
**************************************************************************
C       Determine the temperature and density, first finding the best value
C       and then the max & min values
C*************************************************************************

        k = 1.38062E-23                       ! Joules/K
        To = 386.0                            ! Kelvin at 120 km
        dT = 15                               ! Kelvin
        dz = 1                                ! km
        zo = start                            ! 120 km reference altitude
        Call flux (year,doy,sflux,df)         ! get 10.7 flux for that date
        alt = int(z)                          ! get the altitude

        Tinf = temp*(379 + 3.24*sflux)        ! thermospheric temperature
        sigma = (dT/dz)/(Tinf-To)

        Do 10, i = 1,3                        ! Calculate values for
                                              !   each of the constituents
         If (i .eq. 1) then
            m(i) = 16/(Avogad*1000)           ! mass of oxygen atom (kg)
            nz = 7.69E16                      ! molecules/m**3 at 120 km
          else if (i .eq. 2) then
            m(i) = 28/(Avogad*1000)           ! mass of nitrogen molecule (kg
            nz = 2.98E17                      ! molecules/m**3 at 120 km
          else if (i .eq. 3) then
            m(i) = 32/(Avogad*1000)           ! mass of oxygen molecule (kg)
            nz = 3.38E16                      ! molecules/m**3 at 120 km
          endif

          Do 15, j = 120,alt
            T(j) = Tinf - (Tinf-To)*exp(-sigma*(j-zo))! temperature
            g(j) = go*(Re/(Re + j))**2        ! gravity
            H(j) = ((k*T(j))/(m(i)*g(j)))/1000  ! scale height (km)
            n(i,j) = nz*exp(-dz/H(j))         ! number density
            pdens(i,j) = n(i,j)*m(i)          ! mass density
            nz = n(i,j)                       ! save n(i,j)
            Call error2 (m(i),g(j),H(j),nz,df,dq(i))
15        continue
10      continue

        densty = 0.0
        Do 20, i = 1,3
          densty = pdens(i,alt) + densty
          ddq(i) = qextd (dq(i))
20      continue

        dden = qsqrt (ddq(1)**2 + ddq(2)**2 + ddq(3)**2)
        result = dbleq(dden)

        Return
        END
```

```
      Subroutine flux (year,doy,flx,df)
C*****************************************************************************
C     This function uses the date to determine the interpolated 10.7 cm
C     solar flux value and returns the uncertainty.
C*****************************************************************************

      Implicit        none
      Real*8                  flx,f107(3,6,248),df,dfl,dfh
      Integer*2               year
      Integer*2               doy,mo,day
      Integer*2               month(12)
      Integer*2               i,j,k
      Common  /solflx/        f107

      Data month / 31,28,31,30,31,30,31,31,30,31,30,31 /
      If (((((year .eq. 1984) .or.
     2        (year .eq. 1988)) .or.
     3        (year .eq. 1992)) .or.
     4        (year .eq. 1996)) .or.
     5        (year .eq. 2000)) month(2) = 29        ! leap years

      Do 10, i = 1,248                               ! get the right year
        If (year .ne. f107(2,1,i)) then
          continue
        else
          goto 11
        endif
10    continue
11    continue

      mo = month(1)
      If (mo .lt. doy) then
        Do 15, j = 2,12                              ! convert doy to month
          If (mo .lt. doy) then
            mo = month(j) + mo
            day = month(j) - (mo - doy)
          else
            goto 16
          endif
15      continue
      else
        j = 2
        day = month(j-1) - (mo - doy)
      endif
16    continue

      j = j - 1                                      ! j is now month index
      k = i + j - 1                                  ! pointer for f10.7

      flx = f107(2,3,k) -
     2      (day/real(month(j)))*(f107(2,3,k)-f107(2,3,k+1))! interpolate
      dfl = dabs(f107(2,3,k) - f107(1,3,k))
      dfh = dabs(f107(2,3,k) - f107(3,3,k))
      df = (dfl + dfh)/2.0

      Return
      End
```

```
      Subroutine Solarf
C***************************************************************************
C     This subroutine reads the 10.7 cm solar flux for Jan 1, 1982 to Aug
C     2002 from a previously established data file (SOLARF.DAT). It then
C     places the data in an array for interpolation and access by other
C     program modules.
C***************************************************************************

      Implicit        none
      Real*8          f107(3,6,248)          ! 248 months of F10.7
      Integer*2       year                   ! year buffer
      Integer*2       month                  ! month buffer
      Integer*2       i                      ! loop control
      Character*80    header                 ! data file header
      Character*80    sdev                   ! standard deviation note
      Common          /solflx/ f107

      Open (unit=1,file='SOLARF.DAT',status='old')

      Read (1,101) header                    ! read past headers in file
      Read (1,101) sdev                      ! read past standard dev note

      Do 10, i = 1,248                       ! read all flux values
        Read (1,103)
     2        year,month,f107(1,3,i),f107(2,3,i),f107(3,3,i),
     3        f107(2,4,i),f107(2,5,i),f107(2,6,i)
        f107(2,1,i) = real(year)             ! and place in f107 array
        f107(2,2,i) = real(month)
10    continue

      Close(1)

101   Format (A)
103   Format (x,I4,x,I2,3(x,F6.2),x,F8.5,x,E10.3,x,F8.4)

      End
```

```
        Function den (year,doy)
C*******************************************************************************
C       This function uses the date to determine the interpolated density value
C*******************************************************************************

        Implicit                 none
        Real*8                   den,f107(3,6,248)
        Integer*2                year
        Integer*2                doy,mo,day
        Integer*2                month(12)
        Integer*2                i,j,k
        Common  /solflx/         f107

        Data month / 31,28,31,30,31,30,31,31,30,31,30,31 /
        If (((((year .eq. 1984) .or.
     2          (year .eq. 1988)) .or.
     3          (year .eq. 1992)) .or.
     4          (year .eq. 1996)) .or.
     5          (year .eq. 2000)) month(2) = 29        ! leap years

        Do 10, i = 1,248                               ! get the right year
          If (year .ne. f107(2,1,i)) then
            continue
          else
            goto 11
          endif
10      continue
11      continue

        mo = month(1)
        If (mo .lt. doy) then                          ! convert doy to month
          Do 15, j = 2,12
            If (mo .lt. doy) then
              mo = month(j) + mo
              day = month(j) - (mo - doy)
            else
              goto 16
            endif
15        continue
        else
          j = 2
          day = month(j-1) - (mo - doy)
        endif
16      continue
                                                       ! j is now month index
        j = j - 1                                      ! pointer for f10.7
        k = i + j - 1

        den = f107(2,5,k) -
     2        (day/real(month(j)))*(f107(2,5,k)-f107(2,5,k+1))! interpolate

        Return
        End
```

```
      Subroutine error1 (r,dr,rho)
C**********************************************************************************
C     This subroutine calculates the error in the radius and returns the
C     uncertainty (dr).
C**********************************************************************************

      Implicit        none
      Real*8          q
      Real*8          dq
      Real*8          x
      Real*8          dx
      Real*8          y
      Real*8          r
      Real*8          dr
      Real*8          rho
      Real*8          dy
      Real*8          darea,K2,c1,c2,c3,drho
      Real*16         ddc2
      Real*16         ddy
      Real*16         ddr
      Real*16         ddrho
      Real*16         KK2
      Integer*4       dt

      Common  /err1/  darea,K2,c1,c2,c3,dt,drho

      KK2 = qextd (K2)
      ddc2 = KK2 * darea
      y = c2 * r * rho * dt
      ddr = qextd (dr)
      ddrho = qextd (drho)
      ddy = qsqrt ((ddc2/c2)**2 + (ddr/r)**2 + (ddrho/rho)**2) * y
      dy = dbleq (ddy)
      dx = dsqrt (dr**2 + dy**2)
      x = c1*dsqrt(r**3) - c2*r*rho*dt
      dr = (2.0/3.0) * dx/dabs(x) * r

      Return
      End
```

```
        Subroutine error2 (m,g,H,nz,df,dq)
C*******************************************************************************
C       This subroutine calculates the error in density and returns the
C       uncertainty (dq).
C*******************************************************************************

        Implicit        none

        Real*8          dTi
        Real*8          dsigma
        Real*8          sigma
        Real*8          x
        Real*8          dx
        Real*8          y
        Real*8          dy
        Real*8          z
        Real*8          dzi
        Real*8          df
        Real*8          dT
        Real*8          P
        Real*8          dP
        Real*8          dH
        Real*8          H
        Real*8          B
        Real*8          dn
        Real*8          dden
        Real*8          m
        Real*8          g
        Real*8          nz
        Real*8          dq
        Real*8          Tinf
        Real*8          To
        Real*8          zo
        Real*8          k
        Integer*2       dz,j

        Common  /err2/  Tinf,To,sigma,j,zo,k,dz

        dTi = 3.73*df
        dsigma = (dTi/Tinf) * sigma
        x = (Tinf - To)*exp(-sigma*(j-zo))
        y = Tinf*exp(-sigma*(j-zo))
        z = -To*exp(-sigma*(j-zo))
        P = exp(-sigma*(j-zo))
        dP = dabs (exp(-sigma*(j-zo)) * (-(j-zo))) * dsigma
        dzi = dabs (-To * exp(-sigma*(j-zo)) * (-(j-zo))) * dsigma
        dy = dsqrt ((dTi/Tinf)**2 + (dP/P)**2) * y
        dx = dsqrt (dy**2 + dzi**2)
        dT = dsqrt (dTi**2 + dx**2)
        B = (k*1000.0)/(m*g)
        dH = dabs (B) * dT
        dn = dabs (nz * exp(-dz/H) * (dz/H**2)) * dH
        dden = dabs (m) * dn
        dq = dden

        Return
        End
```

```
      Program actalt
C*******************************************************************************
C      This program averages the daily 10.7 cm fluxes for Jan 1, 1982 to Sept
C      29, 1984, includes in the data the monthly averages for Oct 1984 to
C      Dec 1984, and predicts the monthly averages from Jan 1985 to Aug 2002.
C      It also returns the actual period, density, and altitude at the end of
C      every month for definitive data, which has been separately derived.
C*******************************************************************************

      Implicit        none
      Real*8          mof107(3,6,36)          ! 36 months of actual F10.7
      Real*8          f10_7(3,6,248)          ! 248 months of predicted F10.7
                                              !  note: level 1 = minimum flux
                                              !        level 2 = best flux
                                              !        level 3 = maximum flux
      Real*8          flux(32)                ! daily flux values
      Real*8          fraction                ! fraction used in interpol
      Real*8          period                  ! period of SME
      Real*8          altitude                ! altitude of SME
      Real*8          density(32)             ! density derived by SME
      Real*8          diff                    ! difference (uncertainty)
      Real*8          sigma                   ! standard deviation
      Integer*2       date(33)                ! days in each month
      Integer*2       day(32)                 ! consecutive days
      Integer*2       doy(34)                 ! consecutive days of year
      Integer*2       year(32)                ! year
      Integer*2       yr(248)                 ! year
      Integer*2       month(248)              ! month of year for 20.67 years
      Integer*4       count,i,j               ! loop control
      Character*80    line                    ! one line in data file

      Common          /solflx/ f10_7

      Data mof107(2,3,34) /73.5/              ! Oct 1984 averaged F10.7
      Data mof107(2,3,35) /76.3/              ! Nov 1984 averaged F10.7
      Data mof107(2,3,36) /75.9/              ! Dec 1984 averaged F10.7

      Data date       / 31,28,31,30,31,30,31,31,30,31,30,31,31,28,31,
   2  30,31,30,31,31,30,31,30,31,31,29,31,30,31,30,31,31,29 /
      Data yr         / 33*0,3*1984,12*1985,12*1986,12*1987,12*1988,
   2                    12*1989,12*1990,12*1991,12*1992,12*1993,
   3                    12*1994,12*1995,12*1996,12*1997,12*1998,
   4                    12*1999,12*2000,12*2001, 8*2002 /

      Open (unit=1,file='PERIOD.DAT',status='old',readonly)
      Open (unit=2,file='SOLARF.DAT',status='old')
      Open (unit=3,file='MOAVE.DAT',status='old')
      Open (unit=4,file='SOL.DAT',status='old')
```

```
 *****************************************************************************
C       Get the monthly averages of the real data between Jan 82 and Dec 84.
C*****************************************************************************

        doy(1) = date(1)
        Do 1, i = 2,34                        ! get end of months in doy
          If (doy(i-1) .le. 334) then
            doy(i) = date(i) + doy(i-1)
          else
            doy(i) = date(i)
          endif
1       continue

        Read (1,'(A)') line                   ! read past headers in file
        Read (1,'(A)') line
        Read (1,'(A)') line
        Read (1,'(A)') line

        Do 2, i = 1,15                        ! read until Jan 1, 1982
          Read (1,'(55x,F6.2)') flux(i)
2       continue

        Do 5, i = 1,33                        ! read all flux beginning
          flux(32) = 0.0                      !  January 1, 1982
          density(32) = 0.0
          count = 0
          Do 3, j = 1,date(i)
            Read (1,'(x,I4,x,I3,6x,F8.5,x,E10.3,x,F8.4,12x,F6.2)')
     2          yr(i),day(j),period,density(j),altitude,flux(j)
            If (flux(j) .eq. 0.0) then          ! eliminate 0's
              continue
            else                                ! count this flux
              count = count + 1
              flux(32) = flux(j) + flux(32)
              density(32) = density(j) + density(32)
              If (day(j) .ge. doy(i)) goto 4
            endif
3         continue

4         mof107(2,3,i) = flux(32)/real(count)  ! 10.7 cm flux monthly average
          mof107(2,4,i) = period                ! SME actual period (eom)
          mof107(2,5,i) = density(32)/real(count)! SME actual density (mo ave)
          mof107(2,6,i) = altitude              ! SME actual altitude (eom)
5       continue
```

```
*******************************************************************************
C       Determine the best value for the predicted 10.7 cm flux.
C******************************************************************************

        Do 10, i = 1,59                         ! Jan 1982 - Nov 1986 (21: min)
          f10_7(2,3,i) = (-3.33831e-5)*(i**3) + (4.08119e-2)*(i**2) -
     2                  (4.4542)*(i) + 193.92
10      continue

        Do 11, i = 60,72                        ! Dec 1986 - Dec 1987 (21: min)
          f10_7(2,3,i) = f10_7(2,3,i-1)
11      continue

        Do 12, i = 73,112                       ! Jan 1988 - Apr 1991 (22: max)
          f10_7(2,3,i) = -0.0023*(i-72)**3 + 0.13812*(i-72)**2 + 66.337
12      continue

        Do 13, i = 113,132                      ! May 1991 - Dec 1992 (22: max)
          f10_7(2,3,i) = f10_7(2,3,i-1)
13      continue

        Do 14, i = 133,208                      ! Jan 1993 - Apr 1999 (22: min
          f10_7(2,3,i) = 0.00034*(i-132)**3 - 0.03895*(i-132)**2 + 140.0
14      continue

        Do 15, i = 209,248                      ! May 1999 - Aug 2002 (23: max
          f10_7(2,3,i) = -0.00338*(i-208)**3 + 0.2025*(i-208)**2 + 65.0
15      continue

        Do 17, i = 1,36                         ! insert actual values of
          f10_7(2,4,i) = mof107(2,4,i)          !   period
          f10_7(2,5,i) = mof107(2,5,i)          !   density
          f10_7(2,6,i) = mof107(2,6,i)          !   altitude
17      continue                                ! into the f10_7 array
C******************************************************************************
C       Find the uncertainty (standard deviation) in the predicted flux which
C       corresponds to the maximum and minimum differences between the actual
C       monthly averages and the curve fit for the period from Jan 82 - Dec 84
C******************************************************************************

        diff = 0
        Do 18, i = 1,36                         ! find standard deviation
          diff = (mof107(2,3,i) - f10_7(2,3,i))**2 + diff
18      continue
        sigma = sqrt(diff/35.0)                 ! 1 standard deviation (68%)
```

```
********************************************************************************
C       Determine the minimum and maximum flux from curves fitted to predicted
C       solar cycle 22 minimum and maximum.
C*******************************************************************************

        Do 21, i = 1,65                          ! Jan 1982 - May 1987
          f10_7(1,3,i) = -0.000204*(i**3) + 0.053302*(i**2)
     2                   - 4.34*i + 172.0
          f10_7(3,3,i) = -0.000029*(i**3) + 0.03626*(i**2)
     2                   - 4.34*i + 208.0
21      continue

        Do 22, i = 66,112                        ! Jun 1987 - Apr 1991
          If (i .le. 72) then
            f10_7(1,3,i) = f10_7(1,3,i-1)
          else
            f10_7(1,3,i) = -0.00206*(i-72)**3 + 0.12375*(i-72)**2 + 59.0
          endif
          f10_7(3,3,i) = -0.00162*(i-65)**3 + 0.11408*(i-65)**2 + 71.0
22      continue

        Do 23, i = 113,132                       ! May 1991 - Dec 1992
          f10_7(1,3,i) = f10_7(1,3,i-1)
          f10_7(3,3,i) = f10_7(3,3,i-1)
23      continue

        Do 24, i = 133,208                       ! Jan 1993 - Apr 1999
          f10_7(1,3,i) = 0.0003*(i-132)**3 - 0.03428*(i-132)**2 + 125.0
          f10_7(3,3,i) = 0.00039*(i-132)**3 - 0.04415*(i-132)**2 + 155.0
24      continue

        Do 25, i = 209,248                       ! May 1999 - Aug 2002
          f10_7(1,3,i) = -0.00275*(i-208)**3 + 0.165*(i-208)**2 + 59.0
          f10_7(3,3,i) = -0.00406*(i-208)**3 + 0.24375*(i-208)**2 + 70.0
25      continue
```

```
*******************************************************************************
C       Write the data into files
C******************************************************************************

        Write (2,'(20x,A)') 'Predicted data'    ! header for predicted data fil
        Write (2,'(10x,A29,I2)') '1 sigma standard deviation = ',
     2          int(sigma)
        Do 30, i = 1,248
          month(i) = i - int((i-1)/12)*12
          f10_7(2,1,i) = yr(i)
          f10_7(2,2,i) = month(i)
          Write (2,'(x,I4,x,I2,3(x,F6.2),x,F8.5,x,E10.3,x,F8.4)')
     2          int(f10_7(2,1,i)),int(f10_7(2,2,i)),f10_7(1,3,i),
     3          f10_7(2,3,i),f10_7(3,3,i),f10_7(2,4,i),f10_7(2,5,i),
     4          f10_7(2,6,i)
30      continue

        Write (3,'(20x,A)') 'Actual data'       ! header for actual data file
        Write (3,'(A)') ' '
        Do 31, i = 1,36
          month(i) = i - int((i-1)/12)*12
          mof107(2,1,i) = yr(i)
          mof107(2,2,i) = month(i)
          Write (3,'(x,I4,x,I2,x,F6.2,x,F8.5,x,E10.3,x,F8.4)')
     2          int(mof107(2,1,i)),int(mof107(2,2,i)),mof107(2,3,i),
     3          mof107(2,4,i),mof107(2,5,i),mof107(2,6,i)
31      continue

        Do 32, i = 1,248
          month(i) = i - int((i-1)/12)*12
          f10_7(2,1,i) = yr(i)
          f10_7(2,2,i) = month(i)
          Write (4,'(x,I4,x,I2,3(x,F6.2),x,F8.5,x,E10.3,x,F8.4)')
     2          int(f10_7(2,1,i)),int(f10_7(2,2,i)),f10_7(1,3,i),
     3          f10_7(2,3,i),f10_7(3,3,i),f10_7(2,4,i),f10_7(2,5,i),
     4          f10_7(2,6,i)
32      continue

        Close(1)
        Close(2)
        Close(3)
        Close(4)

        End
```

APPENDIX B

Tabulated Results

Year	DOY	Prd Per	Prd Dens	Act Dens	10.7	Min Alt	Bst Alt	Max Alt	Act Alt
1982	31	95.3061	0.166E-11	0.110E-11	189	470.725	533.407	596.090	533.919
1982	59	95.2805	0.157E-11	0.113E-11	185	471.380	532.168	592.957	532.550
1982	90	95.2537	0.150E-11	0.899E-12	180	471.386	530.870	590.353	530.898
1982	120	95.2291	0.141E-11	0.472E-12	176	471.966	529.681	587.396	529.872
1982	151	95.2052	0.133E-11	0.427E-12	172	472.808	528.522	584.237	529.139
1982	181	95.1834	0.125E-11	0.450E-12	168	473.734	527.465	581.197	528.572
1982	212	95.1622	0.118E-11	0.434E-12	164	474.726	526.437	578.148	528.158
1982	243	95.1423	0.111E-11	0.647E-12	160	475.769	525.470	575.171	527.447
1982	273	95.1241	0.104E-11	0.999E-12	157	476.864	524.592	572.319	526.563
1982	304	95.1066	0.978E-12	0.900E-12	153	478.005	523.741	569.477	525.402
1982	334	95.0907	0.919E-12	0.910E-12	149	479.620	522.970	566.320	524.172
1982	365	95.0753	0.849E-12	0.507E-12	146	481.010	522.223	563.436	522.837
1983	31	95.0609	0.797E-12	0.411E-12	142	482.158	521.524	560.891	522.310
1983	59	95.0488	0.749E-12	0.450E-12	139	483.519	520.937	558.356	521.804
1983	90	95.0362	0.691E-12	0.383E-12	136	485.124	520.328	555.533	521.213
1983	120	95.0249	0.649E-12	0.396E-12	132	486.255	519.780	553.306	520.639
1983	151	95.0140	0.599E-12	0.387E-12	129	487.913	519.252	550.592	520.088
1983	181	95.0042	0.563E-12	0.295E-12	126	488.983	518.777	548.571	519.750
1983	212	94.9948	0.520E-12	0.316E-12	123	490.533	518.319	546.104	519.435
1983	243	94.9860	0.489E-12	0.312E-12	120	491.545	517.894	544.244	518.967
1983	273	94.9781	0.451E-12	0.408E-12	118	492.950	517.510	542.069	518.618
1983	304	94.9705	0.417E-12	0.354E-12	115	494.302	517.142	539.983	518.168
1983	334	94.9637	0.393E-12	0.283E-12	112	495.154	516.811	538.468	517.841
1983	365	94.9571	0.363E-12	0.259E-12	110	496.383	516.491	536.600	517.553
1984	31	94.9510	0.336E-12	0.355E-12	107	497.527	516.196	534.865	517.166
1984	60	94.9457	0.317E-12	0.483E-12	105	498.286	515.939	533.592	516.757
1984	91	94.9404	0.294E-12	0.519E-12	102	499.279	515.681	532.084	516.121
1984	121	94.9357	0.272E-12	0.314E-12	100	500.233	515.450	530.667	515.656
1984	152	94.9311	0.252E-12	0.258E-12	98	501.118	515.228	529.338	515.322
1984	182	94.9270	0.235E-12	0.235E-12	96	501.940	515.029	528.118	515.081
1984	213	94.9230	0.223E-12	0.199E-12	94	502.447	514.834	527.221	514.816
1984	244	94.9192	0.208E-12	0.236E-12	92	503.157	514.652	526.147	514.638
1984	274	94.9158	0.194E-12	0.000E+00	90	503.820	514.488	525.157	514.484
1984	305	94.9126	0.181E-12	0.000E+00	88	504.424	514.330	524.235	0.000
1984	335	94.9096	0.169E-12	0.000E+00	86	504.985	514.187	523.388	0.000
1984	366	94.9068	0.159E-12	0.000E+00	84	505.495	514.048	522.601	0.000
1985	31	94.9040	0.152E-12	0.000E+00	83	505.785	513.916	522.047	0.000
1985	59	94.9017	0.144E-12	0.000E+00	81	506.213	513.803	521.394	0.000
1985	90	94.8993	0.136E-12	0.000E+00	80	506.614	513.685	520.756	0.000
1985	120	94.8971	0.128E-12	0.000E+00	78	506.976	513.577	520.179	0.000
1985	151	94.8949	0.121E-12	0.000E+00	77	507.303	513.472	519.641	0.000
1985	181	94.8929	0.115E-12	0.000E+00	76	507.597	513.375	519.152	0.000
1985	212	94.8909	0.110E-12	0.000E+00	75	507.864	513.280	518.696	0.000
1985	243	94.8891	0.105E-12	0.000E+00	74	508.101	513.189	518.277	0.000
1985	273	94.8873	0.101E-12	0.000E+00	73	508.314	513.105	517.896	0.000
1985	304	94.8856	0.965E-13	0.000E+00	72	508.502	513.022	517.542	0.000
1985	334	94.8840	0.952E-13	0.000E+00	71	508.564	512.943	517.322	0.000
1985	365	94.8823	0.920E-13	0.000E+00	70	508.714	512.864	517.014	0.000
1986	31	94.8808	0.890E-13	0.000E+00	69	508.846	512.788	516.729	0.000
1986	59	94.8794	0.867E-13	0.000E+00	69	508.960	512.721	516.481	0.000
1986	90	94.8779	0.845E-13	0.000E+00	68	509.053	512.648	516.244	0.000
1986	120	94.8765	0.827E-13	0.000E+00	67	509.129	512.580	516.030	0.000
1986	151	94.8751	0.812E-13	0.000E+00	67	509.190	512.511	515.832	0.000
1986	181	94.8737	0.800E-13	0.000E+00	67	509.238	512.445	515.651	0.000
1986	212	94.8723	0.791E-13	0.000E+00	66	509.269	512.377	515.486	0.000
1986	243	94.8709	0.785E-13	0.000E+00	66	509.284	512.311	515.338	0.000
1986	273	94.8696	0.781E-13	0.000E+00	66	509.288	512.247	515.205	0.000
1986	304	94.8682	0.780E-13	0.000E+00	66	509.278	512.181	515.084	0.000
1986	334	94.8669	0.780E-13	0.000E+00	66	509.258	512.117	514.977	0.000
1986	365	94.8656	0.780E-13	0.000E+00	66	509.230	512.051	514.872	0.000
1987	31	94.8642	0.799E-13	0.000E+00	66	509.133	511.985	514.837	0.000

1987	59	94.8629	0.799E-13	0.000E+00	66	509.093	511.924	514.755	0.000
1987	90	94.8615	0.799E-13	0.000E+00	66	509.046	511.856	514.667	0.000
1987	120	94.8602	0.799E-13	0.000E+00	66	508.990	511.791	514.592	0.000
1987	151	94.8588	0.799E-13	0.000E+00	66	508.927	511.724	514.520	0.000
1987	181	94.8575	0.799E-13	0.000E+00	66	508.866	511.658	514.450	0.000
1987	212	94.8561	0.799E-13	0.000E+00	66	508.722	511.591	514.459	0.000
1987	243	94.8547	0.799E-13	0.000E+00	66	508.529	511.523	514.517	0.000
1987	273	94.8533	0.799E-13	0.000E+00	66	508.292	511.458	514.624	0.000
1987	304	94.8519	0.799E-13	0.000E+00	66	508.009	511.391	514.772	0.000
1987	334	94.8506	0.799E-13	0.000E+00	66	507.686	511.325	514.964	0.000
1987	365	94.8492	0.804E-13	0.000E+00	66	507.305	511.258	515.210	0.000
1988	31	94.8478	0.820E-13	0.000E+00	66	506.848	511.189	515.529	0.000
1988	60	94.8464	0.847E-13	0.000E+00	66	506.382	511.123	515.864	0.000
1988	91	94.8449	0.883E-13	0.000E+00	67	505.868	511.050	516.233	0.000
1988	121	94.8433	0.952E-13	0.000E+00	68	505.174	510.976	516.777	0.000
1988	152	94.8416	0.101E-12	0.000E+00	69	504.537	510.893	517.249	0.000
1988	182	94.8399	0.108E-12	0.000E+00	70	503.840	510.807	517.775	0.000
1988	213	94.8379	0.117E-12	0.000E+00	72	503.071	510.712	518.353	0.000
1988	244	94.8358	0.127E-12	0.000E+00	74	502.224	510.610	518.995	0.000
1988	274	94.8335	0.138E-12	0.000E+00	75	501.299	510.501	519.703	0.000
1988	305	94.8310	0.151E-12	0.000E+00	77	500.288	510.379	520.471	0.000
1988	335	94.8283	0.166E-12	0.000E+00	79	499.194	510.250	521.306	0.000
1988	366	94.8253	0.183E-12	0.000E+00	82	497.998	510.103	522.208	0.000
1989	31	94.8219	0.205E-12	0.000E+00	84	496.432	509.940	523.449	0.000
1989	59	94.8185	0.225E-12	0.000E+00	87	495.086	509.777	524.467	0.000
1989	90	94.8144	0.248E-12	0.000E+00	89	493.598	509.577	525.556	0.000
1989	120	94.8100	0.273E-12	0.000E+00	92	492.033	509.364	526.695	0.000
1989	151	94.8050	0.300E-12	0.000E+00	94	490.372	509.123	527.873	0.000
1989	181	94.7996	0.336E-12	0.000E+00	97	488.242	508.863	529.485	0.000
1989	212	94.7934	0.368E-12	0.000E+00	100	486.410	508.566	530.723	0.000
1989	243	94.7867	0.402E-12	0.000E+00	103	484.514	508.242	531.969	0.000
1989	273	94.7796	0.447E-12	0.000E+00	105	482.106	507.897	533.689	0.000
1989	304	94.7715	0.485E-12	0.000E+00	108	480.072	507.504	534.937	0.000
1989	334	94.7629	0.525E-12	0.000E+00	111	478.052	507.093	536.133	0.000
1989	365	94.7533	0.577E-12	0.000E+00	114	475.393	506.626	537.859	0.000
1990	31	94.7428	0.621E-12	0.000E+00	116	473.255	506.121	538.986	0.000
1990	59	94.7326	0.675E-12	0.000E+00	119	470.622	505.626	540.630	0.000
1990	90	94.7204	0.719E-12	0.000E+00	121	468.529	505.038	541.548	0.000
1990	120	94.7077	0.777E-12	0.000E+00	124	465.780	504.423	543.067	0.000
1990	151	94.6937	0.835E-12	0.000E+00	126	463.006	503.746	544.486	0.000
1990	181	94.6792	0.878E-12	0.000E+00	128	460.999	503.047	545.095	0.000
1990	212	94.6633	0.935E-12	0.000E+00	130	458.263	502.277	546.290	0.000
1990	243	94.6465	0.991E-12	0.000E+00	132	455.581	501.462	547.343	0.000
1990	273	94.6293	0.105E-11	0.000E+00	134	452.956	500.632	548.309	0.000
1990	304	94.6107	0.110E-11	0.000E+00	135	450.377	499.732	549.087	0.000
1990	334	94.5919	0.115E-11	0.000E+00	136	447.987	498.822	549.657	0.000
1990	365	94.5717	0.119E-11	0.000E+00	138	445.613	497.844	550.074	0.000
1991	31	94.5507	0.123E-11	0.000E+00	138	443.207	496.829	550.452	0.000
1991	59	94.5313	0.126E-11	0.000E+00	139	441.270	495.887	550.505	0.000
1991	90	94.5092	0.129E-11	0.000E+00	139	439.042	494.818	550.594	0.000
1991	120	94.4874	0.131E-11	0.000E+00	140	437.014	493.763	550.513	0.000
1991	151	94.4645	0.133E-11	0.000E+00	140	434.854	492.652	550.451	0.000
1991	181	94.4419	0.136E-11	0.000E+00	140	432.730	491.557	550.383	0.000
1991	212	94.4181	0.138E-11	0.000E+00	140	430.541	490.403	550.265	0.000
1991	243	94.3938	0.140E-11	0.000E+00	140	428.312	489.226	550.139	0.000
1991	273	94.3698	0.143E-11	0.000E+00	140	426.082	488.064	550.046	0.000
1991	304	94.3445	0.148E-11	0.000E+00	140	422.864	486.836	550.808	0.000
1991	334	94.3195	0.151E-11	0.000E+00	140	420.348	485.623	550.898	0.000
1991	365	94.2931	0.153E-11	0.000E+00	140	417.898	484.343	550.787	0.000
1992	31	94.2661	0.156E-11	0.000E+00	140	415.421	483.035	550.650	0.000
1992	60	94.2403	0.161E-11	0.000E+00	140	411.993	481.782	551.572	0.000
1992	91	94.2120	0.164E-11	0.000E+00	140	409.176	480.412	551.648	0.000
1992	121	94.1841	0.167E-11	0.000E+00	140	406.562	479.057	551.552	0.000

1992	152	94.1544	0.173E-11	0.000E+00	140	402.596	477.619	552.642	0.000
1992	182	94.1251	0.176E-11	0.000E+00	140	399.806	476.195	552.583	0.000
1992	213	94.0939	0.182E-11	0.000E+00	140	395.689	474.684	553.679	0.000
1992	244	94.0620	0.186E-11	0.000E+00	140	392.635	473.133	553.630	0.000
1992	274	94.0301	0.192E-11	0.000E+00	140	388.303	471.589	554.876	0.000
1992	305	93.9964	0.199E-11	0.000E+00	140	385.119	469.953	554.787	0.000
1992	335	93.9627	0.203E-11	0.000E+00	140	380.474	468.319	556.163	0.000
1992	366	93.9270	0.209E-11	0.000E+00	140	375.852	466.584	557.317	0.000
1993	31	93.8903	0.216E-11	0.000E+00	139	370.265	464.802	559.340	0.000
1993	59	93.8562	0.219E-11	0.000E+00	139	366.766	463.147	559.529	0.000
1993	90	93.8175	0.226E-11	0.000E+00	139	361.916	461.266	560.616	0.000
1993	120	93.7789	0.233E-11	0.000E+00	139	357.103	459.395	561.686	0.000
1993	151	93.7380	0.239E-11	0.000E+00	139	352.215	457.409	562.602	0.000
1993	181	93.6974	0.245E-11	0.000E+00	138	347.452	455.435	563.419	0.000
1993	212	93.6543	0.252E-11	0.000E+00	138	342.531	453.342	564.154	0.000
1993	243	93.6101	0.258E-11	0.000E+00	137	337.659	451.194	564.729	0.000
1993	273	93.5662	0.264E-11	0.000E+00	137	332.800	449.058	565.316	0.000
1993	304	93.5195	0.275E-11	0.000E+00	136	326.697	446.792	566.888	0.000
1993	334	93.4732	0.281E-11	0.000E+00	135	321.110	444.541	567.971	0.000
1993	365	93.4242	0.286E-11	0.000E+00	134	316.062	442.156	568.250	0.000
1994	31	93.3738	0.297E-11	0.000E+00	134	309.501	439.705	569.908	0.000
1994	59	93.3271	0.303E-11	0.000E+00	133	304.236	437.432	570.628	0.000
1994	90	93.2740	0.314E-11	0.000E+00	132	298.308	434.853	571.398	0.000
1994	120	93.2212	0.319E-11	0.000E+00	131	291.769	432.283	572.796	0.000
1994	151	93.1650	0.331E-11	0.000E+00	130	284.390	429.549	574.708	0.000
1994	181	93.1091	0.343E-11	0.000E+00	129	278.131	426.828	575.526	0.000
1994	212	93.0495	0.355E-11	0.000E+00	128	271.176	423.926	576.677	0.000
1994	243	92.9879	0.367E-11	0.000E+00	127	263.151	420.928	578.705	0.000
1994	273	92.9263	0.379E-11	0.000E+00	125	254.947	417.928	580.909	0.000
1994	304	92.8603	0.392E-11	0.000E+00	124	244.613	414.715	584.817	0.000
1994	334	92.7941	0.405E-11	0.000E+00	123	235.110	411.489	587.869	0.000
1994	365	92.7230	0.419E-11	0.000E+00	122	225.454	408.024	590.595	0.000
1995	31	92.6488	0.441E-11	0.000E+00	120	213.046	404.406	595.767	0.000
1995	59	92.5788	0.465E-11	0.000E+00	119	202.934	400.995	599.057	0.000
1995	90	92.4976	0.481E-11	0.000E+00	118	188.813	397.035	605.257	0.000
1995	120	92.4147	0.518E-11	0.000E+00	116	173.989	392.999	612.009	0.000
1995	151	92.3241	0.546E-11	0.000E+00	115	155.488	388.581	621.674	0.000
1995	181	92.2307	0.576E-11	0.000E+00	114	136.912	384.025	631.139	0.000
1995	212	92.1270	0.635E-11	0.000E+00	112	113.365	378.972	644.578	0.000
1995	243	92.0147	0.686E-11	0.000E+00	111	84.379	373.490	662.601	0.000
1995	273	91.8956	0.757E-11	0.000E+00	109	51.728	367.686	683.644	0.000
1995	304	91.7592	0.838E-11	0.000E+00	108	9.646	361.029	712.413	0.000
1995	334	91.6100	0.971E-11	0.000E+00	106	-41.761	353.757	749.275	0.000
1995	365	91.4312	0.113E-10	0.000E+00	105	*******	345.038	809.246	0.000
1996	31	91.2158	0.141E-10	0.000E+00	103	*******	334.550	899.340	0.000
1996	60	90.9615	0.181E-10	0.000E+00	102	*******	322.177	*******	0.000
1996	91	90.5815	0.279E-10	0.000E+00	100	*******	303.764	*******	0.000
1996	121	89.9240	0.600E-10	0.000E+00	99	*******	272.254	*******	0.000
1996	145	84.9340	0.450E-08	0.000E+00	97	0.000	0.000	0.000	0.000

Predicted data

1 sigma standard deviation = 18

1982	1	167.71	189.51	203.70	95.31755	0.766E-12	533.9187
1982	2	163.53	185.17	199.46	95.28923	0.110E-11	532.5496
1982	3	159.45	180.92	195.31	95.25508	0.113E-11	530.8984
1982	4	155.48	176.75	191.22	95.23385	0.899E-12	529.8721
1982	5	151.61	172.67	187.20	95.21869	0.472E-12	529.1389
1982	6	147.83	168.66	183.26	95.20697	0.427E-12	528.5718
1982	7	144.16	164.73	179.39	95.19840	0.450E-12	528.1577
1982	8	140.59	160.88	175.59	95.18370	0.434E-12	527.4467
1982	9	137.11	157.11	171.86	95.16543	0.647E-12	526.5628
1982	10	133.73	153.43	168.20	95.14144	0.999E-12	525.4023
1982	11	130.44	149.82	164.61	95.11601	0.900E-12	524.1723
1982	12	127.24	146.29	161.09	95.08841	0.910E-12	522.8369
1983	1	124.14	142.84	157.64	95.07752	0.507E-12	522.3101
1983	2	121.13	139.47	154.27	95.06706	0.411E-12	521.8037
1983	3	118.20	136.18	150.96	95.05485	0.450E-12	521.2130
1983	4	115.37	132.96	147.72	95.04300	0.383E-12	520.6394
1983	5	112.62	129.83	144.56	95.03161	0.396E-12	520.0883
1983	6	109.96	126.77	141.46	95.02461	0.387E-12	519.7497
1983	7	107.38	123.79	138.43	95.01811	0.295E-12	519.4351
1983	8	104.89	120.89	135.47	95.00843	0.316E-12	518.9667
1983	9	102.48	118.07	132.58	95.00124	0.312E-12	518.6185
1983	10	100.15	115.33	129.76	94.99193	0.408E-12	518.1679
1983	11	97.89	112.66	127.01	94.98517	0.354E-12	517.8410
1983	12	95.72	110.07	124.32	94.97910	0.283E-12	517.5535
1984	1	93.63	107.55	121.71	94.97122	0.259E-12	517.1659
1984	2	91.61	105.11	119.16	94.96277	0.355E-12	516.7566
1984	3	89.66	102.75	116.68	94.94906	0.483E-12	516.1212
1984	4	87.79	100.47	114.27	94.94004	0.519E-12	515.6564
1984	5	85.99	98.26	111.93	94.93313	0.314E-12	515.3219
1984	6	84.26	96.12	109.65	94.92816	0.258E-12	515.0812
1984	7	82.61	94.07	107.44	94.92268	0.235E-12	514.8159
1984	8	81.02	92.08	105.30	94.91901	0.199E-12	514.6384
1984	9	79.49	90.18	103.22	94.91570	0.236E-12	514.4835
1984	10	78.04	88.34	101.22	0.00000	0.000E+00	0.0000
1984	11	76.65	86.59	99.28	0.00000	0.000E+00	0.0000
1984	12	75.32	84.90	97.40	0.00000	0.000E+00	0.0000
1985	1	74.06	83.30	95.59	0.00000	0.000E+00	0.0000
1985	2	72.85	81.76	93.85	0.00000	0.000E+00	0.0000
1985	3	71.71	80.30	92.17	0.00000	0.000E+00	0.0000
1985	4	70.63	78.91	90.56	0.00000	0.000E+00	0.0000
1985	5	69.60	77.60	89.01	0.00000	0.000E+00	0.0000
1985	6	68.63	76.36	87.53	0.00000	0.000E+00	0.0000
1985	7	67.72	75.20	86.12	0.00000	0.000E+00	0.0000
1985	8	66.86	74.10	84.77	0.00000	0.000E+00	0.0000
1985	9	66.05	73.08	83.48	0.00000	0.000E+00	0.0000
1985	10	65.29	72.14	82.26	0.00000	0.000E+00	0.0000
1985	11	64.58	71.26	81.11	0.00000	0.000E+00	0.0000
1985	12	63.93	70.46	80.02	0.00000	0.000E+00	0.0000
1986	1	63.32	69.73	78.99	0.00000	0.000E+00	0.0000
1986	2	62.75	69.07	78.02	0.00000	0.000E+00	0.0000
1986	3	62.24	68.48	77.13	0.00000	0.000E+00	0.0000
1986	4	61.76	67.96	76.29	0.00000	0.000E+00	0.0000
1986	5	61.33	67.52	75.52	0.00000	0.000E+00	0.0000
1986	6	60.95	67.14	74.81	0.00000	0.000E+00	0.0000
1986	7	60.60	66.84	74.16	0.00000	0.000E+00	0.0000
1986	8	60.29	66.61	73.58	0.00000	0.000E+00	0.0000
1986	9	60.02	66.45	73.06	0.00000	0.000E+00	0.0000
1986	10	59.79	66.35	72.60	0.00000	0.000E+00	0.0000
1986	11	59.59	66.33	72.21	0.00000	0.000E+00	0.0000
1986	12	59.42	66.33	71.87	0.00000	0.000E+00	0.0000
1987	1	59.29	66.33	71.60	0.00000	0.000E+00	0.0000

1987	2	59.19	66.33	71.39	0.00000	0.000E+00	0.0000
1987	3	59.13	66.33	71.24	0.00000	0.000E+00	0.0000
1987	4	59.09	66.33	71.16	0.00000	0.000E+00	0.0000
1987	5	59.08	66.33	71.13	0.00000	0.000E+00	0.0000
1987	6	59.08	66.33	71.11	0.00000	0.000E+00	0.0000
1987	7	59.08	66.33	71.44	0.00000	0.000E+00	0.0000
1987	8	59.08	66.33	71.98	0.00000	0.000E+00	0.0000
1987	9	59.08	66.33	72.72	0.00000	0.000E+00	0.0000
1987	10	59.08	66.33	73.65	0.00000	0.000E+00	0.0000
1987	11	59.08	66.33	74.76	0.00000	0.000E+00	0.0000
1987	12	59.08	66.33	76.03	0.00000	0.000E+00	0.0000
1988	1	59.12	66.47	77.47	0.00000	0.000E+00	0.0000
1988	2	59.48	66.87	79.06	0.00000	0.000E+00	0.0000
1988	3	60.06	67.52	80.79	0.00000	0.000E+00	0.0000
1988	4	60.85	68.40	82.65	0.00000	0.000E+00	0.0000
1988	5	61.84	69.50	84.63	0.00000	0.000E+00	0.0000
1988	6	63.01	70.81	86.72	0.00000	0.000E+00	0.0000
1988	7	64.36	72.32	88.91	0.00000	0.000E+00	0.0000
1988	8	65.87	74.00	91.20	0.00000	0.000E+00	0.0000
1988	9	67.52	75.85	93.57	0.00000	0.000E+00	0.0000
1988	10	69.32	77.85	96.01	0.00000	0.000E+00	0.0000
1988	11	71.23	79.99	98.51	0.00000	0.000E+00	0.0000
1988	12	73.26	82.25	101.07	0.00000	0.000E+00	0.0000
1989	1	75.39	84.63	103.67	0.00000	0.000E+00	0.0000
1989	2	77.60	87.10	106.31	0.00000	0.000E+00	0.0000
1989	3	79.89	89.65	108.96	0.00000	0.000E+00	0.0000
1989	4	82.24	92.27	111.64	0.00000	0.000E+00	0.0000
1989	5	84.64	94.95	114.32	0.00000	0.000E+00	0.0000
1989	6	87.08	97.67	116.99	0.00000	0.000E+00	0.0000
1989	7	89.54	100.42	119.64	0.00000	0.000E+00	0.0000
1989	8	92.02	103.18	122.28	0.00000	0.000E+00	0.0000
1989	9	94.50	105.95	124.88	0.00000	0.000E+00	0.0000
1989	10	96.96	108.70	127.43	0.00000	0.000E+00	0.0000
1989	11	99.40	111.42	129.93	0.00000	0.000E+00	0.0000
1989	12	101.80	114.10	132.37	0.00000	0.000E+00	0.0000
1990	1	104.16	116.72	134.73	0.00000	0.000E+00	0.0000
1990	2	106.45	119.28	137.02	0.00000	0.000E+00	0.0000
1990	3	108.67	121.76	139.20	0.00000	0.000E+00	0.0000
1990	4	110.80	124.13	141.29	0.00000	0.000E+00	0.0000
1990	5	112.83	126.40	143.26	0.00000	0.000E+00	0.0000
1990	6	114.75	128.54	145.12	0.00000	0.000E+00	0.0000
1990	7	116.55	130.55	146.84	0.00000	0.000E+00	0.0000
1990	8	118.22	132.41	148.42	0.00000	0.000E+00	0.0000
1990	9	119.73	134.09	149.85	0.00000	0.000E+00	0.0000
1990	10	121.09	135.60	151.12	0.00000	0.000E+00	0.0000
1990	11	122.27	136.92	152.21	0.00000	0.000E+00	0.0000
1990	12	123.27	138.03	153.13	0.00000	0.000E+00	0.0000
1991	1	124.07	138.92	153.86	0.00000	0.000E+00	0.0000
1991	2	124.66	139.58	154.39	0.00000	0.000E+00	0.0000
1991	3	125.03	139.98	154.71	0.00000	0.000E+00	0.0000
1991	4	125.16	140.13	154.81	0.00000	0.000E+00	0.0000
1991	5	125.16	140.13	154.81	0.00000	0.000E+00	0.0000
1991	6	125.16	140.13	154.81	0.00000	0.000E+00	0.0000
1991	7	125.16	140.13	154.81	0.00000	0.000E+00	0.0000
1991	8	125.16	140.13	154.81	0.00000	0.000E+00	0.0000
1991	9	125.16	140.13	154.81	0.00000	0.000E+00	0.0000
1991	10	125.16	140.13	154.81	0.00000	0.000E+00	0.0000
1991	11	125.16	140.13	154.81	0.00000	0.000E+00	0.0000
1991	12	125.16	140.13	154.81	0.00000	0.000E+00	0.0000
1992	1	125.16	140.13	154.81	0.00000	0.000E+00	0.0000
1992	2	125.16	140.13	154.81	0.00000	0.000E+00	0.0000
1992	3	125.16	140.13	154.81	0.00000	0.000E+00	0.0000
1992	4	125.16	140.13	154.81	0.00000	0.000E+00	0.0000

1992	5	125.16	140.13	154.81	0.00000	0.000E+00	0.0000
1992	6	125.16	140.13	154.81	0.00000	0.000E+00	0.0000
1992	7	125.16	140.13	154.81	0.00000	0.000E+00	0.0000
1992	8	125.16	140.13	154.81	0.00000	0.000E+00	0.0000
1992	9	125.16	140.13	154.81	0.00000	0.000E+00	0.0000
1992	10	125.16	140.13	154.81	0.00000	0.000E+00	0.0000
1992	11	125.16	140.13	154.81	0.00000	0.000E+00	0.0000
1992	12	125.16	140.13	154.81	0.00000	0.000E+00	0.0000
1993	1	124.97	139.96	154.96	0.00000	0.000E+00	0.0000
1993	2	124.87	139.85	154.83	0.00000	0.000E+00	0.0000
1993	3	124.70	139.66	154.61	0.00000	0.000E+00	0.0000
1993	4	124.47	139.40	154.32	0.00000	0.000E+00	0.0000
1993	5	124.18	139.07	153.95	0.00000	0.000E+00	0.0000
1993	6	123.83	138.67	153.49	0.00000	0.000E+00	0.0000
1993	7	123.42	138.21	152.97	0.00000	0.000E+00	0.0000
1993	8	122.96	137.68	152.37	0.00000	0.000E+00	0.0000
1993	9	122.44	137.09	151.71	0.00000	0.000E+00	0.0000
1993	10	121.87	136.45	150.98	0.00000	0.000E+00	0.0000
1993	11	121.25	135.74	150.18	0.00000	0.000E+00	0.0000
1993	12	120.58	134.98	149.32	0.00000	0.000E+00	0.0000
1994	1	119.87	134.16	148.40	0.00000	0.000E+00	0.0000
1994	2	119.10	133.30	147.42	0.00000	0.000E+00	0.0000
1994	3	118.30	132.38	146.38	0.00000	0.000E+00	0.0000
1994	4	117.45	131.42	145.30	0.00000	0.000E+00	0.0000
1994	5	116.57	130.41	144.16	0.00000	0.000E+00	0.0000
1994	6	115.64	129.36	142.97	0.00000	0.000E+00	0.0000
1994	7	114.68	128.27	141.74	0.00000	0.000E+00	0.0000
1994	8	113.69	127.14	140.46	0.00000	0.000E+00	0.0000
1994	9	112.66	125.97	139.14	0.00000	0.000E+00	0.0000
1994	10	111.60	124.77	137.78	0.00000	0.000E+00	0.0000
1994	11	110.52	123.53	136.39	0.00000	0.000E+00	0.0000
1994	12	109.40	122.26	134.96	0.00000	0.000E+00	0.0000
1995	1	108.26	120.97	133.50	0.00000	0.000E+00	0.0000
1995	2	107.10	119.65	132.01	0.00000	0.000E+00	0.0000
1995	3	105.91	118.30	130.49	0.00000	0.000E+00	0.0000
1995	4	104.71	116.93	128.95	0.00000	0.000E+00	0.0000
1995	5	103.49	115.54	127.38	0.00000	0.000E+00	0.0000
1995	6	102.25	114.13	125.79	0.00000	0.000E+00	0.0000
1995	7	100.99	112.70	124.19	0.00000	0.000E+00	0.0000
1995	8	99.73	111.26	122.57	0.00000	0.000E+00	0.0000
1995	9	98.45	109.80	120.94	0.00000	0.000E+00	0.0000
1995	10	97.16	108.34	119.29	0.00000	0.000E+00	0.0000
1995	11	95.87	106.86	117.64	0.00000	0.000E+00	0.0000
1995	12	94.57	105.38	115.98	0.00000	0.000E+00	0.0000
1996	1	93.27	103.90	114.31	0.00000	0.000E+00	0.0000
1996	2	91.96	102.41	112.65	0.00000	0.000E+00	0.0000
1996	3	90.66	100.93	110.98	0.00000	0.000E+00	0.0000
1996	4	89.35	99.44	109.32	0.00000	0.000E+00	0.0000
1996	5	88.05	97.96	107.66	0.00000	0.000E+00	0.0000
1996	6	86.76	96.48	106.01	0.00000	0.000E+00	0.0000
1996	7	85.47	95.01	104.37	0.00000	0.000E+00	0.0000
1996	8	84.19	93.56	102.75	0.00000	0.000E+00	0.0000
1996	9	82.92	92.11	101.14	0.00000	0.000E+00	0.0000
1996	10	81.66	90.68	99.54	0.00000	0.000E+00	0.0000
1996	11	80.42	89.26	97.96	0.00000	0.000E+00	0.0000
1996	12	79.20	87.86	96.41	0.00000	0.000E+00	0.0000
1997	1	77.99	86.48	94.88	0.00000	0.000E+00	0.0000
1997	2	76.80	85.13	93.38	0.00000	0.000E+00	0.0000
1997	3	75.63	83.79	91.90	0.00000	0.000E+00	0.0000
1997	4	74.49	82.49	90.46	0.00000	0.000E+00	0.0000
1997	5	73.37	81.21	89.04	0.00000	0.000E+00	0.0000
1997	6	72.28	79.96	87.67	0.00000	0.000E+00	0.0000
1997	7	71.22	78.74	86.33	0.00000	0.000E+00	0.0000

1997	8	70.18	77.56	85.04	0.00000	0.000E+00	0.0000
1997	9	69.18	76.42	83.78	0.00000	0.000E+00	0.0000
1997	10	68.22	75.31	82.57	0.00000	0.000E+00	0.0000
1997	11	67.29	74.24	81.41	0.00000	0.000E+00	0.0000
1997	12	66.39	73.22	80.30	0.00000	0.000E+00	0.0000
1998	1	65.54	72.24	79.24	0.00000	0.000E+00	0.0000
1998	2	64.73	71.31	78.24	0.00000	0.000E+00	0.0000
1998	3	63.96	70.42	77.29	0.00000	0.000E+00	0.0000
1998	4	63.23	69.59	76.40	0.00000	0.000E+00	0.0000
1998	5	62.55	68.81	75.57	0.00000	0.000E+00	0.0000
1998	6	61.93	68.08	74.81	0.00000	0.000E+00	0.0000
1998	7	61.35	67.41	74.11	0.00000	0.000E+00	0.0000
1998	8	60.82	66.80	73.48	0.00000	0.000E+00	0.0000
1998	9	60.35	66.25	72.92	0.00000	0.000E+00	0.0000
1998	10	59.93	65.77	72.44	0.00000	0.000E+00	0.0000
1998	11	59.57	65.34	72.03	0.00000	0.000E+00	0.0000
1998	12	59.27	64.99	71.69	0.00000	0.000E+00	0.0000
1999	1	59.03	64.70	71.44	0.00000	0.000E+00	0.0000
1999	2	58.85	64.49	71.27	0.00000	0.000E+00	0.0000
1999	3	58.74	64.34	71.19	0.00000	0.000E+00	0.0000
1999	4	58.69	64.28	71.19	0.00000	0.000E+00	0.0000
1999	5	59.16	65.20	70.24	0.00000	0.000E+00	0.0000
1999	6	59.64	65.78	70.94	0.00000	0.000E+00	0.0000
1999	7	60.41	66.73	72.08	0.00000	0.000E+00	0.0000
1999	8	61.46	68.02	73.64	0.00000	0.000E+00	0.0000
1999	9	62.78	69.64	75.59	0.00000	0.000E+00	0.0000
1999	10	64.35	71.56	77.90	0.00000	0.000E+00	0.0000
1999	11	66.14	73.76	80.55	0.00000	0.000E+00	0.0000
1999	12	68.15	76.23	83.52	0.00000	0.000E+00	0.0000
2000	1	70.36	78.94	86.78	0.00000	0.000E+00	0.0000
2000	2	72.75	81.87	90.32	0.00000	0.000E+00	0.0000
2000	3	75.30	85.00	94.09	0.00000	0.000E+00	0.0000
2000	4	78.01	88.32	98.08	0.00000	0.000E+00	0.0000
2000	5	80.84	91.80	102.27	0.00000	0.000E+00	0.0000
2000	6	83.79	95.42	106.63	0.00000	0.000E+00	0.0000
2000	7	86.84	99.16	111.14	0.00000	0.000E+00	0.0000
2000	8	89.98	103.00	115.77	0.00000	0.000E+00	0.0000
2000	9	93.17	106.92	120.50	0.00000	0.000E+00	0.0000
2000	10	96.42	110.90	125.30	0.00000	0.000E+00	0.0000
2000	11	99.70	114.92	130.15	0.00000	0.000E+00	0.0000
2000	12	103.00	118.96	135.02	0.00000	0.000E+00	0.0000
2001	1	106.30	123.00	139.89	0.00000	0.000E+00	0.0000
2001	2	109.58	127.02	144.74	0.00000	0.000E+00	0.0000
2001	3	112.83	131.00	149.55	0.00000	0.000E+00	0.0000
2001	4	116.02	134.91	154.27	0.00000	0.000E+00	0.0000
2001	5	119.16	138.75	158.91	0.00000	0.000E+00	0.0000
2001	6	122.21	142.48	163.42	0.00000	0.000E+00	0.0000
2001	7	125.16	146.09	167.78	0.00000	0.000E+00	0.0000
2001	8	127.99	149.56	171.97	0.00000	0.000E+00	0.0000
2001	9	130.70	152.87	175.97	0.00000	0.000E+00	0.0000
2001	10	133.25	155.99	179.76	0.00000	0.000E+00	0.0000
2001	11	135.64	158.91	183.29	0.00000	0.000E+00	0.0000
2001	12	137.85	161.60	186.56	0.00000	0.000E+00	0.0000
2002	1	139.86	164.06	189.54	0.00000	0.000E+00	0.0000
2002	2	141.65	166.24	192.20	0.00000	0.000E+00	0.0000
2002	3	143.22	168.15	194.52	0.00000	0.000E+00	0.0000
2002	4	144.54	169.74	196.48	0.00000	0.000E+00	0.0000
2002	5	145.59	171.02	198.04	0.00000	0.000E+00	0.0000
2002	6	146.36	171.94	199.19	0.00000	0.000E+00	0.0000
2002	7	146.84	172.50	199.91	0.00000	0.000E+00	0.0000
2002	8	147.00	172.68	200.16	0.00000	0.000E+00	0.0000

APPENDIX C

Ephemeris of the Solar Mesosphere Explorer

Goddard Space Flight Center

Ground Tracking and Data

System Ephemeris Program

```
                              GTDS  EPHEM   PROGR                                                    PAGE
JOB IDENTIFICATION:Z0535PET          COMPUTER IDENTIFICATION: C1              STARTING ADDRESS OF MAIN:  400054(075500)
GTDS RUN NUMBER   1  127828          RUN DATE: OCT  31 1983                   TIME: 21 HRS  14 MINS  14.2637 SECS
******************************************************************************************************************

                              GTDS  EPHEM   PROGRAM                                                  PAGE    6
                                    GTDS INITIAL CONDITIONS REPORT
                                          INDEX - GTDS INITIAL CONDITIONS REPORT
                              ORBIT GENERATION

CURRENT TIME OCT 31, 1983, 21 HRS,14 MIN,  22.147 SEC                                     SCOPES NOT  IN USE
SATELLITE NAME          SMF
SATELLITE NUMBER         6110001
SATELLITE CONFIGURATION:
      SATELLITE IS SPHERICAL
      DIAMETER                 =  0.11585520D+01  METERS      COEFFICIENT OF DRAG USED FOR THE RUN =  0.23000000E+01
      MASS                     =  0.41550000D+03  KG
      AREA VARIATION (RHO1)    =  0.0
      REFLECTIVITY CONSTANT    =  0.12000000D+01              AREA FOR RADIATION PRESSURE          =  0.11290000E+01 M**2

* * * * * * * * * * * * * * * * * * * * * * * * *ORBIT GENERATOR OPTIONS* * * * * * * * * * * * * * * * * * * * * * *

ORBIT GENERATOR TYPE-
NUMERICAL INTEGRATION OF COWELL EQUATIONS OF MOTION
      NO STATE PARTIALS CONSIDERED

NON-STATE PARTIALS (COMPUTED BY NUMERICAL INTEGRATION)-
NO NON-STATE PARTIALS CONSIDERED

* * * * * * * * * * * * * * * * * * * * * * * * * * * * * * * * * * * * * * * * * * * * * * * * * * * * * * * * * *

                                    TRAJECTORY INITIAL CONDITIONS
                                    (AS SPECIFIED BY INPUT DATA)
                                      CASE NUMBER        1
                      EPOCH TIME                   =OCT 29, 1983,  0 HRS,  0 MIN,   0.0   SEC
                      END   TIME                   =OCT  1, 1985,  0 HRS,  0 MIN,   0.0   SEC
                      REFERENCE DATE OF INPUT      =OCT 29, 1983
                      TIME SPAN FOR THIS FLIGHT    = 703 DAYS          0.0     HRS
                      PRINT START TIME             =OCT 29, 1983   0 HRS,  0 MIN,      0.0   SEC
                      PRINT FREQUENCY              = EVERY    152 TH NODAL CROSSING
```

```
                                   GTCS   EPHEM    PROGI                                                    PAGE
                                        GTDS INITIAL CONDITIONS REPORT
ADVANCED VECTOR REPORT  FOR    SME        8110001
INITIAL EPOCH AND ELEMENTS FROM 24 HOUR HOLD ELEMENTS FILE
EPOCH TIME=OCT 29, 1983,  0 HRS,  0 MIN,   0.0    SEC WILL BE USED AS ANCHOR POINT . NO EPOCH ADVANCE OCCURS.
CARTESIAN                 ELEMENTS INPUT          CENTRAL BODY = EARTH        TRUE OF REFERENCE
CARTESIAN COORDINATES
          X     0.50517212826643390+03       Y    -0.23852156881373730+04        Z    -0.43712557818684090+04
          DX   -0.10816308469125290+01       DY   -0.69931277692356540+01        DZ    0.37422736532256490+01
KEPLERIAN ELEMENTS
          SMA   0.68835118372486730+04       ECC   0.27088672280944440-02        INC   0.97661540274124840+02
          LAN   0.26415638891479090+03       AP    0.11237220308662410+03        MA    0.17500287053541670+03
SPHERICAL COORDINATES
          RA    0.28273481887082010+03       DEC  -0.67381808115018140+02        VPA   0.89997387124186630+02
          AZ    0.33999113660558480+03       RMAG  0.69021900424942950+04        VMAG  0.75865066530197504D+01
OTHER PARAMETERS (REFERENCED TO CENTRAL BODY AND COORDINATE FRAME OF INTEGRATION)
          EA    0.17980556340158580+03       P     0.94727203739152440+02        SLR   0.68823461386132795D+04
          PR    0.68648708244780180+04       APR   0.65021522580653270+04        PH    0.48673862442881840+03
          APH   0.52401285006932720+03       C3   -0.28553398081394030+02        TA    0.17980825263171840+03
          LAT  -0.67806653116811450+02       LON   0.24597433608482100+03        HGHT  0.64228441313122540+03
*********************************************************************************************************
*                                   DEFINITIONS OF ABBREVIATIONS                                        *
*    X,Y,Z      = POSITION IN KM                                EA    = ECCENTRIC ANOMALY IN DEGREES    *
*    DX,DY,DZ   = VELOCITY IN KM/SEC                            P     = PERIOD IN MINUTES               *
*    SMA        = SEMI-MAJOR AXIS IN KM                         SLR   = SEMI-LATUS RECTUM IN KM         *
*    ECC        = ECCENTRICITY                                  PR    = PERIFOCAL RADIUS IN KM          *
*    INC        = INCLINATION IN DEGREES                        APR   = APOFOCAL RADIUS IN KM           *
*    RAAN       = RIGHT ASCENSION OF ASCENDING NODE DEGREES     PH    = MEAN PERIFOCAL HEIGHT IN KM     *
*    AP         = ARGUMENT OF PERIFOCUS IN DEGREES              APH   = MEAN APOFOCAL HEIGHT IN KM      *
*    MA         = MEAN ANOMALY IN DEGREES                       C3    = ENERGY IN KM**2/SEC**2          *
*    RA         = RIGHT ASCENSION IN DEGREES                    TA    = TRUE ANOMALY IN DEGREES         *
*    DEC        = DECLINATION IN DEGREES                        LAT   = LATITUDE IN DEGREES             *
*    VPA        = VERTICAL FLIGHT PATH ANGLE IN DEGREES         LON   = LONGITUDE IN DEGREES            *
*    AZ         = VELOCITY AZIMUTH IN DEGREES                   HGHT  = HEIGHT IN KM                    *
*    RMAG       = MAGNITUDE OF POSITION VECTOR IN KM                                                    *
*    VMAG       = MAGNITUDE OF VELOCITY VECTOR IN KM                                                    *
*********************************************************************************************************
```

```
GTDS EPHEM  PROGR.                                                  PAGE
                    GTDS INITIAL CONDITIONS REPORT

* * * * * * * * * * * * * * * * * * * * * * * * * * * * * * * * * * * * * * * * * * *
* * * * * * * * * * * * * * * * * * * * * NUMERICAL INTEGRATION OPTIONS AND PARAMETERS * * * * * * * * * * * * * * * * * * * * * * *

NUMERICAL INTEGRATOR TYPE FOR STATE PROPAGATION-
     12 TH ORDER SUMMED COWELL/ADAMS PREDICT-PARTIAL CORRECT
NUMERICAL INTEGRATOR TYPE VARIATIONAL EQUATIONS-
     8 TH ORDER SUMMED COWELL/ADAMS CORRECTOR-ONLY

* * * * * * * * * * * * * * * * * * * * * * * * * * * * * INTEGRATION PARAMETERS* * * * * * * * * * * * * * * * * * * * * * * * * * *
          CONVERGENCE TOLERANCE FOR PREDICTOR-CORRECTOR ITERATIONS            =  0.5000D+00
          MAXIMUM NUMBER OF CORRECTOR ITERATIONS                              =     3
          CORRECTOR TOLERANCE FOR EQUATIONS OF MOTIONS MULTISTEP STARTER      =  0.1000D-12
          CORRECTOR TOLERANCE FOR VARIATIONAL EQUATIONS STARTER               =  0.1000D-12
          MAXIMUM NUMBER OF CORRECTOR ITERATIONS IN STARTER                   =    15

* * * * * * * * * * * * * * * * * * * * * * * * * * * * * * * * * * * * * * * * * * *
* * * * * * * * * * * * * * * * * * * * * * SECTIONING DEPENDENT PARAMETERS * * * * * * * * * * * * * * * * * * * * * * * * * * * *

                              TOTAL NUMBER OF SECTIONS   1

                               FORCE OPTIONS CONSIDERED

     SYSTEM OF INTEGRATION                        TRUE OF REFERENCE
     NAME OF ATMOSPHERIC DENSITY MODEL            1964 HARRIS/PRIESTER ATMOSPHERE (MIN-MAX) 0-2000 KM  P=100
          TIME VARIATION IN ATMOSPHERE DENSITY                              =   0.0
          DIURNAL VARIATION IN ATMOSPHERIC DENSITY                          =   0.0
          ANGLE BETWEEN SUN LINE AND APEX OF DIURNAL ATMOSPHERIC BULGE      =   0.52359878D+00
          POWER OF COSINE FOR COMPUTING ATMOSPHERIC DENSITY                 =   6
     NAME OF EARTH POTENTIAL FIELD MODEL          GEOPOTENTIAL EARTH MODEL NINE (GEM-9)
     NAME OF LUNAR POTENTIAL FIELD MODEL          NOT REQUIRED
     NO SECTION MODEL RETRIEVED FROM PERM FILES(DEFAULT AND CARD INPUT USED)

                    SECTION  1
INTEG STP MODE       FIXED
STEP SIZE (SEC)      180.0
HARMONICS          ZON-TESL
   MAX DEGREE          8
   MAX ORDER           8
RESONANT POTENTIAL  YES
      ORDER           15
CENTRAL BODY       EARTH
NON-CENT BODY1     MOON
NON-CENT BODY2     SUN
2-BODY MOTION      NO
SOL RAD PRESS      YES
DRAG               YES
POLAR MOTION       NO
THRUST             NO
INTEG RESTART    MUL-STEP

ORBIT TYPE         COWELL

                              CROSSOVER CONDITION BY SECTION

     MORE THAN ONE CONDITION MAY BE LISTED, ANY ONE OF WHICH MAY CAUSE SECTIONING.   THE FIRST CONDITION TO BE
     SATISFIED WILL BE THE CROSSOVER CONDITION BETWEEN ANY TWO ADJACENT SECTIONS.  WHEN VEHICLE IMPACTS UPON
     CENTRAL BODY OR WHEN END OF PRINT ARC ( 851001        0.0    ) IS REACHED. RUN WILL TERMINATE.

  FROM SECTION  1 TO TERMINATION

     1) SECTIONING DUE TO TIME FROM EPOCH..... 0.60739201D+08 SECONDS

* * * * * * * * * * * * * * * * * * * * * * * * * * MANEUVERS DATA* * * * * * * * * * * * * * * * * * * * * * * * * * * * *
                              0 MANEUVERS THIS FLIGHT
```

GTDS EPHEM PROGF PAGE

GTDS INITIAL CONDITIONS REPORT

• PHYSICAL CONSTANTS •

UNIVERSAL GRAVITATIONAL CONSTANT = 0.667300000D-22 KM**3/(SEC**2)(GRAM)
ASTRONOMICAL UNIT = 0.149597850+09 KM
SOLAR RADIATION PRESSURE = 0.450000000D-02 (KG/SEC**2)/KM

CONSTANTS OF BODIES CONSIDERED THIS FLIGHT--

GRAV CONST(KM**3/SEC**2)	EARTH	0.398600640D+06	MOON	0.490277800+04	SUN	0.132715440D+12
MEAN EQUATORIAL RADIUS(KM)	EARTH	0.637814000D+04	MOON	0.173800900D+04	SUN	0.695952000D+06
ROTATION RATE(RAD/SEC)	EARTH	0.729211590-04	MOON	0.266169550-05	SUN	0.0
SPHERE OF INFLUENCE(KM)	EARTH	0.925000000D+06	MOON	0.660000000D+05	SUN	0.0
INVERSE FLATTENING COEFF	EARTH	0.298250000D+03	MOON	0.100000000D+31	SUN	0.100000000D+31
GREENWICH HOUR ANGLE	EARTH	0.441591460+00				

HARMONIC COEFFICIENTS EARTH

MAXIMUM DEGREE = 8
MAXIMUM ORDER = 8

ZONALS

INDEX N M	VALUE	INDEX N M	VALUE	INDEX N M	VALUE	INDEX N M	VALUE
2 0	-.108262710000000000D-02	3 0	0.253500000000000000D-05	4 0	0.162461000000000000D-05	5 0	0.228055910000000000D-06
6 0	-.545185720000000000D-06	7 0	0.341391646000000000D-06	8 0	0.210000620000000000D-06		

SECTORALS AND TESSERALS

INDEX N M	VALUE C	VALUE S	INDEX N M	VALUE C	VALUE S
2 1	-.276359570000000000D-09	-.523974540000000000D-08	2 2	0.157114230000000000D-05	-.903131337000000000D-06
3 1	0.215676940000000000D-05	0.272678740000000000D-06	3 2	0.304468250000000000D-06	-.211592500000000000D-06
3 3	0.975660629999999990D-07	0.156818770000000000D-06	4 1	-.505527490000000000D-06	-.441250150000000000D-06
4 2	0.788425149999999990D-07	0.148165580000000000D-06	4 3	0.550737490000000000D-07	-.121400273000000000D-07
4 4	-.415424930000000000D-08	0.631161541000000000D-08	5 1	-.420501650000000000D-07	-.796017130000000000D-07
5 2	0.105151650000000000D-06	-.525778120000000000D-07	5 3	-.155359420000000000D-07	-.686707689999999990D-08
5 4	-.276186640000000000D-08	0.397171160000000000D-09	5 5	0.396577780000000000D-09	-.162554300000000000D-08
6 1	-.593428480000000000D-07	0.124851510000000000D-07	6 2	0.556685639999999990D-08	-.433599640000000000D-07
6 3	0.172544560000000000D-08	0.287119440000000000D-10	6 4	-.395894710000000000D-09	-.174455810000000000D-08
6 5	-.206575410000000000D-09	-.434857380000000000D-09	6 6	0.437558400000000000D-12	-.222723320000000000D-10
7 1	0.195557790000000000D-06	0.783138520000000000D-07	7 2	0.326559600000000000D-07	0.104633280000000000D-07
7 3	0.337422550000000000D-08	-.306768620000000000D-08	7 4	-.600341250000000000D-09	-.269448760000000000D-08
7 5	0.590013180000000000D-11	0.154573450000000000D-10	7 6	-.252163400000000000D-10	0.914117340000000000D-11
7 7	-.171341670000000000D-12	0.493556800000000000D-12	8 1	0.170628350000000000D-07	0.414784200000000000D-07
8 2	0.680777320000000000D-08	0.420582140000000000D-08	8 3	-.100309650000000000D-09	-.252665510000000000D-09
8 4	-.321393030000000000D-09	0.924011750000000000D-10	8 5	-.224452760000000000D-11	0.149237070000000000D-10
8 6	-.266659190000000000D-11	0.908964550000000000D-11	8 7	0.340013160000000000D-12	0.391219440000000000D-11
8 8	-.154537120000000000D-12	0.142083580000000000D-12			

RESONANT TERMS SECTORALS AND TESSERALS

INDEX N M	VALUE C	VALUE S	INDEX N M	VALUE C	VALUE S
15 15	-.101911300000000000D-22	-.385315870000000000D-23	16 15	-.110216160000000000D-23	-.833842700000000000D-23
17 15	0.345751380000000000D-25	0.960673290000000000D-25	18 15	-.390461220000000000D-24	-.111481570000000000D-24
19 15	-.547383700000000000D-25	-.466656240000000000D-25	20 15	-.223470670000000000D-25	0.923890960000000000D-26
21 15	0.434821430000000000D-26	0.443690740000000000D-26			

• •

OUTPUT OPTIONS

SECTION DEPENDENT OPTIONS
SECTION 1
EPHEM REPORT FULL
CENTRAL BODY EARTH

REF COORD SYST TRU-DATE INERTIAL

MAP INIT STATE COV MATRIX NC

NODAL PRINT FREQUENCY EVERY 128TH CROSSING

PRINT AT END OF EACH SECTION NC

COOR. SYSTEM OF OUTPUT PARTIALS CARTESIAN

```
                         GTDS  EPHEM    PROG1                                              PAGE
                      GTDS   SATELLITE EPHEMERIS REPORT   SECTION  1

***************************************************************************************************
DATE    NOV  18, 1983    0HRS    47MINS    50.108SECS  (JULIAN DATE = 2445656.53332)
ELAPSED TIME FROM EPOCH =   20 DAYS    0 HRS   47 MINS    50.108 SECS
FLIGHT CENTRAL BODY IS EARTH    (VEHICLE IS IN SHADOW  )

OUTPUT CENTRAL BODY IS EARTH               INERTIAL SYSTEM    TRUE EQUATOR AND EQUINOX OF OCT 29  1983
X    -1684.557569     Y     6686.784020     Z   -.5634322264      DX   .5671288338      DY   .2244340910      DZ  -7.539071208
SMA  6899.672299      ECC  .15671451730-02  INC  97.55561312      RAAN  284.1405798      AP    111.2222424     MA   68.3800990
EA   68.39217197      P     1.584349781     SLR  6899.655354      PR    6888.859511     APR  6910.485067     PH   510.7195111
APM  532.3450874      C3  -28.88547620      TA   68.41587708      LAT -.47106622810-02  LON  38.67527461     HGT  517.6505082
R    6895.698568      V     7.605108150     RA   104.1396589      DEC -.44615172960-02  VPA  89.91621618     AZ   187.8886131

                 X                    Y                    Z                   DX                  DY                  DZ
RHOI(1)   0.2270830+02         0.5800960+01        -0.1769480+03        0.4814070-01        -0.1910360+00        -0.9517630-04
                         THIS IS DESCENDING NODAL CROSSING NO. 384

***************************************************************************************************
DATE    NOV  28, 1983    0HRS    38MINS    46.557SECS  (JULIAN DATE = 2445666.52669)
ELAPSED TIME FROM EPOCH =   30 DAYS    0 HRS   38 MINS    46.557 SECS
FLIGHT CENTRAL BODY IS EARTH    (VEHICLE IS IN SUN LITE)

OUTPUT CENTRAL BODY IS EARTH               INERTIAL SYSTEM    TRUE EQUATOR AND EQUINOX OF OCT 29  1983
X    2817.437669      Y    -6294.284722     Z    .7074368605      DX  -.9172666761      DY  -.3973827570      DZ   7.538007471
SMA  6899.642777      ECC  .16039451140-02  INC  97.55703361      RAAN  294.1149475      AP    71.33811674     MA   288.2442713
EA   288.7576531      P     1.584139613     SLR  6899.625027      PR    6888.576129     APR  6910.709425     PH   510.4361287
APM  532.5694253      C3  -28.88559980      TA   288.6700125      LAT  .59143247210-02  LON  118.8639448     HGT  517.5440834
R    6896.084683      V     7.604658095     RA   254.1141677      DEC  .58777047900-02  VPA  90.08701820     AZ   282.4429663

                 X                    Y                    Z                   DX                  DY                  DZ
RHOI(1)  -0.4063260+02        -0.2080070+02         0.3556280+03       -0.1018180+00         0.4001010+00         0.1427900-04
                         THIS IS ASCENDING NODAL CROSSING NO. 486

***************************************************************************************************
DATE    NOV  28, 1983    1HRS    26MINS    10.785SECS  (JULIAN DATE = 2445666.5558)
ELAPSED TIME FROM EPOCH =   30 DAYS    1 HRS   26 MINS    10.785 SECS
FLIGHT CENTRAL BODY IS EARTH    (VEHICLE IS IN SHADOW  )

OUTPUT CENTRAL BODY IS EARTH               INERTIAL SYSTEM    TRUE EQUATOR AND EQUINOX OF OCT 29  1983
X   -2821.076557      Y     6293.132107     Z   -1.366462841      DX   .9085914924      DY   .4182977684      DZ  -7.538085252
SMA  6899.609544      ECC  .15806625260-02  INC  97.55625386      RAAN  254.1471767      AP    106.3810386     MA   73.48588396
EA   73.54273193      P     1.584328146     SLR  6899.592205      PR    6888.783587     APR  6910.215581     PH   510.5635866
APM  532.3755807      C3  -28.88573893      TA   73.42561335      LAT -.11423157710-01  LON  26.21285420     HGT  518.3756663
R    6856.519885      V     7.604159468     RA   114.1456734      DEC -.11352472770-01  VPA  89.51316498     AZ   187.8888532

                 X                    Y                    Z                   DX                  DY                  DZ
RHOI(1)   0.4831380+02         0.2190090+02        -0.4007500+03        0.1824840+00        -0.4870380+00        -0.8754690-04
                         THIS IS DESCENDING NODAL CROSSING NO. 486

***************************************************************************************************
DATE    DEC   8, 1983    1HRS    16MINS    55.419SECS  (JULIAN DATE = 2445676.55336)
ELAPSED TIME FROM EPOCH =   40 DAYS    1 HRS   16 MINS    55.419 SECS
FLIGHT CENTRAL BODY IS EARTH    (VEHICLE IS IN SUN LITE)

OUTPUT CENTRAL BODY IS EARTH               INERTIAL SYSTEM    TRUE EQUATOR AND EQUINOX OF OCT 29  1983
X    3067.730756      Y    -5708.091344     Z    1.305668622      DX  -.8383067494      DY  -.5509359279      DZ   7.539666427
SMA  6899.594611      ECC  .15939799620-02  INC  97.55938847      RAAN  304.1225118      AP    66.68543417     MA   294.5178348
EA   294.4346264      P     1.584323823     SLR  6899.577081      PR    6888.556796     APR  6910.652427     PH   510.4567955
APM  532.4524266      C3  -28.88580168      TA   294.3815166      LAT  .18917255180-01  LON  208.6813391     HGT  516.9853030
R    6858.048302      V     7.605776994     RA   304.1810720      DEC  .18849612220-01  VPA  90.08314840     AZ   282.4406994

                 X                    Y                    Z                   DX                  DY                  DZ
RHOI(1)  -0.7581780+02        -0.5215590+02         0.7177430+03       -0.4484080+00         0.6617240+00        -0.2901810-04
                         THIS IS ASCENDING NODAL CROSSING NO. 688

                                    UNITS FOR INFORMATION
                 DISTANCES ARE IN KILOMETERS                  ANGLES         ARE IN DEGREES
                 RATES     ARE IN KM/SEC                      TIME(PERIOD) IS IN HOURS
```

SOLAR MESOSPHERE EXPLORER EPHEMERIS
GENERATED BY GSFC GROUND TRACKING AND DATA SYSTEM EPHEM PROGRAM
PROCESSED BY SME DATA PROCESSING SYSTEM ORBIT/ATTITUDE SOFTWARE

GTDS EPHEM PROGRAM   GTDS STANDARD EPHEM   SATELLITE ID: 8110001.

EPHEM START DATE: 1985 JAN 23 0000: 0.000 UTC   DATE PROCESSED: 1985 FEB 6 2220:30.891
EPHEM STOP DATE: 1985 FEB 6 1000: 0.000 UTC   EPHEM DATA STEP SIZE: 60.0 SEC

****** DEFINITIVE DATA******

INITIAL CONDITIONS AT EPHEM START DATE REFERENCED TO INER EQUATOR AND EQUINOX

KEPLERIAN ORBIT ELEMENTS		CARTESIAN STATE VECTOR	ADDITIONAL ELEMENTS		INTEGRATION FACTORS	
SEMIMAJOR AXIS	= 6893.548 KM	X = -0.6559863D+04 KM	PERIAPSIS ALTITUDE =	507.788 KM	ORBIT THEORY	COWELL
ECCENTRICITY	= 0.001	Y = 0.5581069D+03 KM	APOAPSIS ALTITUDE =	523.635 KM	GRAV HARMONICS	USED
INCLINATION	= 97.616 DEG	Z = -0.2042863D+04 KM	ORBIT PERIOD =	94.941 MIN	LUNAR GRAVITY	USED
ARG OF PERIFOCUS	= 93.679 DEG	VX = 0.2307479D+01 KM/S	TRUE ANOMALY =	103.711 DEG	SOLAR GRAVITY	USED
RT ASC OF ASC NODE	= 357.254 DEG	VY = 0.8522533D+00 KM/S	FLIGHT PATH ANGLE =	89.936 DEG	SOLAR RADIATION	USED
MEAN ANOMALY	= 103.583 DEG	VZ = -0.7192884D+01 KM/S	RATE OF ASCEN NODE =	1.006 D/DA	ATMOSPHERE DRAG	USED

REFLECTIVITY CONST = 1.2000   GREENWICH HR ANGLE = 2.134 HR AT EPOCH OF ELEMENTS

EPOCH OF ELEMENTS: 1985-01-23 00:00: 0.000

****** CONSTANTS FOR DRAG ******

DRAG COEFFICIENT = 2.3000   MASS= 0.4135000D+06 GRAMS   SATELLITE AREA = 1.129 M2   DENSITY MODEL HAR-PRIE

****** COEFFICIENTS OF ZONAL/TESSERAL HARMONICS ******

C(2, 1)	-0.2764E-09	S(2, 1)	-0.5236E-08	C(2, 2)	0.1571E-05	S(2, 2)	-0.9023E-06
C(3, 1)	0.2191E-05	S(3, 1)	0.2727E-06	C(3, 2)	0.3047E-06	S(3, 2)	-0.2126E-06
C(3, 3)	0.9777E-07	S(3, 3)	0.1966E-06	C(4, 1)	-0.5055E-06	S(4, 1)	-0.4413E-06
C(4, 2)	0.7834E-07	S(4, 2)	0.1482E-06	C(4, 3)	0.5907E-07	S(4, 3)	-0.1214E-07
C(4, 4)	-0.4154E-08	S(4, 4)	0.4316E-08	C(5, 1)	-0.4205E-07	S(5, 1)	-0.7900E-07
C(5, 2)	0.1052E-06	S(5, 2)	-0.5258E-07	C(5, 3)	-0.1554E-07	S(5, 3)	-0.6867E-08
C(5, 4)	-0.2267E-08	S(5, 4)	0.5922E-09	C(5, 5)	0.3970E-09	S(5, 5)	-0.1630E-08
C(6, 1)	-0.5935E-07	S(6, 1)	0.1249E-07	C(6, 2)	0.5987E-08	S(6, 2)	-0.4336E-07
C(6, 3)	0.1725E-08	S(6, 3)	0.2871E-10	C(6, 4)	-0.3959E-09	S(6, 4)	-0.1743E-08
C(6, 5)	-0.2066E-09	S(6, 5)	-0.6349E-09				

****** COEFFICIENTS CONTINUED FROM RECORD 2 ******

C(6, 6)	0.4380E-12	S(6, 6)	-0.5637E-10	C(7, 1)	0.1956E-06	S(7, 1)	0.7031E-07
C(7, 2)	0.3266E-07	S(7, 2)	0.1046E-07	C(7, 3)	0.3379E-08	S(7, 3)	-0.3068E-08
C(7, 4)	-0.6063E-09	S(7, 4)	-0.2694E-09	C(7, 5)	0.5900E-11	S(7, 5)	0.1546E-10
C(7, 6)	-0.2522E-10	S(7, 6)	0.9141E-11	C(7, 7)	-0.1713E-12	S(7, 7)	0.4940E-12
C(8, 1)	0.1706E-07	S(8, 1)	0.4348E-07	C(8, 2)	0.6008E-08	S(8, 2)	0.4206E-08
C(8, 3)	-0.1003E-09	S(8, 3)	-0.5927E-09	C(8, 4)	-0.3214E-09	S(8, 4)	0.9840E-10
C(8, 5)	-0.2265E-11	S(8, 5)	0.1492E-10	C(8, 6)	-0.2087E-11	S(8, 6)	0.9090E-11
C(8, 7)	0.3456E-12	S(8, 7)	0.3932E-12	C(8, 8)	-0.1545E-12	S(8, 8)	0.1621E-12

Office of Conference Services

EXECUTIVE EDUCATION PROGRAM

FOR THE

GAS INDUSTRY

June 9 - 21, 1985

University of Colorado Boulder